PREPARATION AND MODIFICATION OF MEDIUM-CHAIN-LENGTH POLY(3-HYDROXYALKANOATES) AS OSTEOCONDUCTIVE AND AMPHIPHILIC POROUS SCAFFOLD

NOR FAEZAH BINTI ANSARI

FACULTY OF SCIENCE
UNIVERSITY OF MALAYA
KUALA LUMPUR

2017

PREPARATION AND MODIFICATION OF MEDIUM-CHAIN- LENGTH POLY(3-HYDROXYALKANOATES) AS OSTEOCONDUCTIVE AND AMPHIPHILIC POROUS SCAFFOLD

NOR FAEZAH BINTI ANSARI

THESIS SUBMITTED IN FULFILMENT OF THE REQUIREMENTS FOR THE DEGREE OF DOCTOR OF PHILOSOPHY

INSTITUTE OF BIOLOGICAL SCIENCES
FACULTY OF SCIENCE
UNIVERSITY OF MALAYA
KUALA LUMPUR

2017

UNIVERSITY OF MALAYA

ORIGINAL LITERARY WORK DECLARATION

Name of Candidate: Nor Faezah Ansari

Matric No: SHC130090

Name of Degree: Doctor of Philosophy

Title of ~~Project Paper/Research Report/Dissertation/~~Thesis ("this Work"):

Preparation and modification of medium-chain-length poly(3-hydroxyalkanoates) as osteoconductive and amphiphilic porous scaffold

Field of Study:

Biotechnology

I do solemnly and sincerely declare that:

(1) I am the sole author/writer of this Work;
(2) This Work is original;
(3) Any use of any work in which copyright exists was done by way of fair dealing and for permitted purposes and any excerpt or extract from, or reference to or reproduction of any copyright work has been disclosed expressly and sufficiently and the title of the Work and its authorship have been acknowledged in this Work;
(4) I do not have any actual knowledge nor do I ought reasonably to know that the making of this work constitutes an infringement of any copyright work;
(5) I hereby assign all and every rights in the copyright to this Work to the University of Malaya ("UM"), who henceforth shall be owner of the copyright in this Work and that any reproduction or use in any form or by any means whatsoever is prohibited without the written consent of UM having been first had and obtained;
(6) I am fully aware that if in the course of making this Work I have infringed any copyright whether intentionally or otherwise, I may be subject to legal action or any other action as may be determined by UM.

Candidate's Signature Date:

Subscribed and solemnly declared before,

Witness's Signature Date:

Name:

Designation:

ABSTRACT

Polyhydroxyalkanoates (PHA) are hydrophobic biopolymers with huge potential for biomedical applications due to their biocompatibility, excellent mechanical properties and biodegradability. A porous composite scaffold made of medium-chain-length poly(3-hydroxyalkanoates) (mcl-PHA) and hydroxyapatite (HA) was fabricated using particulate leaching technique and NaCl as porogen. Different percentages of HA loading was investigated that would support the growth of osteoblast cells. Ultrasonic irradiation was applied to facilitate the dispersion of HA particles into mcl-PHA matrix. Different P(3HO-*co*-3HHX)/HA composites were investigated using Field Emission Scanning Electron Microscopy (FESEM), X-ray Diffraction (XRD), Fourier Transform Infrared Spectra (FTIR) and Energy Dispersive X-ray Analysis (EDXA). The scaffolds were found to be highly porous with interconnecting pore structures and HA particles were homogeneously dispersed in the polymer matrix. The scaffolds biocompatibility and osteoconductivity were also assessed following the proliferation and differentiation of osteoblast cells on them. From the results, it is clear that scaffolds made from P(3HO-*co*-3HHX)/HA composites are viable candidate materials for bone tissue engineering applications. Additionally, glycerol 1,3-diglycerol diacrylate (GDD) was graft copolymerized onto poly(3-hydroxyoctanoate-*co*-3-hydroxyhexanoate) P(3HO-*co*-3HHX) to render the latter more hydrophilic. Grafting of P(3HO-*co*-3HHX) backbone was performed using benzoyl peroxide as free radical initiator in homogenous acetone solution. The graft copolymer of P(3HO-*co*-3HHX)-*g*-GDD was characterized using spectroscopic and thermal methods. The presence of GDD monomer in the grafted P(3HO-*co*-3HHX) materials linked through covalent bond was indicated by spectroscopic analyses. Different parameters affecting the graft yield *viz.* monomer concentration, initiator concentration, temperature and reaction time were also investigated. Water uptake measurement showed that P(3HO-*co*-3HHX)-*g*-GDD

copolymer became more hydrophilic as the GDD concentration in the copolymer increased. Introduction of hydroxyl groups *via* grafted GDD monomers improved the wettability and imparted amphiphilicity to the graft copolymer, thus potentially improving their facility for cellular interaction. Thermal stability of grafted copolymer reduced with increased grafting yield. The activation energy, E_a, for the graft copolymerization was calculated at ~ 51 kJ mol^{-1}. Mechanism of grafting reaction was also proposed in the study. Scaffolds of P(3HO-*co*-3HHX)-*g*-GDD/HA were successfully fabricated *via* graft copolymerization and physical blend in order to improve the hydrophilicity of the mcl-PHA. FTIR analysis showed the presence of new absorption spectra for –OH and PO_4^{3-} which indicated the presence of GDD and HA in mcl-PHA structure, respectively. EDX analysis was applied to ratify the distribution of HA particles within the P(3HO-*co*-3HHX)-*g*-GDD/HA composite matrix. Toxicity of the composite was studied against *Artemia franciscana* in brine shrimp lethality assay (BSLA). No significant mortality of the test organism was recorded, thus implied that the novel scaffold poses negligible toxicity risk to the cell. It is concluded that P(3HO-*co*-3HHX)-*g*-GDD/HA composite is potentially useful for biomedical applications.

ABSTRAK

Polyhydroxyalkanoates (PHA) adalah biopolimer hidrofobik yang mempunyai potensi besar untuk aplikasi bioperubatan kerana biokeserasian, ciri-ciri mekanikal yang sangat baik dan biodegradasi. Kerangka komposit berliang yang diperbuat daripada rantai sederhana panjang poli(3-hydroxyalkanoates) (mcl-PHA) dan hydroxyapatite (HA) telah dihasilkan dengan menggunakan teknik zarah larut-lesap dan NaCl sebagai porogen. Peratusan HA yang berbeza telah disiasat untuk menyokong pertumbuhan sel tulang. Gelombang ultrabunyi telah diaplikasi untuk memudahkan penyebaran zarah HA ke dalam matriks mcl-PHA. Perbezaan komposit P(3HO-co-3HHX)/HA telah disiasat menggunakan mikroskop elektron pengimbas (FESEM), serakan X-ray (XRD), spektroskopi inframerah transformasi fourier (FTIR) dan tenaga serakan X-ray analisis (EDXA). Kerangka terhasil didapati sangat berliang dengan struktur liang yang bersambung dan penyebaran zarah HA yang sekata di dalam matriks polimer. Biokeserasian kerangka dan osteokonduktiviti juga dinilai berdasarkan proliferasi dan pembezaan sel-sel osteoblast pada kerangka. Berdasarkan keputusan, kerangka komposit P(3HO-*co*-3HHX)/HA yang dihasilkan merupakan material yang sesuai untuk aplikasi kejuruteraan tisu tulang. Di samping itu, gliserol 1,3-digliserolat diakrilat (GDD) telah dicantum ke dalam poli(3-hydroxyoctanoate-*co*-3-hydroxyhexanoate) P(3HO-*co*-3HHX) untuk memberi kesan lebih hidrophilic. Cantuman P(3HO-*co*-3HHX) dihasilkan dengan menggunakan benzoil peroksida sebagai radikal pemula bebas di dalam larutan aseton. Cantuman P(3HO-*co*-3HHX)-*g*-GDD dicirikan menggunakan kaedah spektroskopi dan terma. Kehadiran monomer GDD dalam cantuman P(3HO-*co*-3HHX) dihubungkan melalui ikatan kovalen telah ditunjukkan oleh spektroskopi analisis. Parameter berbeza yang mempengaruhi hasil cantuman seperti kepekatan monomer, kepekatan radikal, suhu dan masa tindak balas telah disiasat. Pengukuran untuk kebolehan penyerapan air menunjukkan bahawa P(3HO-*co*-

3HHX)-*g*-GDD kopolimer menjadi lebih hidrofilik apabila kepekatan GDD dalam kopolimer meningkat. Pengenalan kumpulan hidroksil melalui percantuman monomer GDD menambahbaik kebolehbasahan dan memberikan amphiphiliciti untuk percantuman kopolimer, justeru berpotensi meningkatkan interaksi diantara sel-sel. Kestabilan terma kopolimer yang dicantumkan menurun dengan peningkatan hasil cantuman. Tenaga pengaktifan, E_a, untuk cantuman telah dikira pada ~ 51 kJ mol^{-1}. Mekanisme tindak balas cantuman juga telah dicadangkan di dalam kajian ini. Kerangka P(3HO-*co*-3HHX)-*g*-GDD/HA telah berjaya direka melalui cantuman dan gabungan fizikal untuk meningkatkan hidrofilik mcl-PHA. Analisis FTIR menunjukkan kehadiran spektrum penyerapan baru bagi -OH dan PO_4^{3-} yang menunjukkan kehadiran GDD dan HA dalam struktur mcl-PHA. Analisis EDX telah dijalankan untuk mengesahkan penyebaran zarah HA dalam matriks polimer. Ketoksikan komposit telah diuji terhadap *Artemia franciscana* di dalam ujian "*brine shrimp lethality assay*" (BSLA). Tiada kematian organisma yang ketara dicatatkan, justeru menunjukkan bahawa kerangka baru dihasilkan tidak menimbulkan risiko ketoksikan kepada sel. Kesimpulannya, komposit P(3HO-*co*-3HHX)-*g*-GDD/HA berpotensi digunakan untuk aplikasi bioperubatan.

ACKNOWLEDGEMENTS

Alhamdulillah, all praises to Allah S.W.T for the strengths and His blessing to complete my PhD research project successfully. I would like to express my sincere gratitude and deepest appreciation to my supervisor, Prof. Dr. Mohamad Suffian Mohamad Annuar for his limitless guidance and support throughout the course of my study. His valuable advice, comments and motivation have guided me in completing my research successfully. I also appreciate his guidance and scientific views very much.

I would like to express my humble appreciation to Assoc. Prof Ir. Dr. Belinda Pingguan-Murphy (Department of Biomedical Engineering, Faculty of Engineering, UM) who was willing to collaborate and extensively revised the scientific paper I have published.

I would like to express my deepest gratitude goes to my beloved parents Mr. Ansari b. Abdul Hamid and Mrs. Masrah bt Abdul Rashid, and also to my siblings Dr Azmah Ansari and Dr Aminuddin Ansari for their boundless support, prayers and love which kept me motivated throughout. I also acknowledge all my family members Haris, Salwana, Syifa, Irfan and Aiman for their support. I would also like to thank Mr Amirul for his moral support.

I would like to thank my fellow labmates in Integrative Bioprocess and Enzyme Technology research group, especially Dr. Ahmad Gumel, Naziz, Syairah, Nadia, Haziq, Suhaiyati, Ana, Hindatu, Syed, Rafais and Haziqah for their guidance, assistance and endless support during the research work.

Finally, I am grateful to International Islamic University Malaysia for awarding me fellowship SLAB/SLAI to sustain my life throughout the candidature. I also would like to credit to the grant from IPPP University Malaya (PG043-2014A) for a full financial support for my project.

TABLE OF CONTENTS

CHAPTER 3: MATERIALS AND METHODS

LIST OF FIGURES

LIST OF TABLES

LIST OF SYMBOLS AND ABBREVIATIONS

NH_4Cl	Ammonium chloride
NH_4OH	Ammonium hydroxide
ALP	Alkaline phosphate
E_a	Activation energy
BPO	Benzoyl peroxide
β	Beta
Ca	Calcium
$CaCI_2.2H_20$	Calcium chloride dehydrate
CDW	Cell dry weight
CoA	Coenzyme-A
$CoCl_2.6H_2O$	Cobalt (II) chloride hexahydrate
$CuCl_2.2H_2O$	Copper (II) chloride dehydrate
$CDCl_3$	Deuterated chloroform
DCM	Dichloromethane
DSC	Differential scanning calorimetry
dH_2O	Distilled water
Na_2HPO_4	Disodium hydrogen phosphate
Da	Dalton
DSC	Differential Scanning Calorimeter
^oC	Degree Celcius
wt%	Dry weight percent
T_d	Degradation temperature
EDX	Energy dispersive X-ray
FESEM	Field emission scanning electron microscopy

FTIR	Fourier transform infrared
FID	Flame ionization detector
g	Gravity
g	Gram
GC	Gas Chromatography
GDD	Glycerol, 1-3 diglycerol diacrylate
g/g	Gram per gram
g/L	Gram per liter
GPC	Gel Permeation Chromatography
T_g	Glass transition temperature
HA	Hydroxyapatite
h	Hour
ΔH_m	Heat of fusion
$FeCl_3$	Iron (III) chloride
J/g	Joule per gram
kDa	Kilo Dalton
kg	Kilogram
L	Liter
µg	Microgram
µg/ml	Microgram per mililiter
µL	Microliter
µm	Micrometer
µM	Micromolar
M_w	Molecular weight
mcl	Medium-chain-length
min	Minute

mg	Miligram
mg/L	Miligram per liter
T_m	Melting temperature
$MgSO_4$	Magnesium sulphate
$MgSO_4.7H_2O$	Magnesium sulphate heptahydrate
mL	Mililiter
mM	Milimolar
Mol %	Mole percent
NR	Nutrient rich
M_n	Number-average molecular weight
NMR	Nucleur Magnetic Resonance
C	Oxygen concentration
C*	Oxygen solubility
K_La	Oxygen mass transfer coefficient
OD	Optical density
pO_2	Oxygen partial pressure
KH_2PO_4	Potassium dihydrogen phosphate
KOH	Potassium hydrogen
%	Percentage
M_w/ M_n	Polydispersity index
PO_4^{3-}	Phosphate
P(3HO-*co*-3HHX)	Poly(3-hydroxyoctanoate-*co*-3-hydroxyhexanoate)
P(3HO-*co*-3HHX)/HA	Poly(3-hydroxyoctanoate-*co*-3-hydroxyhexanoate)/blend with hydroxyapatite
P(3HO-*co*-3HHX)-*g*-GDD	Poly(3-hydroxyoctanoate-*co*-3-hydroxyhexanoate) grafted with glycerol, 1,3-diglycerol diacrylate
P(3HO-*co*-3HHX)-*g*-GDD/HA	Poly(3-hydroxyoctanoate-*co*-3-hydroxyhexanoate) grafted with glycerol, 1,3-diglycerol diacrylate/ blend with hydroxyapatite

Pd	Polydispersity index
PHA	Polyhydroxyalkanoate
PhaA; *phaA*	*β*-ketothiolase; gene encoding *β*-ketothiolase
PhaB; *phaB*	NADPH-dependent acetoacetyl-CoA dehydrogenase; gene encoding NADPH-dependent acetoacetyl-CoA dehydrogenase
PhaC; *phaC*	PHA synthase; gene encoding PHA synthase
rpm	Revolutions per minute
scl	Short-chain-length
sp.	Species
NaCl	Sodium chloride
Na_2CO_3	Sodium carbonate
H_2SO_4	Sulphuric acid
MT	Trace element
TCA	Tricarboxylic acid
v/v	Volume per volume
w/v	Weight per volume
w/w	Weight per weight
H_2O	Water
XRD	X-ray diffraction
$ZnSO_4.7H_2O$	Zinc sulfate heptahydrate
3HX	3-hydroxyhexanoate
3HO	3-hydroxyoctanoate

LIST OF APPENDICES

CHAPTER 1

INTRODUCTION

The increasing demand on sustainability, eco-efficiency and green chemistry has generated tremendous search for materials that are renewable and environmental friendly. Biodegradable polymers offer a sustainable alternative to petroleum-derived sources. Polyhydroxyalkanoates (PHA) comprised a group of natural biodegradable polyesters that are synthesized by microorganisms. PHA exhibits a wide range of physical and mechanical properties owing to the diversity in their chemical structures. Among its sought after attributes are biodegradability and excellent biocompatibility, making this class of biopolymer attractive as the potential biomaterial for various applications, particularly in biomedical field (Ali & Jamil, 2016; Kim *et al.*, 2007).

Medium-chain-length poly(3-hydroxyalkanoates) (mcl-PHA) is structurally diverse polyester and could be suitably tailored for various biomedical applications. They are biodegradable, biocompatible and thermoprocessable, hence suitable platform materials for applications in both conventional medical devices and tissue engineering (e.g. sutures, cardiovascular application, bone marrow scaffolds, matrices for controlled drug delivery etc.) (Chen & Wu, 2005; Hazer *et al.*, 2012). However, direct application of these polyesters, mcl-PHA included, has been hampered by their strong hydrophobic character and other physical shortcomings (Kim *et al.*, 2008; Rai *et al.*, 2011). Hence, native mcl-PHA needs to be modified in order to improve its performance in specialized applications such as environmentally biodegradable polymers and functional materials for biomedical and industrial applications (Lee *et al.*, 2010; Li *et al.*, 2016).

Synthetic and natural hydroxyapatites (HA) ($HCa_5O_{13}P_3$) have similar chemical composition and crystallographic properties to a human bone (Xi *et al.*, 2008). Their biocompatibility and osteoconductive behavior are suitable for making bone implants.

Studies have shown that incorporation of HA into biomaterials could help to enhance mechanical performance and osteoblast responses (Baei & Rezvani, 2011; Wang *et al.*, 2005). Currently, composites of polymers and ceramics are being developed with the aim to increase the mechanical scaffold stability and to improve tissue interactions. In addition, efforts have also been invested in developing scaffolds with drug-delivery capacity. These scaffolds allow for local release of growth factors or antibiotics and enhance bone in-growth to treat bone defects and even support wound healing (Rezwan *et al.*, 2006). Pores are necessary for bone tissue formation because they allow migration and proliferation of osteoblasts and mesenchymal cells as well as vascularization. In addition, a porous surface improves mechanical interlocking between the implant biomaterial and the surrounding natural bone thus providing for greater mechanical stability at this critical interface (Wei & Ma, 2004).

Microbial polyesters can be further diversified *via* both chemical modification reaction and genetic engineering of the biosynthetic pathways. Chemical modification is a promising approach to obtain new types of PHA-composite materials including a wide range of monomers for graft/block copolymerization with synthetic and other natural polymers that cannot be obtained by biotechnological processes (Hazer & Steinbüchel, 2007). For instance, chemical modification of PHA could involve grafting reactions through graft/block copolymerization, chlorination, cross-linking, epoxidation, hydroxyl and carboxylic acid functionalization. Insertions of an additional different polymer segment into an existing polymer backbone or at the side chain of an existing polymer yields block or graft copolymers (Gumel *et al.*, 2014).

Moreover, mcl-PHA has attracted great interest in research due to its potential wide applicability as biomaterials. Nevertheless, its strong hydrophobicity, slow degradation under physiological conditions and lack of chemical functionalities hinder the realization of its potentials. These factors restrict the scope of their applications in

biomedical field. In order to expand the range of its versatilities, other properties such as mechanical strength, surface features, amphiphilicity and degradation rate have to be modified to match the requirements of specific applications (Kai & Loh, 2013). For example, intrinsic hydrophobic properties of mcl-PHA restrict their applications as cell colonizing materials. Therefore, chemical modification with suitable functional groups or modification of the surface topography of mcl-PHA is needed in order to minimize hydrophobic interactions with the surrounding tissue. Amphiphilic copolymers could be produced through chemical modification reactions by inserting the hydrophilic segments into the hydrophobic PHA (Hazer, 2010).

In this study, a mcl-PHA *viz.* poly(3-hydroxyoctanoate-*co*-3-hydroxyhexanoate) P(3HO-*co*-3HHX) was investigated as a potential material for bone cells regeneration scaffold both in its pure form and as P(3HO-*co*-3HHX)/HA composite. The physical, thermal and mechanical properties of the composite P(3HO-*co*-3HHX)/HA scaffold were investigated. The biocompatibility and osteoconductivity of the porous composite P(3HO-*co*-3HHX)/HA scaffold was also studied. In order to enhance hydrophilicity of the polymer, graft copolymerization of P(3HO-*co*-3HHX) with the glycerol 1,3-diglycerolate diacrylate (GDD) was investigated *via* free radical polymerization reaction. The P(3HO-*co*-3HHX)-*g*-GDD was prepared by thermal treatment of homogenous solution of P(3HO-*co*-3HHX), GDD monomer and benzoyl peroxide (BPO) as a chemical initiator. Differently selected parameters affecting the graft yield were studied such as monomer concentration, chemical initiator concentration, temperature and reaction time. In addition, the grafted copolymer P(3HO-*co*-3HHX)-*g*-GDD was characterized and the grafting mechanism was proposed. It is hypothesized that if scaffolds of P(3HO-*co*-3HHX)-*g*-GDD/HA are successfully fabricated *via* graft copolymerization and physical blend, the resulting biomaterials will possess the desired properties as described earlier. The objectives of the investigation includes :

Biosynthesis of mcl-polyhydroxyalkanotes (mcl-PHA)

1. To produce mcl-PHA from *Pseudomonas putida* BET001 in fed-batch fermentation;

Blending of poly(3-hydroxyoctanoate-*co*-3-hydroxyhexanoate) P(3HO-*co*-3HHX) with hydroxyapatite (HA)

1. To study the effects of different concentrations of HA loading onto P(3HO-*co*-3HHX);

2. To characterize the polymer before and after blending with HA using FTIR, DSC, XRD, EDX and FESEM;

3. To determine the osteoblast cell response towards the P(3HO-*co*-3HHX)/HA blend;

Functionalization of P(3HO-*co*-3HHX) as amphiphilic material by graft copolymerization with glycerol 1,3-diglycerol diacrylate (GDD)

1. To study graft copolymerization of P(3HO-*co*-3HHX) with glycerol 1,3-diglycerolate diacrylate *via* free radical polymerization reaction;

2. To determine the effects of monomer concentration, reaction time, initiator concentration and temperature on graft copolymerization of P(3HO-*co*-3HHX)-*g*-GDD;

3. To characterize the P(3HO-*co*-3HHX)-*g*-GDD graft copolymer using FTIR, ^{1}H NMR, STA, DSC, GPC and propose the possible radical polymerization mechanism;

4. To determine the water uptake ability of the grafted copolymer.

P(3HO-*co*-3HHX)-*g*-GDD/HA composite scaffold

1. To fabricate composite scaffold of P(3HO-*co*-3HHX)-*g*-GDD/HA *via* graft copolymerization and physical blend;
2. To characterize the newly developed scaffold by using FTIR and EDX;
3. To study the toxicity effect of the P(3HO-*co*-3HHX)-*g*-GDD/HA.

CHAPTER 2

LITERATURE REVIEW

2.1 Polyhydroxyalkanoates (PHA)

Polyhydroxyalkanoates (PHA) are versatile polyesters produced by a large number of bacteria as intracellular granules under metabolic stress conditions (Bassas-Galià *et al.*, 2015). Bacterial-synthesized PHA has attracted attention because they can be produced from a variety of renewable resources and are truly biodegradable and highly biocompatible thermoplastic materials (Yu *et al.*, 2006). Microorganisms are able to accumulate various types of PHA in the form of homopolymer, copolymer and polymer blends (Bhatt *et al.*, 2008). The properties of PHA copolymers depend strongly on the type, content and distribution of comonomer units which comprise the polymer chains, as well as the molecular weight distribution (Chanprateep *et al.*, 2008). In addition, the nature and proportion of different monomers are also influenced by the bacterial strains, type and relative quantity and quality of carbon sources supplied to the growth medium (Shamala *et al.*, 2009).

PHA is a family of optically active biological polyesters which composed of repeating units of 3-hydroxyalkanoic acids, each carries an aliphatic alkyl side chain (R). Carbon, oxygen and hydrogen are the main components in the structure of PHA. The general structure of PHA is shown in Figure 2.1. The carboxyl group of one monomer forms an ester bond with the hydroxyl group of the adjacent monomer. Each monomer contains the chiral carbon atom and has the (R) stereochemical configuration on the hydroxyl-substituted carbon (Madison & Huisman, 1999). According to Williams and Martin (2005), there are various kind of side chain groups attached including alkyl, aryl, halogen, aromatic and branched monomers. The variation in side chain endows the PHA family with excellent properties ranging from rigid and stiff

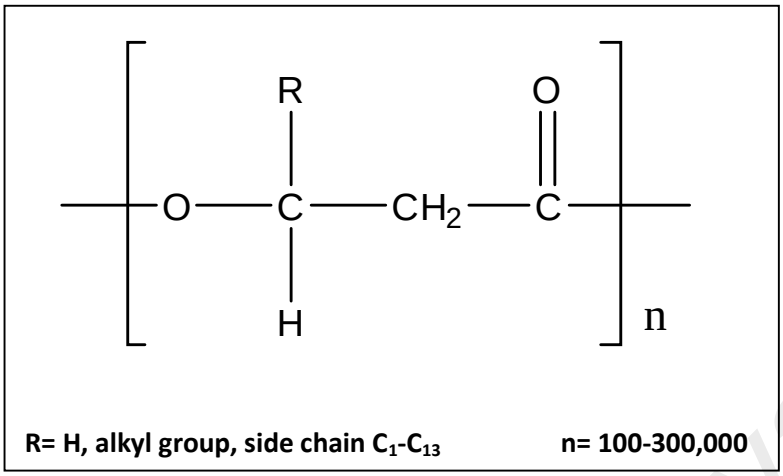

Figure 2.1: General structure of PHA

to flexible and elastomeric. Hence, it significantly expands PHA potential for various applications, particularly in biomedical field.

Several strains of PHA producing bacteria were studied such as *Bacillus* sp., *Alcaligenes* sp., *Pseudomonas* sp., *Aeromonas hydrophila, Rhodopseudomonas palustris, Escherichia coli, Burkholderia sacchari* and *Halomonas boliviensis* (Verlinden *et al.*, 2007). Over 150 types of PHA have been identified as homopolymers or as copolymers. The flexibility of PHA biosynthesis makes it possible to design and produce biopolymers with useful physical properties ranging from stiff and brittle plastic to rubbery polymers (Bhatt *et al.*, 2008; Sudesh *et al.*, 2000). Examples of PHA produced at commercial scale under various trademarks including Biomer®, Mirel ™, Biocycle®, ICI® and Biopol® (Sudesh & Iwata, 2008).

2.1.1 Medium-chain-length poly(3-hydroxyalkanoates)

PHA is classified based on the number of carbon atom present in the monomeric unit. Monomeric unit of short-chain-length PHA (scl-PHA) consisted of 3-5 carbon atoms, while medium-chain-length PHA (mcl-PHA) consisted of 6-14 carbon atoms. Scl-PHA like poly(3-hydroxybutyrate), P(3HB) is hard and brittle compared to mcl-PHA and their copolymers like poly(3-hydroxyhexanoate-*co*-3-hydroxyoctanoate), P(3HHx-*co*-3HO), which are soft and elastomeric. Mcl-PHA and its copolymers exhibit low crystallinity, low glass transition temperature, low tensile strength and high elongation-to-break ratio compared to scl-PHA, which is brittle and stiff (Muhr *et al.*, 2013; Rai *et al.*, 2011; Sudesh *et al.*, 2000).

Mcl-PHA biosynthesis is a general property of the flourescent pseudomonads belonging to the rRNA homology group I. Most of these bacteria are able to grow on various carbon sources that can be incorporated into mcl-PHA. Depending on the nature of the carbon substrate available, the hydroxyacyl monomers are derived from the intermediates of fatty acid *β*-oxidation or *de novo* fatty acid biosynthesis pathways (Chardron *et al.*, 2010; Zinn *et al.*, 2001). Figure 2.2 shows the structure of the mcl-PHA with various types of monomers.

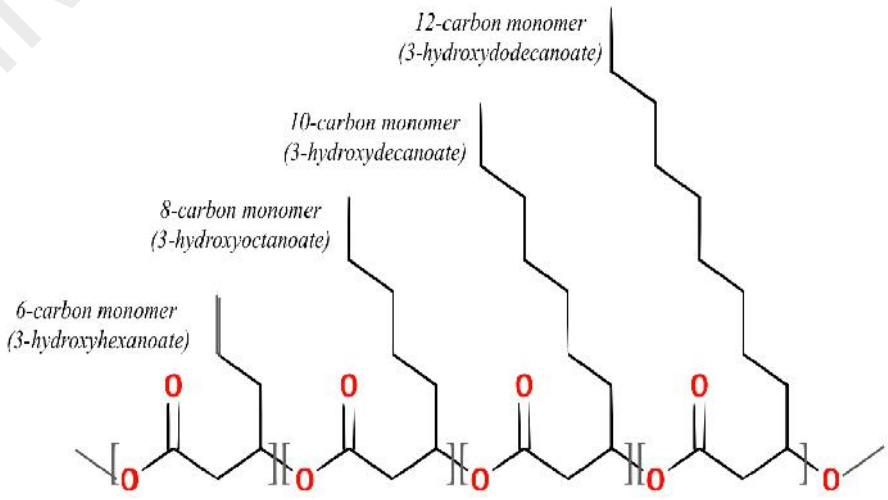

Figure 2.2: Medium-chain-length PHA with different types of monomers

2.2 Biosynthetic pathway of PHA

The properties of microbial polymers produced can be regulated by manipulating the compositions of the copolymers (Doi, 1990). Accordingly, various kinds of copolymers can be expected when a bacterial culture is grown on mixtures of different precursors (Sudesh *et al.*, 2000). Different types of PHA are made from different monomers. The main reason for the possible formation of these diverse types of PHA is due to the extraordinarily broad substrate specificity of PHA synthases (the biological catalyst that polymerizes PHA in the bacterial cell) as well as the effects of carbon source identities fed to the microorganisms, and the metabolic pathways that are active in the cell (Kim *et al.*, 2007; Steinbüchel & Lütke-Eversloh, 2003; Verlinden *et al.*, 2007)

In the bacterial cell, carbon substrates are metabolized by many different pathways. The three most studied metabolic pathways are shown in Figure 2.3. Sugars such as glucose and fructose are mostly processed *via* pathway I, yielding P(3HB) homopolymer (Aldor & Keasling, 2003; Steinbüchel & Lütke-Eversloh, 2003). The biosynthetic pathway of P(3HB) consists of three enzymatic reactions catalyzed by three different enzymes. The first reaction consists of the condensation of two acetyl coenzyme A (acetyl-CoA) molecules into acetoacetyl-CoA by the enzyme *β*-ketothiolase (encoded by *pha*A gene). The second reaction is the reduction of acetoacetyl-CoA to (R)-3-hydroxybutyryl-CoA by acetoacetyl-CoA reductase (encoded by *pha*B gene). Lastly, the (R)-3-hydroxybutyryl-CoA monomers are polymerized into P(3HB) by P(3HB) polymerase, encoded by *pha*C (Reddy *et al.*, 2003; Steinbüchel & Lütke-Eversloh, 2003; Verlinden *et al.*, 2007).

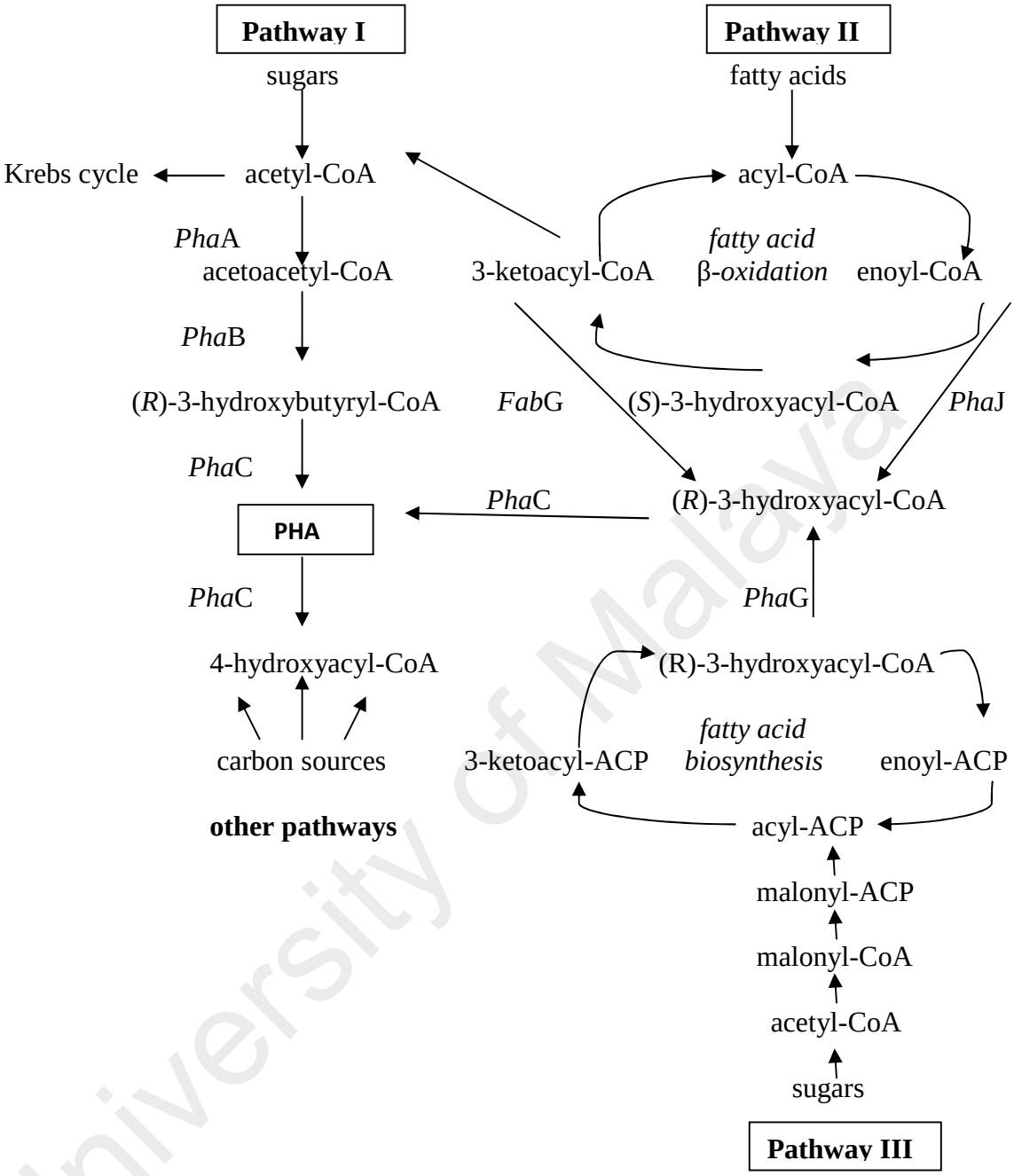

Figure 2.3: Metabolic pathways that supply various hydroxyalkanoate (HA) monomers for PHA biosynthesis. *Pha*A, 3-Ketothiolase; *Pha*B, NADPH-dependent acetoacetyl-CoA reductase; *Pha*C, PHA synthase; *Pha*G, 3-hydroxyacyl-ACP-CoA transferase; *Pha*J, (R)-specific enoyl-CoA hydratase; *Fab*G, 3-ketoacyl-ACP reductase (Tsuge, 2002; Verlinden *et al.*, 2007).

Pathways II and III involved in fatty acid metabolism to generate different HA monomers based on the different carbon sources utilized in PHA biosynthesis (Tsuge, 2002). Intermediates generated from the fatty acid *β*-oxidation pathway are usually inter-related with mcl-PHA biosynthesis in a strain of producer. The carbon sources used includes alkanes, alkenes and alkanoates. The monomers incorporated depend on the carbon sources used. The *β*-oxidation intermediate, trans-2-enoyl-CoA is converted to *(R)*-hydroxyacyl-CoA by a *(R)*-specific enoyl-CoA hydratase (Aldor & Keasling, 2003; Steinbüchel & Lütke-Eversloh, 2003).

The intermediates for the biosynthesis are obtained from the fatty acid biosynthetic pathway. These pathways are significant of interest because they help generate monomers for PHA synthesis from structurally unrelated, simple and inexpensive carbon sources such as glucose, sucrose and fructose. The *(R)*-3-hydroxyacyl-ACP (acyl carrier protein) intermediates from the fatty acid biosynthetic pathway are converted to the *(R)*-3-hydroxyacyl-CoA by the enzyme acyl-ACP-CoA transacylase (encoded by *pha*G gene). This enzyme plays a key role in linking fatty acid synthesis and PHA biosynthesis (Verlinden *et al.*, 2007).

The *β*-oxidation intermediate, trans-2-enoyl-CoA is converted to *(R)*-3-hydroxyacyl-CoA by *(R)*-specific enoyl-CoA hydratase (encoded by *Pha*J gene). Several other enzymes have been found to possess the ability to supply the monomers. The 3-ketoacyl-ACP reductase (encoded by *Fab*G gene) is a constituent of the fatty acid biosynthesis pathway. It has been demonstrated that the product of *Fab*G could accept not only acyl-ACP but also acyl-CoA as a substrate and is capable of supplying mcl-(R)-3HA-CoA from fatty acid β-oxidation in *E. coli* (Tsuge, 2002).

2.3 Biosynthesis of PHA

The choice of operation strategy for the production of bacterial PHA depends on various factors including carbon source, culture condition, modes of fermentation (batch, fed-batch, continuous), bioreactor type (air-lift reactor, continuous stirred tank reactor (CSTR) or sequencing batch system (SBR)) (Amache *et al.*, 2013; Annuar *et al.*, 2008). The carbon source fed to the bacterial culture may include alkanes, alkenes, alcohol and carbohydrate instead of fatty acid, and they affect the polymer structure, quantity and quality (Bassas-Galià *et al.*, 2015). Several mcl-PHA production strategies in the bioreactor such as batch and continuous (Jung *et al.*, 2001), fed-batch (Jiang *et al.*, 2013; Poblete-Castro *et al.*, 2014) and high-cell-density process (Le Meur *et al.*, 2012) under various cultivation conditions have been studied. The imbalance of nutrient provisions, such as oxygen, nitrogen, phosphorus, sulphur and magnesium forced the bacteria to accumulate excess carbon intake by polymerization into PHA within the cells as carbon assimilation for energy reservoir. Thus, the physiological condition can be regulated in the fermentation process in order to achieve high PHA yields and PHA productivity (Annuar *et al.*, 2006).

Furthermore, batch fermentation for PHA production is a common process due to its flexibility, low operation cost and suitable for growth studies and screening of potential PHA accumulating organisms. However, it is associated with low PHA productivity since after utilization of the carbon source, bacterial cells degrade the accumulated PHA resulting in reduced PHA content (Amache *et al.*, 2013). Basically, the fed-batch culture is a batch culture that is continuously supplemented with selected nutrients after it enters the late exponential phase. Fed-batch fermentation yields higher PHA productivity but the overall PHA production is still considered low, when nitrogen is the limiting nutrient. Thus, batch and fed-batch processes are combined in order to obtain higher PHA content. The combined process is the most common fermentation

strategy used for PHA production. In this strategy, the process is divided into two stages: in the first stage the microorganism is grown under batch mode until the desired biomass is achieved and PHA accumulation has started. In the second stage the fermentation is shifted to fed-batch, where usually one or more essential nutrients (most common is nitrogen) are maintained in limited concentration and carbon source is continuously fed into the reactor to further produce and accumulate PHA in the cells (Zinn *et al.*, 2001).

In addition, the removal of cellular endotoxin from Gram-negative bacteria is needed for further application especially in biomedical field. Solvent extraction has undoubted advantages over the other extraction methods of PHA in terms of efficiency. This method is also able to remove bacterial endotoxin and causes negligible degradation to the polymers (Chen & Wu, 2005; Wang *et al.*, 2005; Baei & Rezvani, 2011). Most methods to recover intracellular PHA involve the use of organic solvents, such as acetone, chloroform, methylene chloride or dichloroethane (Furrer *et al.*, 2007; Verlinden *et al.*, 2007). Lower chain ketone such as acetone is the most prominent solvent especially for the extraction of mcl-PHA. However, the consumption of large quantities of solvent makes the procedure economically and environmentally unattractive (Kunasundari & Sudesh, 2011). For medical applications, the solvent extraction is a good method as it yields high purity PHA (Chen & Wu, 2005).

2.4 Biodegradability and biocompatibility of PHA

PHA has been emerged as potentially useful materials in the biomedical field for different applications due to their unique properties of being biodegradable and biocompatible. *In vivo* implant of PHA have been made possible due to their non-toxic degradation products, biocompatibility, desired surface modifications, wide range of physical and chemical properties, cellular growth support, and attachment without carcinogenic effects. In addition, lower acidity and bioactivity of PHA pose minimal risk compared to other biopolymers such as poly-lactic acid (PLA) and poly-glycolic acid (PGA) (Ali & Jamil, 2016; Chen *et al.*, 2013).

For medical applications, materials must be biocompatible, which means that they cannot cause severe immune reactions when introduced to soft tissues or blood of a host organism. Moreover, PHA also considered as biocompatible material when the material does not elicit immune responses during degradation in the body. Generally, PHA polymers are degraded by the action of non-specific lipases and esterases in nature. This is presumably how PHA implants and other medical devices are degraded at the site of implantation in animals. Degradation of PHA matrices in the tissues of the host organism offers the possibility of coupling this occurrence with the release of bioactive compounds, such as antibiotic or anti-tumor drug. Kabilan *et al.* (2012) reviewed the strategies adapted to make functional polymer from mcl-PHA to be utilized as drug delivery system. When PHA is impregnated with a compound, the degradation over time will release the compound, consequently acting as an automatic dosing agent. The kinetics of dosing of a compound from PHA matrix can be fine-tuned by altering the polymer properties, including using different types of PHA with different monomer side chains (Brigham & Sinskey, 2012).

2.5 Modification of PHA

PHA is emerging as a sought-after class of biodegradable polymers for applications in tissue engineering. Over the years, efforts have been made to extend the functionalities of PHA and to investigate their uses in numerous biomedical applications, such as sutures, cardiovascular patches, wound dressings, guided tissue repair/regeneration devices, and tissue engineering scaffolds (Misra *et al.*, 2006). PHA is a promising material for tissue engineering and drug delivery system owing to its properties of being natural, renewable, biodegradable and biocompatible thermoplastics (Hazer, 2010). However, several limitations constrained its competition with traditional synthetic plastics or its applications as ideal biomaterials. These include their poor mechanical properties, high production cost, limited functionalities, incompatibility with conventional thermal processing techniques and susceptibility to thermal degradation (Li & Loh, 2015; Rai *et al.*, 2011). Thus, PHA needs to be modified to ensure improved performance in specific applications. Furthermore, in order for mcl-PHA to serve as the material of choice in the biomedical field, their hydrophilicity must be tailored to the requirements of a particular application. Therefore, attempts to modify the properties of mcl-PHA by chemical and physical methods, such as blending, crosslinking (curing) and graft copolymerization, have attracted a great deal of interest (Kim *et al.*, 2007). Blending is the physical mixture of two or more polymers to obtain the desired properties (Figure 2.4). Grafting is a method where monomers are covalently bonded onto the polymer chain, whereas in crosslinking (curing), the polymerization of an oligomer mixture forms a coating which adheres to the substrate by physical forces (Bhattacharya & Misra, 2004).

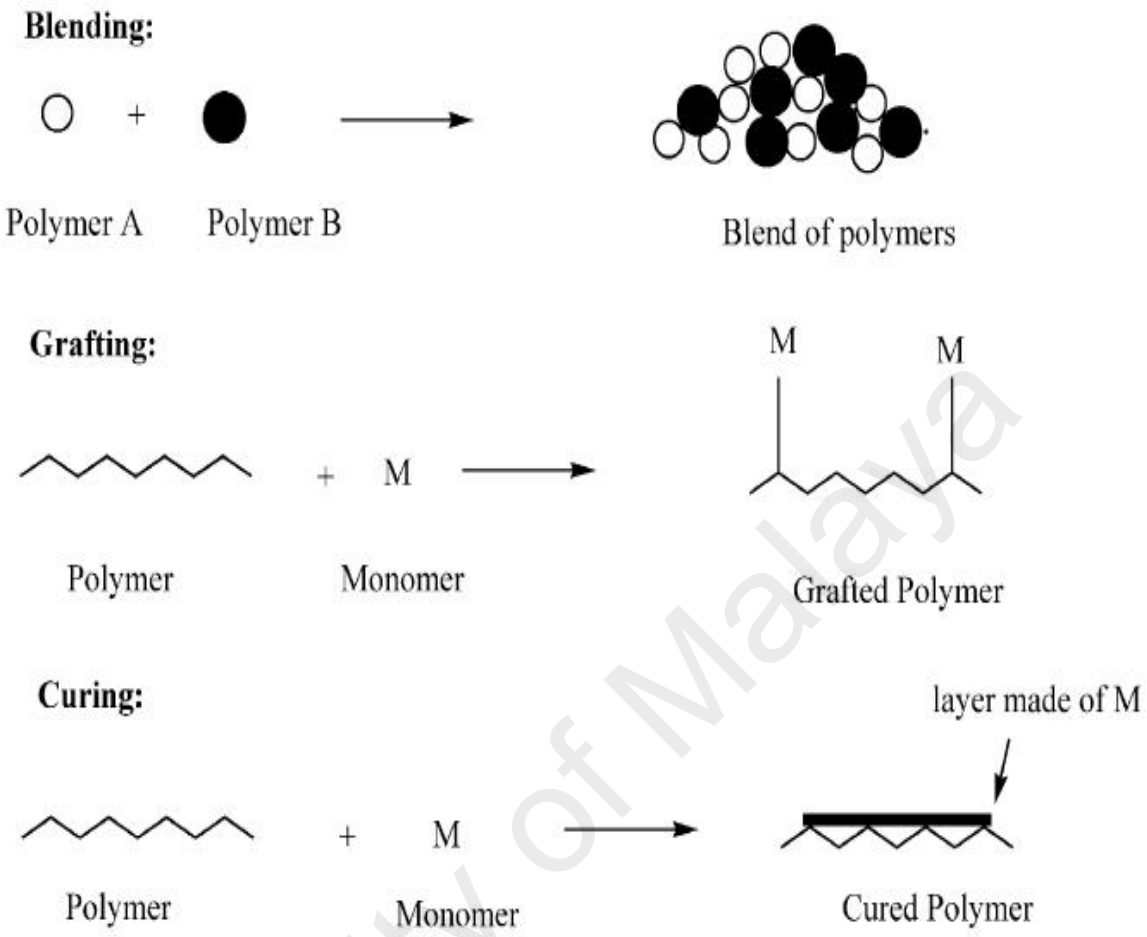

Figure 2.4: Schematic representation of the methods of polymer modification. [adapted from Bhattacharya and Misra (2004)].

Generally, polymers from PHA family are not osteoconductive, thus they are generally overlooked for bone tissue engineering application. One of the major limitations is the inability of PHA to form strong interfacial bonding with the surrounding bone tissue by means of forming biologically active apatite layer on the implant surface (Misra *et al.*, 2006). Therefore, one of the approaches to overcome this lack of osteoconductivity and mechanical competence is by combining mcl-PHA with inorganic bioactive particles or fibres. Incorporation of inorganic phases may lead to mcl-PHA composites with different mechanical properties suitable for tissue engineering application. Extensive research is being carried out on the development of bioactive and biodegradable composite materials in the form of dense and porous system, where the bioactive inorganic phase incorporated as either filler or coating (or both) into the biodegradable polymer matrix (Misra *et al.*, 2006; Rai *et al.*, 2011).

With respect to the development of PHA, researchers have looked into the possibility of designing composites in combination with inorganic phases to further improve the mechanical properties, rate of degradation, and also impart bioactivity. Poly(3-hydroxybutyrate), poly(3-hydroxybutyrate-*co*-3-hydroxyvalerate), and poly(3-hydroxybutyrate-*co*-3-hydroxyhexanoate) are some of the polymers that have been extensively studied to fabricate composites in combination with hydroxyapatite, bioactive glass, and glass-ceramic fillers or coatings (Misra *et al.*, 2006) (Table 2.1). In order to improve the properties, PHA is also blended with natural raw materials or other biodegradable polymers, including starch, cellulose derivatives, lignin, poly(lactic acid), polycaprolactone and different PHA-type blends (Li *et al.*, 2016) .

Bioceramics are inorganic materials specially developed for use as medical and dental implants such as alumina and zirconia, bioactive glasses, glass-ceramics, hydroxyapatite, and resorbable calcium phosphates (Misra *et al.*, 2006). So far, only

Table 2.1: Biomedical applications of PHA and PHA/inorganic phase composites

Applications	**Material**	**References**
Patches		
Gastrointestinal	Poly(3HB)	(Freier *et al.*, 2002)
Right vertical, pulmonary artery	Poly(3HB)	(Malm *et al.*, 1994)
Nutritional/ Therapeutic applications	Poly(4HB) Poly(3HB)	(Löbler *et al.*, 2011)
Orthopedic		
Femur	poly(3HB-*co*-3HV)/hydroxyapatite	(Knowles *et al.*, 1992)
Bone analogue material	poly(3HB)/hydroxyapatite	(Doyle *et al.*, 1991)
	poly(3HB)/hydroxyapatite	(Shishatskaya *et al.*, 2006)
Cortico-cancelous bone graft	poly(3HB-*co*-3HV)/hydroxyapatite	(Boeree *et al.*, 1993)
Bone reconstruction	poly(3HB-*co*-3HV)/hydroxyapatite	(Wang *et al.*, 2004)
	poly(3HB-*co*-3HHX)/hydroxyapatite	(Wang *et al.*, 2005)
Tissue scaffolds		
Muscle	poly(3HB)/bioactive glass	(Misra *et al.*, 2007)
Bone cell proliferation	poly(3HB-co-3HHX)	(Tesema *et al.*, 2004)
Cartilage generation	poly(3HB-*co*-3HV)	(Köse *et al.*, 2003)
Bone tissue regeneration	blend of P(3HB-co-3HHX)/Poly(3HB)	(Zhao *et al.*, 2003)
	poly(3HB-*co*-3HHX)	(Kai *et al.*, 2003), Wang *et al.* (2005)

Applications	**Material**	**References**
Drug release Tetracycline Sulperazone, Gentamicin	poly(3HB-*co*-3HV) poly(3HB-*co*-3HV) poly(3HB-*co*-3HV)/wollastonite	(Panith *et al.*, 2016) (Gursel *et al.*, 2002) (Li & Chang, 2005)
Suture	poly(3HB-*co*-3HV) poly(3HB-co-4HB)	(Shishatskaya *et al.*, 2004) (Chen *et al*., 2010)
Conduits	poly(3HB-*co*-3HV)	(Mosahebi *et al.*, 2002)
Nerve regeneration	Poly(3HB-*co*-3HHX) poly(3HB-*co*-3HV) poly(3HB)	(Bian *et al.*, 2009) (Mosahebi *et al.*, 2002) (Novikov *et al.*, 2002)
Wound healing	poly(3HB-*co*-3HV) poly(4HB)/hyaluronic acid	(Leenstra *et al.*, 1998) (Peschel *et al.*, 2008)
Cardiovascular applications	Poly(4HB) PHO	(Martin & Williams, 2003) (Sodian *et al.*, 2000)

hydroxyapatite, wollastonite and bioactive glasses have been extensively studied in combination with PHA to form composites (Rai *et al.*, 2011). The mechanical and biological performances of bioactive ceramic/polymer composites can be controlled using different particulate bioceramics and also by varying the amount of bioceramic particles in the composite (Boccaccini & Blaker, 2005). Hydroxyapatite is the major mineral component of bone, and it is one of the most common biomaterials studied in bone tissue engineering (Xi *et al.*, 2008). The thermodynamic stability of hydroxyapatite at physiological pH and its ability to actively take part in bone bonding by forming strong chemical bonds with surrounding bone make it a suitable bioactive ceramic for preparing composites (Kokubo *et al.*, 2003).

2.6 Modification of PHA *via* physical blending

2.6.1 PHA/hydroxyapatite blending as an osteoconductive scaffold

Mcl-PHA are structurally more diverse than scl-PHA such as PHB, and this imparts a wider and crucial flexibility in determining the physical and mechanical properties of mcl-PHA in order to meet the requirements of engineered tissue (Muhr *et al.*, 2013; Rezwan *et al.*, 2006; Zinn *et al.*, 2001). Concomitantly, mcl-PHA such as poly(3-hydoxyoctanoate), poly(3-hydroxyhexanoate), copolymers like poly(3-hydroxybutyrate-*co*-3-hydroxyhexanoate), poly(3-hydroxyoctanoate-*co*-3-hydroxyhexanoate) is being increasingly studied to develop osteosynthetic materials, surgical sutures, stents, scaffolds for tissue engineering and matrices for drug delivery (Chen & Wu, 2005). Nevertheless, extensive studies on mcl-PHA in general remain limited because of inavailability of these polymers in testing quantities (Rai *et al.*, 2011).

Synthetic and natural hydroxyapatites (HA) ($HCa_5O_{13}P_3$) have similar chemical composition and crystallographic properties to a human bone (Xi *et al.*, 2008). Their biocompatibility and osteoconductive behavior are suitable for making bone implants. Studies have shown that incorporation of HA into biomaterials could help to enhance mechanical performance and osteoblast responses (Baei & Rezvani, 2011; Wang *et al.*, 2005). Currently, composites of polymers and ceramics are being developed with the aim to increase the mechanical scaffold stability and to improve tissue interactions. In addition, efforts have also been invested in developing scaffolds with drug-delivery capacity. These scaffolds allow for local release of growth factors or antibiotics and enhance bone in-growth to treat bone defects and even support wound healing (Rezwan *et al.*, 2006).

Polymer-based composite scaffold showed great potential in bone tissue engineering. Efforts have been made to form porous PHB/HA and PHBV/HA composites for bone tissue repair by utilizing the osteoconductivity property of HA (Baek *et al.*, 2012; Saadat *et al.*, 2013; Sultana & Khan, 2012; Sultana & Wang, 2008). For instance, particulate hydroxyapatite (HA) incorporated into poly(3-hydroxybutyrate) (PHB) formed a bioactive and biodegradable composite for applications in hard tissue replacement and regeneration (Saadat *et al.*, 2013). Wang *et al.* (2005) reported that the presence of hydroxyapatite increased the growth of osteoblast and cell proliferation compared to neat P(3HB). Studies by them have shown that the presence of hydroxyapatite particles on the surface helps the formation of tenacious bonds with osteoblast cells. Moreover, the presence of hydroxyapatite in P(3HB) matrices helped to increase the strength of the composite along with its bioactivities. Ni and Wang (2002) demonstrated the formation of apatite crystals on the surface of their P(3HB) composite containing hydroxyapatite after 1-3 days of immersion in simulated body fluid (SBF), which is an acellular fluid designed with a

composition equivalent to blood plasma. They showed that the quantity of the apatite crystals formed is directly proportional to the amount of hydroxyapatite used in the composite. The storage modulus of P(3HB)/HA composites was found to increase with increasing percentage of hydroxyapatite.

Jack *et al.* (2009) fabricated PHBV/HA composite scaffolds with high porosity and controlled pore architectures. They found that incorporation of HA nanoparticles increased the stiffness and strength, thus improved the *in vitro* bioactivities of the scaffolds. Baek *et al.* (2012) incorporated collagen into PHBV/HA scaffold fabricated using a hot-press machine and salt leaching method. Their results showed that the PHBV/HA/Col composite scaffolds allowed for better cell adhesion and significantly higher proliferation and differentiation than the PHBV/HA composite scaffolds and the PHBV scaffolds. An ideal biocompatible material should be non-toxic and should not act as immunostimulant at molecular level (Shabna *et al.*, 2013). Furthermore, various PHA blends have been developed to improve the performance of scaffold for bone defect repairs or bone tissue engineering. Several studies on bone tissue engineering have been conducted using PHA/HA such as poly(3-hydroxybutyrate), poly(3-hydroxybutyrate-*co*-3-hydroxyvalerate) and poly(3- hydroxybutyrate-*co*-3-hydroxyhexanoate) (Saadat *et al.*, 2013; Sultana & Khan, 2012; Xi *et al.*, 2008). To date, there are still limited studies on mcl-PHA as a composite scaffold for bone tissue engineering.

Scaffolds should exhibit high porosity, high interconnectivity and proper pore sizes in order to facilitate cell adhesion, tissue in-growth and mass transfer. The appropriate pore characteristics of scaffolds are vital in tissue engineering particularly during the late stage of implantation when cells need to migrate deep into the scaffold (Sultana & Wang, 2008). The scaffold should positively interact with cells, enhance cell adhesion, growth, migration and differentiated function. The basic challenges to the

material selection and scaffold design are to achieve the initial strength and stiffness. For instance, the material for the scaffold must have sufficient inter-atomic and inter-molecular bonding or physical and chemical structures that allow for hydrolytic attachment and breakdown. In addition, porosity and proper pore size are important design parameters for the scaffold design, and high surface area necessary for mechanical stability (Sabir *et al.*, 2009).

Pores are necessary for bone tissue formation because they allow migration and proliferation of osteoblasts and mesenchymal cells as well as vascularization. In addition, a porous surface improves mechanical interlocking between the implant biomaterial and the surrounding natural bone thus providing for greater mechanical stability at this critical interface (Wei & Ma, 2004). Porosity of scaffolds for tissue engineering should be high enough to provide sufficient space for cell adhesion (Chen *et al.*, 2002). The most common techniques applied to create porosity in a biomaterial are porogen leaching technique, gas foaming, phase separation, electrospinning, freeze-drying and sintering depending on the material used to fabricate the scaffold (Karageorgiou & Kaplan, 2005). Among these methods, particle leaching method has been identified as a convenient way to fabricate sponge-like scaffold besides being reproducible (Sodian *et al.*, 2000). Moreover, porogen leaching technique also provides easy control of pore structure and has been well established in the preparation of porous scaffolds for tissue engineering. This technique involves the casting of a polymer/porogen composite followed by aqueous washing out of the incorporated porogen. The pore size, porosity and pore morphology can be easily controlled by the properties of porogen (Tan *et al.*, 2011).

2.7 Functionalization of PHA

Microbial polyesters can be further diversified *via* both chemical modification reaction and genetic engineering of the biosynthetic pathways. Chemical modification is a promising approach to obtain new types of PHA-composite materials including a wide range of monomers for graft/block copolymerization with synthetic and other natural polymers that cannot be obtained by biotechnological processes (Hazer & Steinbüchel, 2007). For instance, chemical modification of PHA could involve grafting reactions through graft/block copolymerization, chlorination, cross-linking, epoxidation, hydroxyl and carboxylic acid functionalization (Figure 2.5). Insertion of an additional different polymer segment into an existing polymer backbone or at the side chain of an existing polymer yields block or graft copolymers (Gumel *et al.*, 2014).

Moreover, chemical modification of PHA enables easy and precise modulation of the polymer structure with predictable functionalities (Li *et al.*, 2016). PHA are predominantly hydrophobic and surface modification of the PHA is necessary to improve their hydrophilicity, wettability, and surface charge for biomedical applications (Guzmán *et al.*, 2011). Amphiphilic polymers can be synthesized by introducing hydrophilic groups such as hydroxyl, carboxyl, amine, glycol, and hydrophilic polymers such as PEG, poly(vinyl alcohol), polyacryl amide, poly acrylic acids, hydroxy ethyl methacrylate, poly vinyl pyridine, and poly vinyl pyrrolidone to a hydrophobic moiety. In grafting reactions, some hydrophilic groups have been attached in the PHA chain to obtain amphiphilic polymer (Hazer, 2010). Furthermore, improvement on mechanical and hydrophilic characteristics of the unsaturated microbial polyesters can be performed by using thiol-ene photo click reaction (Hazer, 2015). Generally, the hydroxylation and carboxylation modification reactions of the double bonds of the unsaturated PHA usually lead to dramatic molecular weight decrease. Pendant hydroxyl and carboxyl

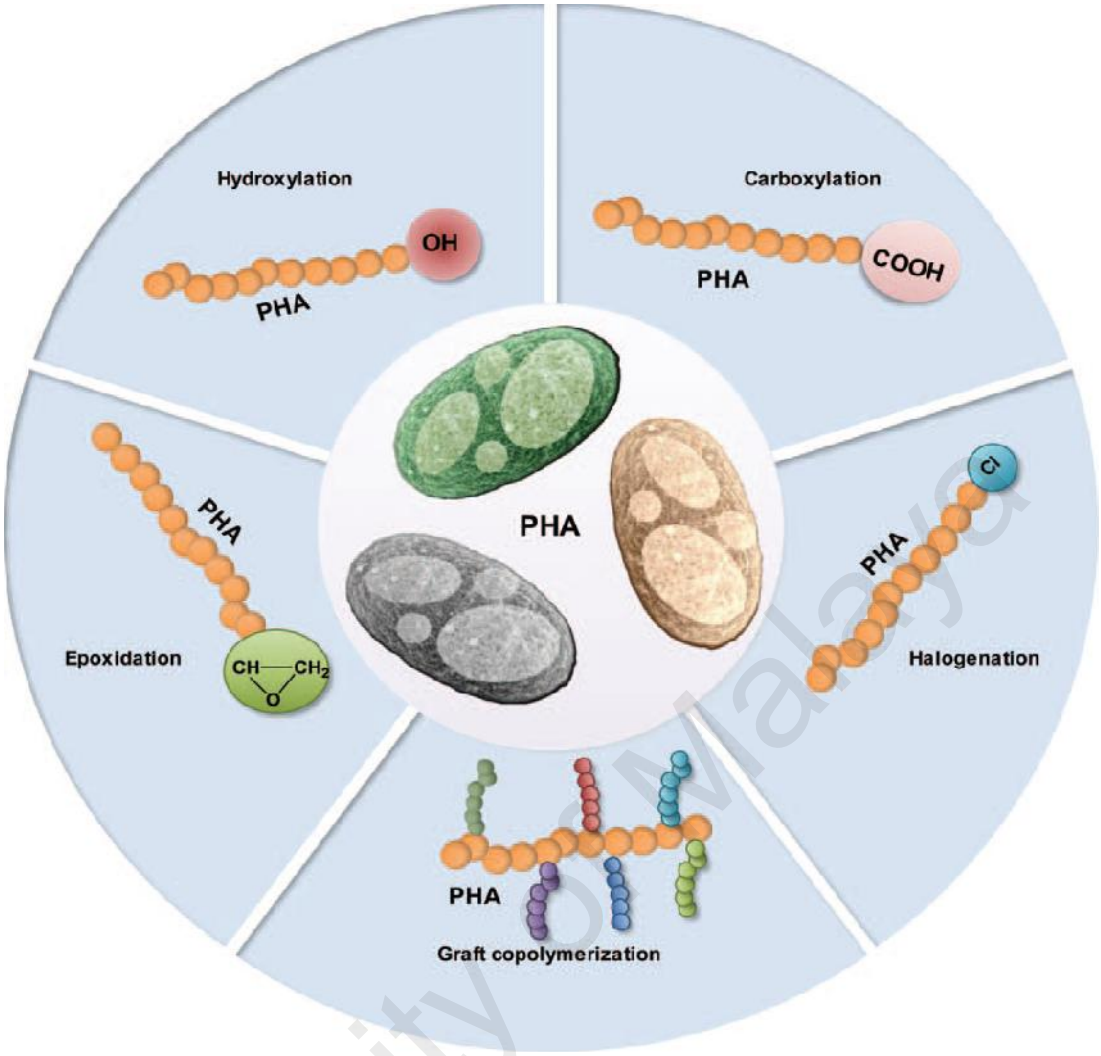

Figure 2.5: Typical methods for the chemical modification of PHA to yield different types of functionalized polymers [adapted from Gumel *et al.* (2014)].

groups are also open for further modification reactions in order to prepare novel modified biodegradable polymers for drug delivery system and industrial applications (Hazer *et al*., 1994).

Whilst mcl-PHA has attracted great interest in research due to its potential wide applicability as biomaterials, its strong hydrophobicity, slow degradation under physiological conditions and lack chemical functionalities hinder the realization of its potentials. These factors restrict the scope of their applications in biomedical field. In order to expand the range of its versatilities, other properties such as mechanical strength, surface features, amphiphilicity and degradation rate have to be modified to match the requirements of specific applications (Kai & Loh, 2013). For example, intrinsic hydrophobic properties of mcl-PHA restrict their applications as cell colonizing materials. Therefore, chemical modification with suitable functional groups or modification of the surface topography of mcl-PHA is needed in order to minimize hydrophobic interactions with the surrounding tissue. Amphiphilic copolymers could be produced through chemical modification reactions by inserting the hydrophilic segments into the hydrophobic PHA (Hazer, 2010).

2.7.1 Graft copolymerization

Graft copolymerization is one of the method to modify PHA, which results in the formation of a modified segmented copolymer with improved properties such as increased wettability and thermo-mechanical strength (Gumel *et al.*, 2014). Several studies on graft copolymerization of mcl-PHA have been conducted in order to modify mcl-PHA properties by chemical and physical methods, such as blending, crosslinking, and graft copolymerization (Hazer & Steinbüchel, 2007; Meng *et al.*, 2014). Among the various methods, graft copolymerization is a versatile technique to introduce functional

groups on a polymer (Chung *et al.*, 2012). Effective chemical modifications include changes in chemical group functionality, surface charge, hydrophilicity, and wettability (Lao *et al.*, 2007). Grafting reaction can be induced by either chemical, radiation or plasma discharge method (Kim *et al.*, 2007; Nguyen, 2008). There are several established ways of grafting, focusing on PHA as the polymer of interest namely "grafting onto", "grafting from" and "grafting through" or macromonomer method (Nguyen, 2008).

"Grafting onto" method involved the covalent coupling of reactive sites distributed along the copolymer main chain with end groups of copolymer segments (Nguyen, 2008). Examples of grafting onto process include amidation or condensation reaction between carboxylic group of PHO, PHBV and linoleic acid with amine groups of chitosan (Arslan *et al.*, 2007a), esterification of PHB and PHBV treated by ozone treatment with acylic acids (Hu *et al.*, 2003) and also free radical reaction of polystyrene consisting active peroxide group reaction with poly(*β*-hydroxynonanoate) (Hazer, 1996). "Grafting from" method is another grafting mechanism of having active sites along the main polymer chain, with grafting monomer polymerized from the sites. For instance, the monomer can be copolymerized using the main polymer chain as macroinitiator with multiple initiation sites along its chain (Nguyen, 2008). Arslan *et al.* (2007b) reported that ''grafting from'' technique led to poly(3-hydroxybutyrate)-*g*-poly(methylmethacrylate) (PHB-*g*-PMMA) brush type graft copolymers following atom transfer radical polymerization of methyl methacrylate, MMA, in the presence of cuprous bromide as catalyst.

Furthermore, "grafting through" or macromonomer method can be achieved by copolymerization of a low molecular weight monomer with a macromonomer, which can be defined as a polymer or oligomer bearing at least one polymerizable end group. This method offers more control on branching formation (Nguyen, 2008). The

macromonomer is selected and prepared prior to copolymerization, whereas the macromonomer arrangement can be homopolymer, random or block copolymer. The size of the side chains is also selected with the length of the macromonomers and their distribution along the main chain is controlled by the comonomer reactivity ratios. Nguyen and Marchessault (2004) studied the synthesis of PMMA-*g*-PHB by copolymerizing PHB macromonomers with methyl methacrylate. PHB macromonomers were prepared from the esterification of oligomers with 2-hydroxyethyl methacrylate at their carboxylic acid end.

Covalent grafting of functional groups is preferred to physical coating (adsorption) in order to achieve a surface chemistry that would remain stable in biological environment. In covalent modification, the presence of functional group facilitates better attachment of bioactive molecules or species onto the surface that leads to a higher surface stability. Moreover, chemically modified surface offer greater biocompatibility towards cell growth and flow of body fluids due to their enhanced wettability (Katti *et al.*, 2008).

2.7.2 Chemical modification of PHA *via* graft copolymerization reaction

PHA-grafted copolymer can also be produced by radical polymerization of monomers/oligomers that contain vinyl or methacrylate groups. Several studies on graft copolymerization of PHA have been conducted by using graft chains of polyethylene glycol (PEG) (Chung *et al.*, 2003), 2-hydroxyethylmethacrylate (HEMA) (Lao *et al.*, 2007), poly(methylmethacrylate) (PMMA) (Ilter *et al.*, 2001), poly(styrene peroxide) (PS-P) (Cakmakli *et al.*, 2001) and poly(*N*-vinylpyrrolodone) (Wang *et al.*, 2007) (Figure 2.6). Chung *et al.* (2003) reported that the presence of PEG chains in the

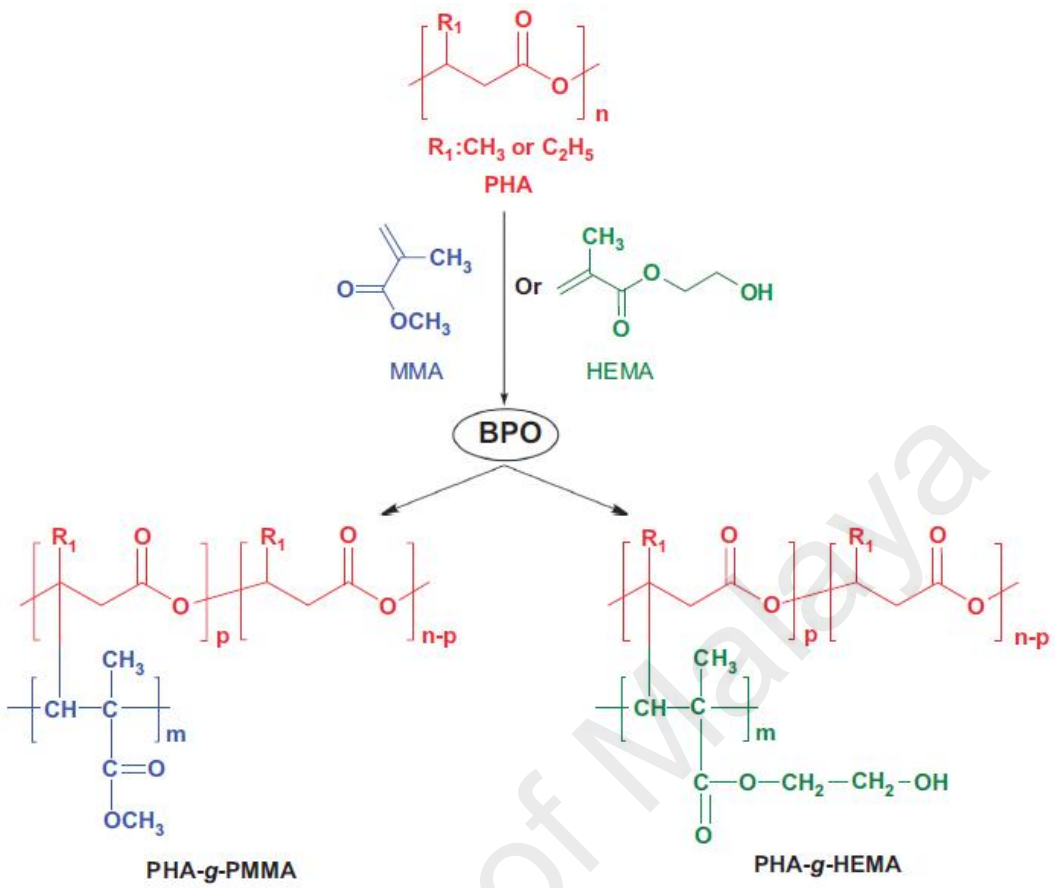

Figure 2.6: Free radical grafting of MMA and HEMA on PHA using benzoyl peroxide (BPO) as an initiator [adapted from Li *et al.* (2016)].

polymer network helped to increase the hydrophilicity of the final product. Their results showed significant concentrations of water within the PHO-*g*-PEG polymers hence resulting in low interfacial tension with blood. Thus, PHO-*g*-PEG polymer network could form an essential component for materials that are employed in blood contacting devices (Li *et al.*, 2016). Similar study was reported by Kim *et al.* (2005b) where the water uptake of the PHO-*g*-PEO copolymer increases up to 30 % in comparison with the water uptake of PHO that is only 2 %. These graft copolymers could potentially be used as blood-contacting devices in a broad range of biomedical applications because of their excellent blood compatibilities. Kim *et al.* (2008) grafted glycerol 1,3-diglycerolate acetate (GDD) onto poly-3-hydroxyoctanoate (PHO) using free radical

polymerization reaction. The surface and bulk of GDD-*g*-PHO copolymers became increasingly hydrophilic as the grafting density increased. *In vitro* studies showed the biocompatibility of Chinese hamster ovary (CHO) cells and adsorption of blood proteins and platelets towards PHO were enhanced by GDD grafting. Ilter *et al.* (2001) studied the graft copolymerization of methyl methacrylate (MMA) onto unsaturated mcl-PHA. They reported that the presence of double bond opens up potential site for functionalization of biopolyester in order to improve its mechanical and viscoelastic properties. For a number of graft copolymers reported, the nature of copolymer and graft copolymer composition affect properties such as thermal stability, mechanical resilience, as well as enzymatic degradability, biodegradability, antibacterial activities and cell compatibility (Nguyen, 2008).

The use of multifunctional monomers in graft copolymerization of polymers is very effective in producing novel copolymers with high thermal stability and mechanical strength (Avci & Mathias, 2004). Glycerol 1,3-diglycerolate diacrylate (GDD) is an excellent example of a multifunctional monomer that could be potentially grafted onto mcl-PHA. It possesses a number of hydroxyl groups useful for enhancing the hydrophilicity of its polymer graft. Furthermore, unreacted pendant hydroxyl groups in grafted polymers provide potential target sites for chemical modifications to further improve the physical properties of the main polymer. For example, GDD-*g*-PHO copolymer is envisaged for a broad range of biomedical applications due to their improved physical properties, and excellent blood and cell compatibilities (Kim *et al.*, 2008). Therefore, development of novel mcl-PHA grafts with improved physico-chemical and biocompatibility properties is needed to extend their range of applications.

2.7.3 Mechanism and kinetic of free radical polymerization

The kinetic of a chemical reaction depends on the mechanism involved in the reaction. It is possible to investigate the mechanism of polymer grafting by considering its kinetics. The mechanism of polymer networks grafting can be classified depending on relative dimensions of the reacting species (ex: polymer/polymer mechanism, polymer/monomer mechanism or monomer/monomer mechanism) or the chemical nature of the intermediate in the reaction (Bhattacharya *et al.*, 2009). The most important intermediates for grafting are free radicals. In polymer/monomer mechanisms, a polymer may be subjected to conditions where the reactive centres are generated on it from which new polymer chains may grow ("grafting from" reaction), or to which new growing polymer chains may be attached ("grafting onto" reaction) (Pham *et al.*, 2000). Radicals can be introduced *via* thermal or chemical decomposition of an initiator, by redox reaction between two species, or by excitation of a photoinitiator. Radical intermediates can also be introduced by exposure of a material to energies sufficient to cleave chemical bonds homolytically, using γ irradiation, photoirradiation, thermal treatment, or an electron beam (Bhattacharya & Misra, 2004; Li *et al.*, 2016).

The mechanism for the graft copolymerization generally consists of three major steps namely initiation, propagation and termination. The mechanism can be described as an addition reaction of radicalized unit to the reactive site to form higher molecular mass polymer. As the reaction proceeds, monomer concentration will decrease, expected to be linked to the polymer backbone (Jenkins & Hudson, 2001). In the chemical process, free radicals are produced from the initiators and transferred to the substrate to react with monomer to form the graft copolymers (Bhattacharya & Misra, 2004).

Initiation is the first reaction of a chain carrier with a polymer or monomer molecule to generate a new covalent bond and regenerate the reactive centre at a new location. This initiation may occur by addition, where the radical adds across a double bond, or by abstraction, where the radical removes a labile atom from a substrate. The thermodynamic driving force of these reactions is the replacement of a high energy π bond by an σ bond (addition) or the replacement of a weaker R−H or R−X bond by a stronger R′−H or R′−X bond (abstraction) (Bhattacharya *et al.*, 2009). In addition, initiation step begin with the radicalization of monomer or polymer substrate by the action of radical initiator such as benzoyl peroxide and eventually generating radicals. Radicalized monomers undergo chain transfer to the backbone of the polymer. Therefore, radical formation is the process to enable the monomer to transfer to the main polymer backbone (Wang *et al.*, 2007).

Propagation is the next step in generating a graft copolymer by a free radical polymer/monomer mechanism. The overall kinetics of free radical polymerization reaction will be dominated by this step (Bhattacharya *et al.*, 2009). Moreover, a particular polymer reactive site grafted with monomer will create propagation of radicalization, thus radicalizing other site of the backbone. This will allow another chain transfer reaction, forming successful graft copolymerization. However, radicalized monomers from the initiation step also have the ability to perform chain transfer among themselves to undergo unintended homopolymerization process (Wang *et al.*, 2007).

Termination occurs by the pairing of two radicals, stopping both the kinetic of chain reaction and physical polymer chain extension. Discontinuation of chain extension in radical polymerization occurs with the pairing of two radicals to form nonradical species. Termination step will come ultimately, resulting in graft copolymer and homopolymer as final product due to recombination process. The occurrence is affected by several factors such as temperature, monomer concentration and initiator

concentration, and consequently determines the grafting yield of the copolymer (Lao *et al.*, 2007; Lao *et al.*, 2010; Lee & Lee, 1997; Wang *et al.*, 2007).

2.8 Mcl-PHA in pharmaceutical and medical applications

2.8.1 Bone tissue engineering

Recently, several bone tissue engineering strategies such as cell transplantation, acellular scaffolds, gene therapy, stem cell therapy, and growth factor delivery have been applied to address the challenging requirements of a suitable biomimetic bone scaffold (Porter *et al.*, 2009). Bone forms the structural framework of the body and is composed of an inorganic mineral phase of hydroxyapatite (60% by weight) and an organic phase, which is mainly type I collagen. Tissue engineering has developed in recent years to overcome the problem of bone loss or defect. Therefore, extensive studies on various materials for scaffold preparation have been conducted in order to meet osteocompatibility demand and mechanical properties which are similar to native bones. Wang *et al.* (2004) studied the *in vitro* biocompatibility of 3D scaffold PLA, P(3HB), and P(3HB-*co*-3HHx) inoculated on rabbit bone marrow cells. Their results showed that the cells on the P(3HB-*co*-3HHx) scaffolds were able to sustain osteoblast phenotypes, high alkaline phosphatase activity (ALP), round cell shape, fibril collagen synthesis and strong calcium deposition. The cells also showed best proliferation on the P(3HB-*co*-3HHx) scaffolds. They found that after incubation for 10 days, the number of cells grown on P(3HB-*co*-3HHx) scaffolds was approximately 40 % higher than on P(3HB) scaffolds, and 60 % higher than on PLA scaffolds. ALP activity of the cells grown on P(3HB-*co*-3HHx) scaffolds increased to about 65 U g^{-1} of the scaffold, 50 % higher than P(3HB) and PLA scaffolds, respectively. From SEM analysis, it was observed that P(3HB-*co*-3HHx) scaffolds had suitable roughness for osteoblast

attachment and proliferation compared to the ones made from P(3HB) and PLA. Thus, P(3HB-*co*-3HHx) was determined as an attractive biomaterial for osteoblast attachment, proliferation and differentiation for bone marrow cells (Hazer *et al.*, 2012).

2.8.2 Drug delivery system

Polymers could play a central role in controlled of drug release systems and fabrication of drug delivery devices. Controlled drug delivery systems deal with releasing therapeutic compounds at a desired rate so that the drug level in the body can be sustained within the therapeutic time frame (Bayram *et al.*, 2008; Nair & Laurencin, 2006). The drug delivery systems are developed for releasing, targeting, uptaking, retaining, activating, bringing and localizing the drugs at the right time, place, dose and period. The drug release kinetics can be controlled *via* manipulating the PHA matrix parameters to reach desired degradation rates (Hazer *et al.*, 2012). Scl-PHA are primarily degraded by surface erosion that makes them an attractive candidate to be applied as drug carriers. However, since scl-PHA are crystalline and hydrophobic, many pores are formed on the surface. It results in too rapid release of drugs without significant polymer degradation. On the other hand, mcl-PHA copolymers have low melting point and low crystallinity, therefore they are more suitable for drug delivery applications (Rai *et al.*, 2011).

Drug delivery systems can be prepared in different shapes and attributes such as gels, films, microcapsules, microspheres, nanoparticles, porous matrices, polymeric micelles and polymer-linked drugs. The physical interactions are generally preferred in order to bind the drug to the polymer since it will not damage the molecular structure of the drug (Hazer *et al.*, 2012; Kabilan *et al.*, 2012). Drugs can be entrapped or microencapsulated in a PHA homopolymer or copolymer. Microsphere or microcapsule-based delivery systems have been extensively used for the delivery of a

number of drugs such as anesthetics, antibiotics, anti-inflammatory agents, anticancer agents, hormones, steroids, and vaccines. In addition, the introduction of such a delivery system at the target location also results in site-specific drug delivery (Shrivastav *et al.*, 2013). The biocompatible and biodegradable properties of PHA serve as a real advantage to provide excellent matrix for controlled drug delivery (Kabilan *et al.*, 2012; Pouton & Akhtar, 1996).

Kim *et al.* (2005a) synthesized monoacrylate-poly(ethylene glycol)-grafted poly(3-hydroxyoctanoate) (PEGMA-*g*-PHO) copolymer to develop a swelling controlled release delivery system for ibuprofen as a model drug. Their results showed hydrolytic degradation of the copolymer was strongly dependent on the degree of grafting of the PEGMA group. The *in vitro* degradation rate of the copolymer films increased with higher degree of grafting of PEGMA group on the P(3HO) chain. The copolymer films showed a controlled delivery of ibuprofen to the medium in certain periods of time depending on the composition, hydrophilic/hydrophobic characteristics, initial drug loading amount and film thickness of the graft copolymer support. The research showed that a combination of low degree grafting of PEGMA group in the P(3HO) chains and low ibuprofen solubility in water led to a long-term constant release from these matrices *in vitro*.

2.8.3 Cardiovascular system

PHA has been widely used in the cardiovascular area such as artery augments, cardiologic stents, vascular grafts, heart valves, pericardial patches, implants, dressing tablets and microparticulate carriers (Philip *et al.*, 2007). Vascular grafting is a frequently used technique in cardiovascular pathologies. The ideal cardiovascular patch material should have resistance to degradation and infection, in addition to long durability, amendable to various size tailoring to suit cardiac and peripheral vascular reconstructions, lack of immunogenicity and non-toxic (Hazer *et al.*, 2012).

Tissue-engineered heart valves may have the potential to overcome shortcomings of prosthetic valves and homograft valves that are currently being used in valve replacements. Many studies have been carried out using several synthetic absorbable polyesters such as PGA, PLA and scl-PHA *viz*. P(3HB), as potential scaffolding materials for heart valves. However, these materials are too stiff to function as flexible leaflets inside a trileaflet valve and therefore the relatively elastomeric PHA is considered to be more promising (Rai *et al.*, 2011). One of the early studies using an elastomeric P(3HO) for the fabrication of a trileaflet heart valve scaffold was carried out by Sodian *et al.* (2000). Vascular cells were harvested from ovine carotid arteries, expanded *in vitro* and seeded onto the heart valve scaffold. They reported that when the artificial trileaflet scaffold was incorporated in the animal model, all test subjects survived the procedure and the valves showed minimal regurgitation (Sodian *et al.*, 2000).

Biotechnology start-up such as Tepha Inc., based in Cambridge, MA, has been devoted to manufacturing pericardial patches, artery augments, cardiological stents, vascular grafts, heart valves, implants and tablets, sutures, dressings, dusting powders, prodrugs and microparticulate carriers using PHA (Philip *et al.*, 2007). The first PHA-

based product approved by the United States Food and Drug Administration (FDA) for clinical application is the TephaFLEX® absorbable suture prepared from P(4HB). The most remarkable property of P(4HB) is its very high elasticity that benchmarks closely to ultrahigh molecular weight polyethylene which can be stretched 10 times than its original length before breaking (Martin & Williams, 2003). In 2007, the FDA had cleared its marketing in the US, indicating a bright future for PHA practical applications in the biomedical field (Wu *et al*., 2009).

CHAPTER 3

MATERIALS AND METHODS

3.1 Materials

3.1.1 Microorganism

The bacterial species used in the studies is a Gram-negative *Pseudomonas putida* BET001 able to biosynthesize medium-chain-length polyhydroxyalkanoates (mcl-PHA). The microorganism was obtained from Bioprocess and Enzyme Technology Laboratory, Institute of Biological Science, Faculty of Science, University of Malaya. It was isolated from a palm oil mill effluent (POME) (Gumel *et al*., 2012).

3.1.2 Media

Two types of media were used for growth and PHA accumulation by *P. putida* BET001. Nutrient rich (NR) was used for growing cell biomass and E2 mineral medium was used for PHA accumulation by the microorganism (Gumel *et al*., 2012). Compositions of NR (Table 3.1) and E2 media (Table 3.2) are as follows:

Table 3.1: Nutrient rich medium (NR)

Ingredients	Mass (g) in 1.0 L distilled water
Yeast extract	10.0
Nutrient broth	15.0
Ammonium sulphate	5.0

Table 3.2: E2 medium

Ingredients	Mass (g) in 1.0 L distilled water
$NaNH_4HPO_4.H_2O$	3.5
K_2HPO_4	5.7
KH_2PO_4	3.7
Mineral solutions	**Volume (mL) in 1.0 L distilled water**
$MgSO_4.7H_2O$ (0.1 M)	10.0
Trace elements (MT)	1.0

The trace elements (MT) were dissolved in 1.0 L of 1 M HCl and its composition is shown below:

Table 3.3: MT solution

Ingredients	Mass (g) in 1.0 L of 1 M HCl
$CaCl_2.2H_2O$	1.5
$CoSO_4.7H_2O$	2.4
$CuCl_2.2H_2O$	0.2
$FeSO_4.7H_2O$	2.8
$MnCl_2.4H_2O$	2.0
$ZnSO_4.7H_2O$	0.3

3.1.3 Shaker incubator set-up

Shake-flask fermentation was carried out in an orbital shaker incubator (HOTECH, Model 721, Taiwan). The incubation temperature and agitation speed for the incubator were set at 30 °C and 200 rpm, respectively, throughout the experiments.

3.1.4 Stirred tank bioreactor set-up

The fed-batch fermentation for mcl-PHA production was performed in a 2-L stirred fermenter (Biostat®A, Sartorius, Germany), a culture vessel made of borosilicate glass equipped with a cooling finger for temperature regulation. The pH, temperature and partial pressure of oxygen (pO_2) of the culture media were measured and regulated by a digital system. All the reservoir bottles that contained the carbon substrate (octanoic acid), ammonium solution, antifoam, acid and base solutions were connected to the bioreactor with autoclavable peroxide-cured silicone tubings. Before autoclaving, all the tubes and filters were clamped except the exhaust line filter. The filters were wrapped with non-absorbent wool and aluminium foil to prevent water vapor from entering into the filters. The temperature sensor, pH probe (Mettler-Toledo) and pO_2 probe (Mettler-Toledo) were checked and calibrated prior to the experiments. The pH probe and temperature sensor were connected to the bioreactor and calibration of pH probe was carried out using pH 4 and 7 buffer solutions at 25 °C before autoclaving. After the glass vessel setup was autoclaved at 121 °C and 103 kPa for 15 min and allowed to cool down to room temperature, the pO_2 electrode was connected to the digital system to polarize the pO_2 probe for at least 6 hours. Upon polarization, the pO_2 probe was calibrated using industrial grade nitrogen gas followed by industrial grade oxygen gas. Cool circulating water was allowed to pass through the cooling finger to help regulate the temperature. The stirrer motor was fitted to the bioreactor and the pH and temperature of the medium was set at pH 7 and 30 °C, respectively. Agitation of the liquid culture was achieved using a single impeller (six-bladed Rushton turbine) placed directly above the ring-shaped gas sparger. Aeration of the culture was provided by pressurized filtered air supplied at 0.5 vvm. The impeller speed was set at 600 rpm throughout the fermentation (Annuar, 2004; Chan, 2012). The setup of the bioreactor for fed-batch fermentation is shown in Figure 3.1.

Figure 3.1: Setup of a 2-L stirred tank bioreactor for fed-batch fermentation

3.1.5 Sterilizer

Sterilization was carried out at 121 °C and 103 kPa for 15 minutes using Tomy SX-500 autoclave (Japan).

3.1.6 Centrifugation

Centrifugation was carried out using Thermo-Line MLX-210 mini centrifuge (China), Hettich Zentrifugen EBA 20S bench-top centrifuge and Thermo Scientific Sorvall RC-5C Plus ultracentrifuge (USA) for liquid volumes of 1.0, 10.0 and 50.0 mL, respectively. The revolution speed and temperature of the ultracentrifuge machine were fixed at 3,578 × *g* and 4 °C respectively.

3.1.7 Vacuum evaporation

Rotary evaporator model RE300 from Yamato Scientific Co., Ltd. (Japan) was used to carry out evaporation of volatile liquid samples.

3.1.8 Spectrophotometer

Spectrophotometric analysis was performed using Jasco V-630 spectrophotometer equipped with temperature controller (Model EHC-716 Japan).

3.2 Method

3.2.1 Maintenance of culture stock

P. putida BET001 was maintained on nutrient rich (NR) agar slant and stored at 4 °C. Weekly sub-culture was made on NR agar plate to check for viability and contamination. For long term maintenance, 40 % glycerol stock was added into the agar slant in the ratio of 1:1 and then kept at -20 °C.

3.2.2 Media preparation

Nutrient rich (NR) medium was prepared by mixing the components as listed in Table 3.1 in 1.0 L distilled water. Then, medium was autoclaved at 121 ºC and 103 kPa for 15 minutes.

The E2 medium was prepared by dissolving ammonium and phosphate salts in 1.0 L distilled water followed by autoclaving at 121 ºC and 103 kPa for 15 minutes. $MgSO_4.7H_2O$, carbon source and trace elements (MT) were autoclaved separately. Aforementioned step was taken to avoid the possible precipitation of salt ingredients due to the high heat and pressure during autoclaving. The initial pH of the medium was 7.0 ± 0.2.

3.2.3 Estimation of total biomass

The total biomass (residual biomass and PHA) was determined by gravimetry method. During sampling, 1.0 mL of the culture was pipetted into Eppendorf microfuge tube. The cells were spun down at 3,578 $\times g$ for 5 minutes. The supernatant was decanted and the pellet was washed twice with saline solution (0.9 % w/v). After that, the tubes were dried inside an oven at 65 °C until constant weight.

The total biomass was also determined using spectrophotometer. 1.0 mL culture was centrifuged and washed as described above. Then the cell pellet was diluted with saline solution and the optical density of the cells was read at 600 nm ($OD_{600\ nm}$). The calibration of known amount of dried biomass to its corresponding optical density at 600 nm was used for quick estimation of total biomass in the culture during fermentation run. The calibration was done as follows:

Bacterial culture was grown in 100 mL of NR medium in shake-flasks for 24 hours at 30 °C. Then, 50 mL of culture was harvested and spun down at 3,578 $\times g$ for 5 minutes at 4 °C. The cell pellet was then washed with saline solution and re-centrifuged. The washing and centrifugation steps were repeated three times before the cell pellet was dried in hot air oven at 65 °C until constant weight. Another 50 mL of the liquid culture was diluted accordingly in saline solution to obtain $OD_{600\ nm}$ less than 1.0. Several calibration points were recorded (Figure 3.2) with a replicate for each. The difference within the replicate did not exceed ± 0.1 unit $OD_{600\ nm}$.

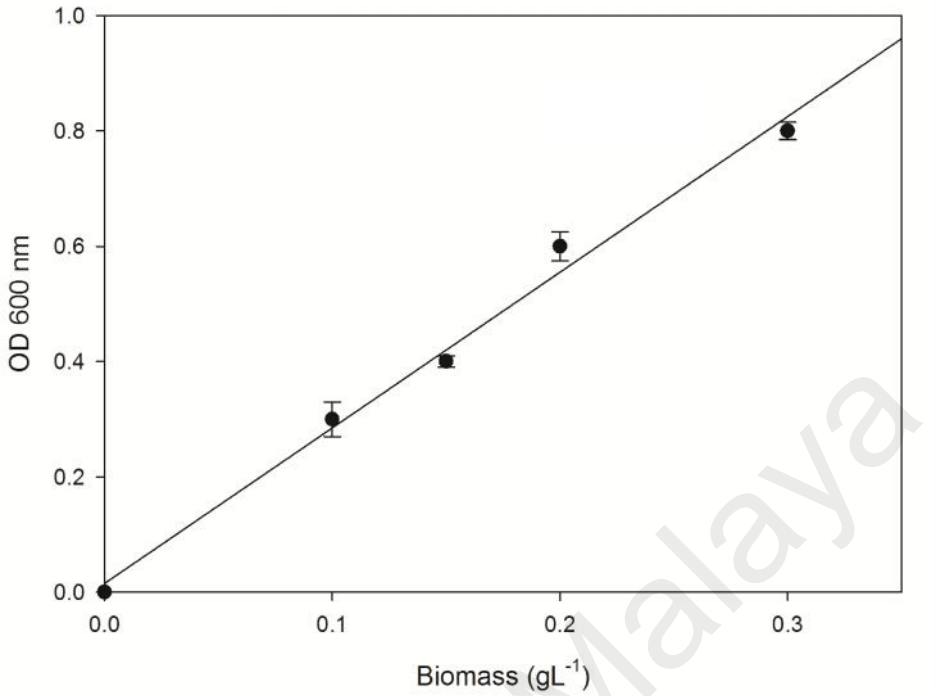

Figure 3.2: Standard calibration of optical density at 600 nm ($OD_{600\ nm}$) to dried total biomass (g L^{-1})

The biomass concentration was calculated from the following relationship:

$$y = 2.6543 \cdot x \qquad \text{(Eq 3.1)}$$

where, *x*, is the $OD_{600\ nm}$ and *y* is the calculated total biomass concentration (g L^{-1}).

3.2.4 Determination of optimum carbon-to-nitrogen (C/N) mol ratio to be used as supplementation solution in the fed-batch fermentation

P. putida Bet001 was used as the producer strain for mcl-PHA accumulation. Effects of different initial C/N mol ratio on dry cell weight (g L^{-1}) and mcl-PHA content (wt %) were determined in shake flasks. Different C/N mol ratios of carbon (octanoic acid, $C_8H_{16}O_2$) and nitrogen (sodium ammonium hydrogen phosphate tetrahydrate, $NaNH_4HPO_4.H_2O$) sources were prepared at 5, 10, 15, and 20. Sterile NR medium (30 mL per each 100 mL conical flask) was used as medium for growing the bacterial inoculum. A loopful of culture from NR agar was aseptically introduced into 30 mL NR liquid medium in shake flasks and cultivated in an aerobic condition at 25 °C and 200 rpm for 24 h. Then, 10 % (v/v) of cell inoculum from NR broth was transferred into E2 medium with different C/N mol ratios (100 mL per each 250 mL conical flask). The cultures were incubated for 24 hours at 30 ºC with 200 rpm agitation in shake flasks. After 24 hours cultivation, the culture was centrifuged at 3, 578 × *g* for 5 minutes at 4 °C. Then, the cells were washed twice with saline solution (0.9 % w/v) followed with *n*-hexane before oven dried (60 °C) until constant weight.

3.2.5 Determination of volumetric oxygen mass transfer coefficient (K_La) using static gassing-out method

The volumetric oxygen mass transfer coefficient, K_La was determined in a stirred tank bioreactor using static gassing-out method. The experiment was carried out in order to estimate the oxygen mass transfer efficiency of the bioreactor system. The conditions were similar to the actual fermentation run and using the same equipment setup. The aqueous phase consisted of actual composition of the fermentation E2 medium with 3 g L^{-1} of octanoic acid in 1.0 L of total working volume. The aqueous medium was first deoxygenated by sparging gaseous nitrogen until all traces of oxygen

was stripped away (oxygen partial pressure, pO_2 = 0 %). Then pressurized air was sparged into the bioreactor at 0.6 L min^{-1} and at 600 rpm agitation rate. The increase in % pO_2 was recorded at regular intervals until readings became constant which indicated the saturation of the liquid medium with oxygen (Annuar *et al*., 2007).

The K_La was determined using the relationship:

$$dC_L/dt = K_La\ (C^*_L - C_L) \qquad \text{(Eq. 3.2)}$$

where,

C_L : % pO_2 value at time t;
C^*_L : dissolved oxgen concentration in equilibrium with the gas phase (constant % pO_2);
t : time (second);
K_La : volumetric oxygen mass transfer coefficient (s^{-1}).

Integration of equation (Eq 3.2) yields

$$\ln (C^*_L - C_L) = - K_La \,.\, t + \ln C^*_L \qquad \text{(Eq. 3.3)}$$

K_La value was determined directly from the slope by plotting of $\ln (C^*_L - C_L)$ versus t.

3.2.6 Batch cultivation of *P. putida* BET001 in stirred tank bioreactor

Bacterial cells were pre-cultured in NR liquid medium using orbital shaker incubator at 30 ˚C and 200 rpm agitation for 24 hours. Then, 10 % (v/v) of inoculum from the broth was transferred into 100 mL of E2 medium in shake flasks. Octanoic acid (3 g L^{-1}) was included in the E2 medium as the sole carbon and energy source. The shake flasks were incubated in an orbital shaker incubator at 30 ˚C and 200 rpm agitation for 18 hours. Subsequently, the whole content of a flask was used to inoculate E2 medium in a 2-L stirred tank bioreactor.

Batch fermentation was employed to study the growth profile of the bacteria in a controlled stirred tank bioreactor in order to determine the appropriate feeding points of C/N solution to the culture during fed-batch fermentation later. Batch cultures were cultivated at 30 ˚C, 600 rpm agitation, constant pH 7.0 regulated by the addition of 0.5

N KOH and 0.5 N H_2SO_4 and 0.5 vvm aeration in the stirred tank bioreactor. Inoculum at 10 % (v/v) was seeded into 0.9 liter of E2 medium in the bioreactor (concentration of E2 components were adjusted for 1-L). The initial concentration of octanoic acid in the bioreactor was 3 g L^{-1}. After 48 hours of fermentation, the culture medium was pumped out from the vessel. The biomass was subsequently harvested by centrifugation.

3.2.7 Biosynthesis of mcl-PHA in fed-batch cultivation

Bacterial cells were pre-cultured in NR medium using orbital shaker incubator at 30 ˚C and 200 rpm agitation for 24 hours. Then, 10 % (v/v) of inoculum from the broth was transferred into 100 mL of E2 medium in shake flasks. Octanoic acid (3 g L^{-1}) was included in the E2 medium as sole carbon and energy source to acclimatize the culture to the carbon substrate and therefore helped to reduce the lag phase during cell cultivation in 2-L bioreactor later. The shake flask culture was incubated in an orbital shaker incubator at 30 ˚C and 200 rpm agitation for 18 hours. Subsequently, the whole flask content was used to inoculate E2 medium for mcl-PHA production in a 2-L stirred tank bioreactor.

Fed-batch fermentation was employed in order to extend the cell growth phase and concomitant mcl-PHA accumulation. Fed-batch cultures were cultivated at 30 ˚C in the stirred tank bioreactor. About 10 % inoculum (v/v) was used to inoculate 0.9 liter of E2 medium in the bioreactor (concentration of E2 components were adjusted for 1-L). The initial concentration of octanoic acid in the bioreactor was 3 g/L. A solution with C/N mol ratio of 10 (10.3 ml/L) was added to the culture at 12- and 24-hour intervals. After 48 hours of fermentation, the culture medium was pumped out from the vessel. The biomass was subsequently harvested by centrifugation.

3.2.8 Cell harvesting

Bacterial cells were aseptically harvested by centrifugation (Thermo Scientific Sorvall RC-5C Plus ultracentrifuge, USA) at 3,578 × *g* for 10 minutes at 4 °C. The cells were washed twice with sterile saline (0.9 % w/v) and then with *n*-hexane to remove excess fatty acids. The pellets were dried in dry-air oven (60 °C) until constant weight. Cell concentration was expressed as total cell dry weight concentration (CDW, g L^{-1}).

3.2.9 PHA extraction and purification

Intracellular PHA was extracted by suspending the dried cells in analytical grade acetone (C_3H_6O, *Mw* 58.08 g mol^{-1}, Merck) and refluxed for 4 hours at 70 ˚C. The PHA-acetone solution was filtered through Whatman No. 1 filter paper to remove cellular debris, and the filtrate was concentrated by rotary evaporation (EYELA N-1000 rotary evaporator, Japan). The polymer was purified by drop-wise addition of the extract into rapidly stirred analytical grade methanol (CH_3OH, *Mw* 32.04 g mol^{-1}, Merck) chilled in ice bath. Further purification was performed by re-dissolving the PHA extract in a small amount of acetone and re-precipitating it in cold methanol. Then, it was dried in a vacuum oven (JEIOTECH Model OV-11/12, Korea) at 40 ˚C, 0.6 atm for 24 hours (Baei & Rezvani, 2011; Chardron *et al*., 2010).

3.3 Fabrication of P(3HO-*co*-3HHX)/HA composite scaffold

3.3.1 Material

Hydroxyapatite (HA) powder ($HCa_5O_{13}P_3$, *MW* 502.31, CAS 12167-74-7) was purchased from Sigma Aldrich (~15-20 µm). Acetone (CAS 67-64-1) and sodium chloride (CAS 7647-14-5) were purchased from Merck Millipore, Darmstadt, Germany. Analytical grade chemicals were used throughout the study.

3.3.2 Preparation of composite P(3HO-*co*-3HHX)/HA scaffold

The P(3HO-*co*-3HHX)/HA composite scaffold was fabricated using solvent casting-particulate leaching technique (Figure 3.3). Agglomeration of the particles was prevented by placing the solution in a Multi-frequency Ultrasonic Bath SB-300DTY (Ningbo Scientz Biotechnology Co., Zhejiang, China). A combination of ultrasonication and solution casting method was applied to achieve a well-dispersed P(3HO-*co*-3HHX)/HA matrix. The scaffold was fabricated as follows: 0.6 g of the polymer was dissolved in 6 mL of acetone followed by the addition of HA powder. The amount of HA particles was 10 weight % and 30 weight % relative to the polymer (Moradi *et al*., 2013). After 20 minutes ultrasonication (25 kHz, 340 W), NaCl was added to the mixture and stirred for 15 min. The size range of salt particles was 100 - 200 µm and its weight fraction was 90 %, based on the total mass of polymer and salt. Subsequently, the mixture was poured into a glass Petri dish (6-cm diameter) as a casting mold. After 48 h of drying at room temperature (25 ± 1 °C), samples were dried in an oven (40 °C) under vacuum for 24 h. After the drying process, dried and solidified sample was removed from the Petri dish. The samples from salt-leaching process were soaked in deionized water (minimum 300 mL) with light stirring using magnetic stirrer. The soaking was carried out for five consecutive days with daily changes of fresh deionized water. Then, the samples were dried out at 25 ± 1 °C under vacuum for 48 h. The pure P(3HO-*co*-3HHX) scaffold for control experiment was fabricated using the same method without the addition of HA particles.

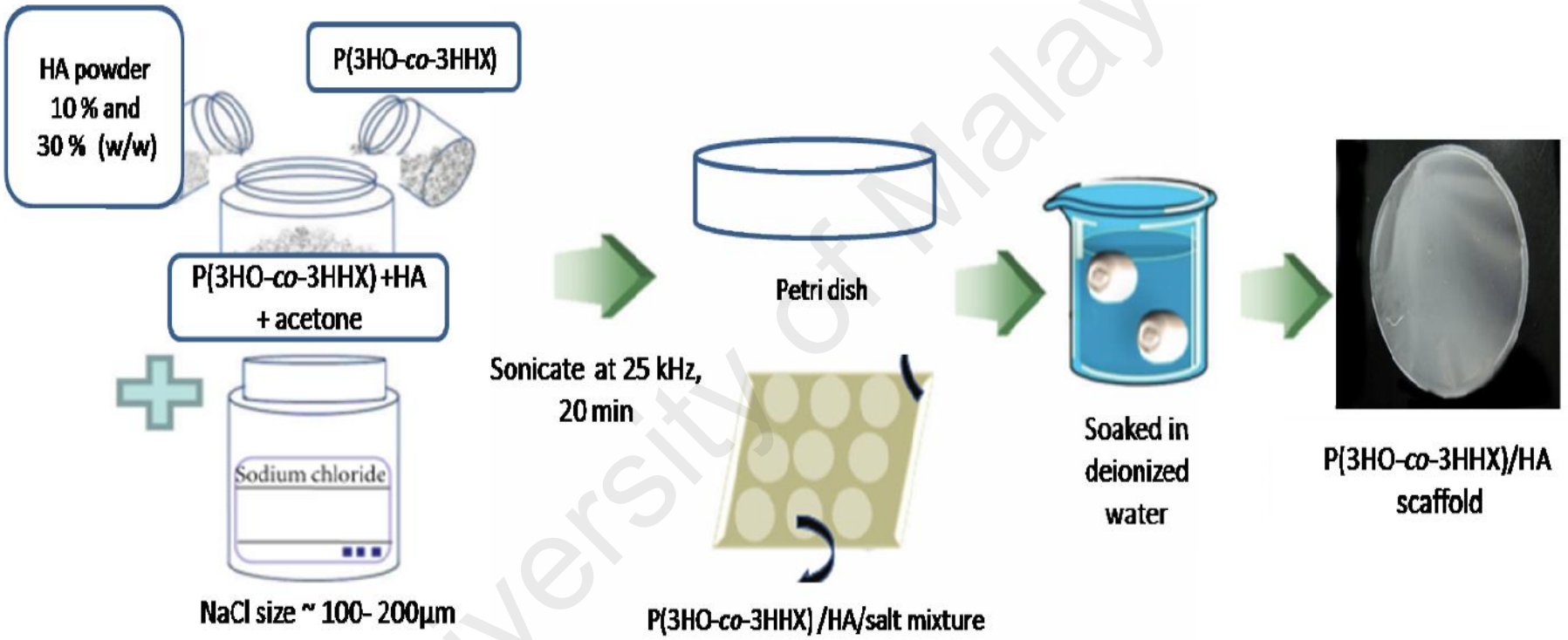

Figure 3.3: Schematic diagram for preparation of composite P(3HO-*co*-3HHX)/HA scaffold

3.3.3 Characterization of polymer composite

3.3.3.1 FTIR-ATR spectroscopy

A nondestructive attenuated total reflectance Fourier transform infrared spectra of the control references and the composite polymer were recorded on Perkin-Elmer Spectrum 400 FT-IR and FT-NIR Spectrometer (Perkin-Elmer Inc., Wellesley, MA, USA) equipped with PIKE GladiATR hovering monolithic diamond ATR accessory (Pike Technologies Inc., Fitchburg, USA). Control samples and their composites were placed on the monolithic diamond ATR probe and clamped against the diamond crystal plate using the force adapter. Thereafter, the samples were scanned over a range of 4000–400 cm^{-1} at 25 °C (Gumel *et al.*, 2014).

3.3.3.2 X-ray diffraction (XRD) analysis

Crystallinity of mcl-PHA was investigated using a PANalytical EMPYREAN (PANalytical, Almelo, Netherlands). Five milligrams of PHA was dissolved in 2 mL dichloromethane. Then, it was casted on a glass slide, and allowed to dry overnight. A 20-minute scan was run on each sample with the X-ray settings held at 40 kV and 40 mA. The scan range was from 10° to 70° 2θ.

3.3.3.3 Differential scanning calorimetry (DSC)

The analysis was carried out using a Mettler-Toledo differential scanning calorimeter (DSc 822e;Mettler-Toledo, Columbus, OH, USA) running on STARe DSc ver 8.10 software, equipped with a HAAKE EK90/MT digital immersion cooler (Thermo Fischer Scientific, USA). About 5 mg sample was encapsulated in an aluminium pan. Analysis was performed at a programmed temperature range of −50 to 200 °C with a heating rate of 10 °C min^{-1} under a nitrogen flow rate 50 mL min^{-1} at a head pressure of 1.5 bars. The melting temperature (T_m) was taken at the endothermic

peak of the DSC thermogram. The degree of crystallinity in polymer was calculated based on the endothermic melting enthalpy (ΔH_m) value obtained from DSC endotherm with respect to ΔH_m of PHB with 100 % crystallinity (140.1 J g^{-1}) (Doi, 1990).

3.3.3.4 Surface analysis

The morphological characteristics of both control and composited polymers were viewed in a high-resolution field emission scanning electron microscope (FESEM) (Quanta FEG 450) (FEI, Oregon, USA). The microscope was operated at high vacuum mode with an electron acceleration voltage of 5 kV and a working distance of about 10 mm. Thin films of neat polymer and polymer composites were mounted on brass stubs using double-sided cellophane tape and introduced into the viewing chamber of the instrument (Gumel *et al.*, 2014). Energy dispersive X-ray spectrometry (INCAEnergy200, Oxford Inst., UK) was performed in order to determine the presence and distribution of HA particles in the composite scaffolds (Sultana & Wang, 2008).

3.3.3.5 Porosity of the scaffold

To evaluate the porosity of the composite scaffolds, they were weighed and immersed in 95 % ethanol for one hour. Then, the samples were soaked in deionized water overnight and their wet weights were recorded. The percentage of porosity of the composite scaffolds was calculated using the following equation (Kuo & Leou, 2006; Saadat *et al.*, 2013):

$$\text{Porosity}\ (\%) = \frac{W_w - W_d}{V_a} \qquad \text{(Eq. 3.4)}$$

where, W_w is the wet weight of scaffold (g), W_d is the dry weight of scaffold (g) and V_a is the apparent scaffold volume (mL).

3.3.3.6 Biocompatibility study

3.3.3.6.1 *In vitro* cell culture

Prior to culture initiation, 5-mm diameter disks were cut from both pure P(3HO-*co*-3HHX) and P(3HO-*co*-3HHX)/HA composite scaffolds, and sterilized through immersion in 70 % ethanol for 15 minutes. Then, the scaffolds were rinsed with sterilized phosphate-buffered saline and retained at room temperature for 2 hours under aseptic condition prior to cell culture. Then, osteoblast cells were suspended in 500 µL Dulbecco's modified Eagle's medium (DMEM) containing 10 % fetal bovine serum (FBS), 2 mM *L*-glutamine, penicillin and streptomycin (all from Gibco-Invitrogen, USA), and were placed on the surfaces of the disks located in the wells of 24-well culture plates. Osteoblast cells were inoculated in a plating density of 1 x 10^5 per scaffold. Cell cultures were incubated at 37 °C, 5 % CO_2 and saturated humidity to allow cell adhesion to the surface of the materials and infiltration into the porous structure. Three samples of each material were used in replicated experiments.

3.3.3.6.2 Alamar Blue assay

Alamar Blue (Biosource Int, Camarillo, USA), which detects the number of viable cells, was used to measure the growth of cells on polymer scaffolds. At the indicated time endpoints, the wells received 100 µL Alamar Blue per well. After incubation at 37 °C for 3 h, the reduced resazurin dye was quantitated by FLUOstar® Omega (BMG Optima, Ortenberg, Germany) fluorescence cell reader at 570 nm to 595 nm wavelengths. The percentage of resazurin dye reduction was calculated in order to determine the growth of osteoblast cells.

3.3.3.6.3 Alkaline phosphatase (ALP) activity

The differentiation of osteoblast cells was evaluated by the expression of ALP activity (Baek *et al.*, 2012). For ALP activity measurement, total protein of cells on scaffolds was extracted using 100 µl M-PER mammalian protein extraction reagent to lyse the cells. The lysate was then centrifuged at 14,000 × *g* at 4 °C for 15 minutes to separate cell debris. Supernatant was collected and ALP activities were measured using *p*-nitrophenyl phosphate (*p*-NPP) as a substrate. Following the ALP-catalyzed reaction, *p*-nitrophenyl phosphate was converted to *p*-nitrophenol and the absorbance at 405 nm was measured with a microplate reader (FLUOstar® Omega, BMG Optima, Ortenberg, Germany).

3.4 Functionalization of mcl-PHA by graft copolymerization of P(3HO-*co*-3HHX) with glycerol 1,3-diglycerolate acetate (GDD)

3.4.1 Material

Glycerol 1,3-diglycerol diacrylate ($C_{15}H_{24}O_9$ *MW* 348.35 CAS 60453-84-1) was purchased from Sigma Aldrich (Saint Louis, USA). Octanoic acid (CAS 124-07-2), acetone (CAS 67-64-1) and benzoyl peroxide (with 25 % H_2O) for synthesis ($C_4H_{10}O_4$ *MW* 242.23 CAS 94-36-0) were purchased from Merck Millipore (Darmstadt, Germany). Analytical grade chemicals were used throughout the study.

3.4.2 Preparation of P(3HO-*co*-3HHX)-*g*-GDD copolymer

P(3HO-*co*-3HHX)-*g*-GDD copolymer was prepared by thermal treatment of homogeneous acetone solution of P(3HO-*co*-3HHX), GDD monomer and benzoyl peroxide (BPO) initiator (Figure 3.4). 0.2 g P(3HO-*co*-3HHX) was used throughout the experiment. The reaction was carried out under nitrogen-saturated atmosphere. To remove dissolved oxygen from the solution, nitrogen gas was bubbled into the solution at 25 ± 1 °C for 10 minutes, and then the tube was sealed air-tight and incubated at 80 °C for 4 hours. Then, the solution was poured into vigorously stirred methanol to precipitate the copolymer. The resulting suspension was filtered and the solid product was dried to a constant weight in a vacuum oven at 25 ± 1 °C. The product was purified by dissolving in acetone and precipitating into methanol, followed by filtration and vacuum drying. The mass increase of P(3HO-*co*-3HHX)-*g*-GDD due to successful grafting was calculated according to the following equation:

$$\underset{\text{(Graft yield)}}{\text{Mass increase due to succesful grafting (\%)}} = \frac{M_f - M_i}{M_i} \times 100 \qquad \text{(Eq. 3.5)}$$

where M_f is the mass after grafting and M_i is the initial mass of P(3HO-*co*-3HHX).

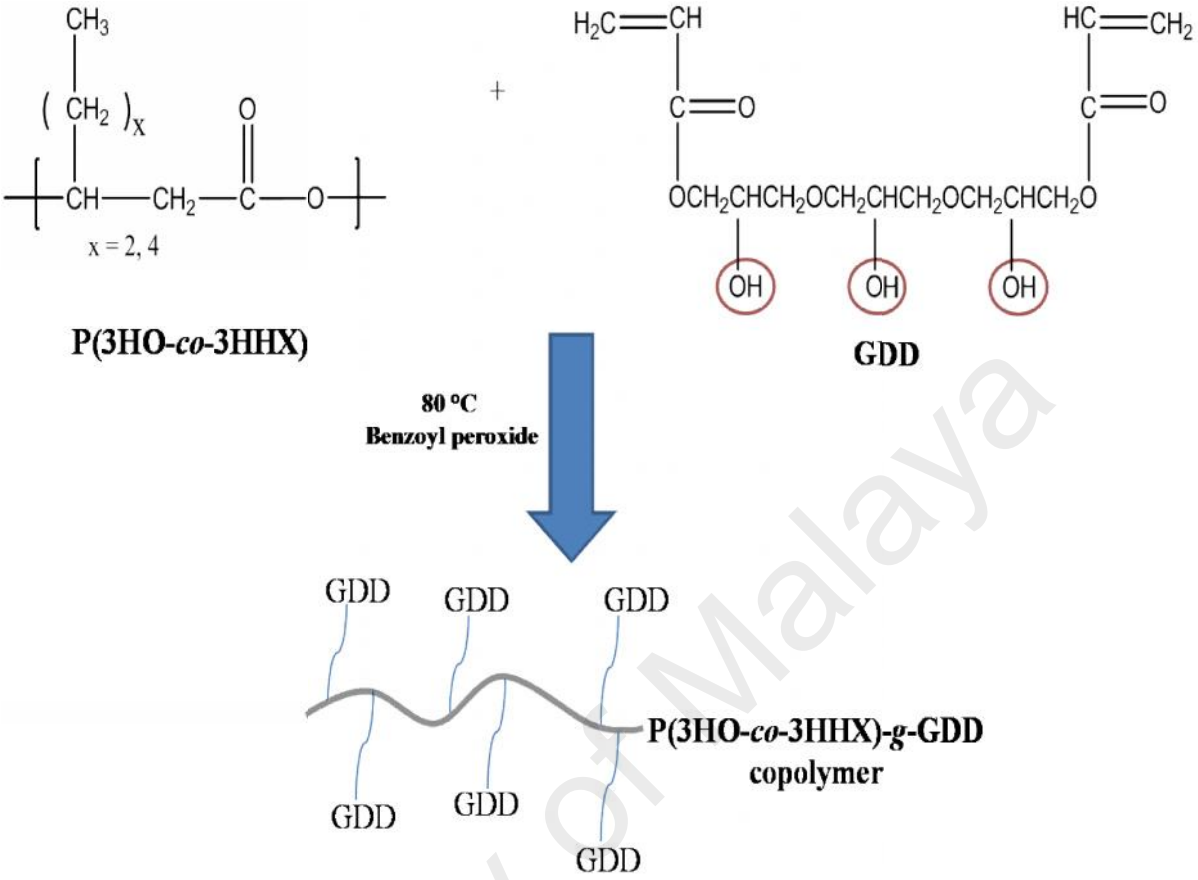

Figure 3.4: Schematic diagram showing the formation of P(3HO-*co*-3HHX)-*g*-GDD copolymer

3.4.3 Effects of the initial monomer concentration

The procedure was carried out as described in section 3.4.2. The reaction mixture was incubated at 80 °C with 0.04 mM BPO for 2 hours. The mass of P(3HO-*co*-3HHX) was fixed at 0.2 g for the experiment. The concentrations investigated for GDD monomer were 0.1, 0.3, 0.4, 0.6 and 0.9 mM.

3.4.4 Effects of reaction time

The procedure was carried out as described in section 3.4.2. Different concentrations of GDD monomer (0.1, 0.3, 0.4, 0.6 and 0.9 mM) were studied at different reaction times (0.5, 1.0, 2.0, 3.0 and 4.0 hours). The reaction mixture consisted of 0.2 g P(3HO-*co*-3HHX), 0.04 mM BPO and pre-determined GDD monomer concentration.

3.4.4.1 Determination of activation energy

The activation energy (E_a, J mol^{-1}) for the graft copolymerization reaction was calculated using the linearized Arrhenius equation:

$$\ln k = \ln A - \frac{E_a}{RT} \qquad \text{(Eq. 3.6)}$$

where A is the frequency factor, R is the gas constant (8.3145 J mol^{-1} K^{-1}), and T is the absolute temperature (K).

3.4.5 Effects of reaction temperature

The procedure was carried out as described in section 3.4.2. Different reaction temperatures *viz.* 70 °C, 80 °C and 90 °C were studied. The reaction mixture consisted of 0.2 g P(3HO-*co*-3HHX), 0.4 mM GDD and 0.04 mM BPO incubated at pre-determined temperature for 2 hours.

3.4.6 Effects of benzoyl peroxide

The procedure was carried out as described in section 3.4.2. Different concentrations of radical (BPO) 0.01, 0.02, 0.04, 0.10, 0.15 and 0.20 mM were studied. The reaction mixture consisted of 0.2 g P(3HO-*co*-3HHX), 0.4 mM GDD and BPO incubated at 80 °C for 2 hours.

3.4.7 Characterization of P(3HO-*co*-3HHX)-*g*-GDD copolymers

3.4.7.1 FTIR-ATR Spectroscopy

The analysis was carried out as described in section 3.3.3.1.

3.4.7.2 Proton (^{1}H) Nuclear Magnetic Resonance (NMR)

Five milligrams of mcl-PHA sample was dissolved in 2 mL deuterated chloroform ($CDCl_3$) and filtered into Nuclear Magnetic Resonance (NMR) tube using a borosilicate glass syringe equipped with 0.22 μm polytetrafluoroethylene (PTFE) disposable filter (11807–25; Sartorius Stedim, Goettingen, Germany). The spectrum was acquired using a JEOL JNM-GSX 270 FT-NMR spectrometer (JOEL, Tokyo, Japan) at 400 MHz against tetramethylsilane (TMS) as internal reference.

3.4.7.3 Simultaneous Thermal Analysis (STA)

The thermal stability of the neat polymer and its composite was evaluated by simultaneous thermal analysis (STA) using Perkin Elmer STA 6000 machine (Perkin-Elmer Inc., Wellesley, MA, USA) operated as tandem differential scanning calorimetry (DSC) and thermogravimetric analysis (TGA) at nitrogen gas flow rate of 20 mL min^{-1}. Samples (8 mg) were compressed in an aluminium boat and heated from 30 to 550 °C at a heating rate of 10 °C min^{-1}.

3.4.7.4 Differential Scanning Calorimetry (DSC)

The analysis was carried out as described in section 3.3.3.3.

3.4.7.5 Gel Permeation Chromatography (GPC)

The number average molecular weight (M_n) and the polydispersity index (M_w/M_n) of the grafted copolymer were investigated by gel permeation chromatography (GPC) using Waters 600 (Waters Corporation, Milford, MA, USA) instrument equipped with a Waters refractive index detector (model 2414) employing the following gel columns (7.8 mm internal diameter, 300 mm length) in series: HR1, HR2, HR5E, and HR5E Waters Styragel HR-THF. The sample was dissolved in tetrahydrofuran (THF) at a concentration of 2.0 mg mL^{-1} and was filtered through a 0.22 μm PTFE filter. Then, 100 μL of the sample was injected at 40 °C. THF was used as the eluent at a flow rate of 1.0 mL min^{-1}. The instrument was calibrated using monodisperse polystyrene standards with different molecular weights (162, 380, 1020, 1320, 2930, 6770, 13030, 29150, 51150, 113300, 215000, and 483400 g mol^{-1}).

3.4.7.6 Water Uptake Ability

The swelling behavior of grafted copolymers was studied using gravimetric method (Kim *et al.*, 2008). Dry films were immersed in phosphate-buffered saline (pH 7.4) at 37 °C. The swollen films were recovered, blotted quickly with absorbent paper to eliminate surface water and weighed. The measurement was repeated until constant weight of swollen sample was observed. The water uptake ability was calculated using the following equation:

$$\text{Water uptake (\%)} = \frac{W_t - W_0}{W_t} \times 100 \qquad \text{(Eq. 3.7)}$$

where W_t is the weight of swollen film (g) at time t (min) and W_o is the initial weight of the film (g).

3.5 Preparation of P(3HO-*co*-3HHX)-*g*-GDD/HA

P(3HO-*co*-3HHX)-*g*-GDD/HA was prepared by thermal treatment of homogeneous solution of P(3HO-*co*-3HHX), 0.1 mM GDD monomer and 0.04 mM benzoyl peroxide (BPO) initiator (as described in section 3.4.2). After the grafted copolymer P(3HO-*co*-3HHX)-*g*-GDD was obtained, 10 weight % of HA powder was added into the solution and sonicated at 25 kHz, 340 W for 20 minutes. Subsequently, the mixture was poured into a glass Petri dish (6-cm diameter) as a casting mold. After 48 h of drying at room temperature (25 ± 1 °C), the samples were dried in an oven (40 °C) under vacuum for 24 h. After the drying process, dried and solidified samples were removed from the Petri dishes.

3.5.1 Characterization of the P(3HO-*co*-3HHX)-*g*-GDD/HA

3.5.1.1 FTIR-ATR Spectroscopy

The analysis was carried out as described in section 3.3.3.1.

3.5.1.2 Energy Dispersive X-ray Analysis (EDX)

Energy dispersive X-ray spectrometry (INCAEnergy200, Oxford Inst., UK) was performed in order to determine the presence and distribution of HA particles in the composite scaffolds. The instrument was operated at high vacuum mode with an electron acceleration voltage of 10 keV and a working distance of about 10 mm. Thin films of P(3HO-*co*-3HHX)-*g*-GDD/HA were mounted on brass stubs using double-sided cellophane tape and introduced into the viewing chamber of the instrument.

3.5.4 Toxicity test by brine shrimp lethality assay (BSLA)

In order to ascertain the potential toxicity of the P(3HO-*co*-3HHX)-*g*-GDD/HA composite, cytotoxicity assay was carried out involving brine shrimp lethality assay (BSLA) with *Artemia franciscana* as the test organism (Nunes *et al.*, 2006; Rajabi *et al.*, 2015). The ARTOXKIT M toxicity kit employing *A. franciscana* cysts were purchased from MicroBioTests Inc., Belgium. The toxicity assays were performed according to the manufacturer's instruction. The 24-hour assay was performed using instars II-III larvae (nauplii) of the *A. franciscana* hatched from its cysts. Mortality of the test organism upon exposure to the P(3HO-*co*-3HHX)-*g*-GDD/HA composite is the toxicity endpoint employed in this assay.

Artificial seawater was prepared by dissolving salt and concentrated salt solution (NaCl, KCl, $CaCl_2$, $MgCl_2$, $MgSO_4$, $NaHCO_3$ and H_3BO_3) provided with the kit in 1-L of distilled water. *A. franciscana* cysts were hatched in the artificial seawater under continuous illumination by light-emitting diode (LED) illuminator system at 6,000 lux

(MicroBioTests Inc.,) for 24 hours at room temperature (25 ± 1 °C). The nauplii (larva) were then transferred into 24-well plates with 10 nauplii per well. Wells without aqueous elution of test material served as a negative control.

Aqueous stock solutions of P(3HO-*co*-3HHX)-*g*-GDD/HA were prepared by dissolving 10 mg material in 10 mL of distilled water and incubated at 37 °C under gentle shaking for 48 hours (Pelka *et al.*, 2000). Toxicity assays were performed on aqueous dilutions of P(3HO-*co*-3HHX)-*g*-GDD/HA stock ranging from 12.5- to 100 % and incubated for 24-hours in darkness at room temperature (25 ± 1 °C). The number of surviving nauplii was counted and recorded after 24-hour exposure period. A nauplii is considered to be dead if it does not exhibit any movement after 10 seconds observation. The experiment was performed in triplicates and mortality of nauplii was recorded.

CHAPTER 4

RESULTS AND DISCUSSION

4.1 Biosynthesis of medium-chain-length poly(3-hydroxyalkanoates)

4.1.1 Determination of optimum carbon-to-nitrogen (C/N) mol ratio to be used as supplementation solution in the fed-batch fermentation

The optimal C/N mol ratio for supplementation during mcl-PHA accumulation by *P. putida* BET001 in fed-batch cultivation was determined using shake-flasks fermentation as described in section 3.2.4. Different C/N mol ratios of carbon (octanoic acid, $C_8H_{16}O_2$) and nitrogen source (sodium ammonium hydrogen phosphate tetrahydrate, $NaNH_4HPO_4.H_2O$) were studied. Figure 4.1 shows the effects of different C/N mol ratios (5, 10, 15 and 20) on dry cell weight and mcl-PHA content. The optimum C/N mol ratio was observed at C/N 10 (3 g L^{-1} octanoic acid) with maximum cell dry weight and mcl-PHA content of 0.83 g L^{-1} and 10.2 %, respectively. Furthermore, higher C/N mol ratios of 15 and 20 led to lower cell dry weight and mcl-PHA content, thus indicated possible inhibitory effects on both cell and mcl-PHA accumulation at a relatively higher concentration of octanoic acid (Du and Yu, 2002; Finkeova *et al*., 2013). The C/N ratios used in this study represented the octanoic acid concentrations ranging from 1.5 to 6.0 g L^{-1}. Fatty acids are toxic to cells of *P. putida* even at low concentration, and for octanoic acid the inhibition was observed when its concentration exceeds 4 g L^{-1} (Chardron *et al*., 2010). The optimum C/N mol ratio obtained would be used in the subsequent batch and fed-batch experiments. The C/N ratio experiment serves as a basis for the design of an ammonium-limited medium with excess carbon source to be fed during the fed-batch cultivation (Annuar *et al*., 2007).

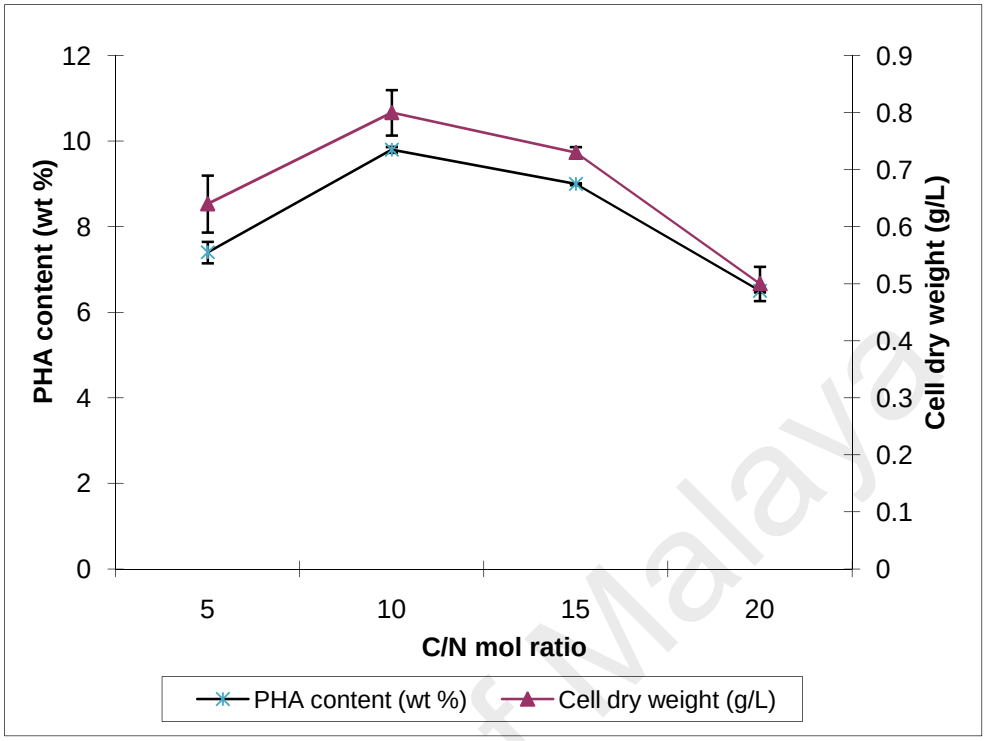

Figure 4.1: Effects of different C/N mol ratios on cell dry weight and mcl-PHA content of *P. putida* BET001

4.1.2 Determination of volumetric oxygen mass transfer coefficient (K_La) using static gassing-out method

The volumetric oxygen mass transfer coefficient, K_La was determined in the stirred tank bioreactor using static gassing-out method. This experiment was carried out to estimate the K_La of the bioreactor system. From Figure 4.2, the K_La value was calculated from the slope of the straight line plot ln (C^*_L-C_L) versus time (seconds). The estimated K_La value at 3 g L^{-1} of octanoic acid was 0.0126 s^{-1}. The response time for the same model of electrode to achieve 63 % oxygen saturation has been measured by Annuar *et al*. (2007), and it was concluded that for reliable determination when using the same electrode model, the K_La value should be less or equal to 0.03125 s^{-1}.

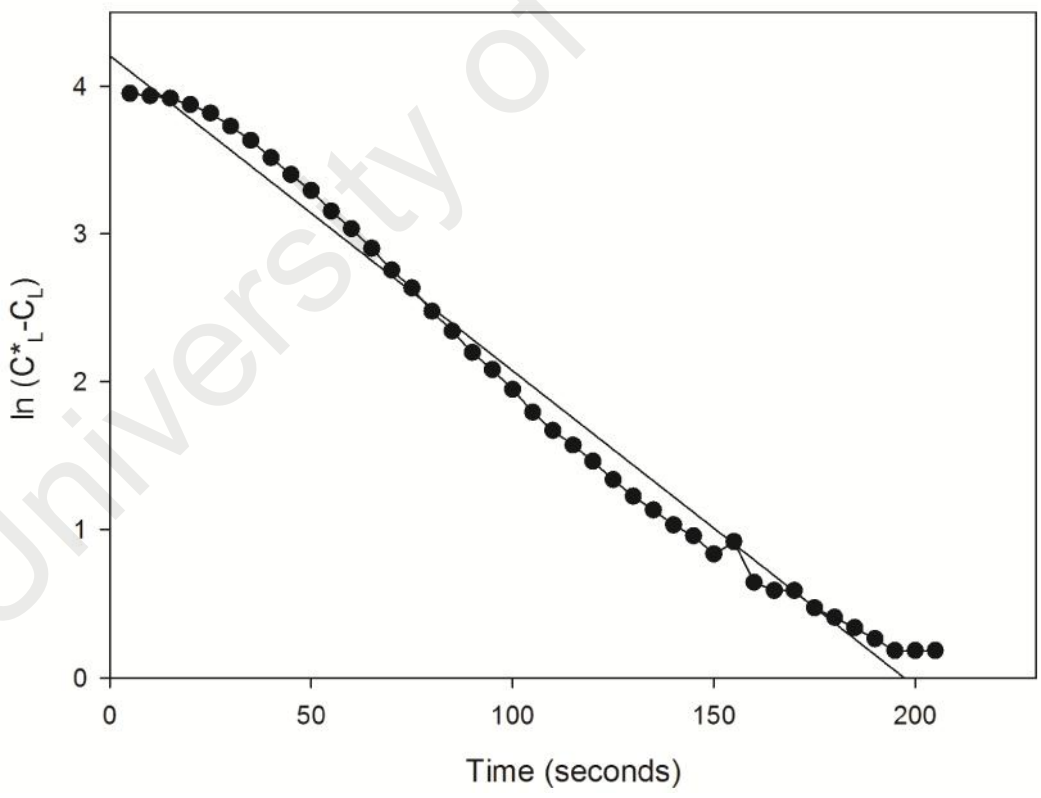

Figure 4.2: Estimation of the K_La value

4.1.3 Growth profile of *P.putida* BET001 from batch cultivation in controlled stirred tank bioreactor

Batch fermentation was employed to study the growth profile of the culture in a controlled stirred tank bioreactor in order to determine the appropriate feeding points of C/N solution during fed-batch fermentation. A solution containing C/N 10 mol ratio of octanoic acid-to-$NaNH_4HPO_4.4H_2O$ was added to supplement the consumption of carbon and nitrogen sources during fermentation as described in section 3.2.5. Figure 4.3 shows the growth profile of *P. putida* BET001 from three separate batch fermentation runs for 30 h cultivation time. The cell dry weight increased from 0.05 to 3.5 g L^{-1} after 24 h cultivation. Subsequently, it decreased to 2.2 g L^{-1} possibly due to the depletion of carbon source and nitrogen limitation condition in the culture. In order to increase cell biomass, supplementation of nutrient during PHA production phase was required to increase the accumulation of intracellular PHA (Kim, 2002). In addition, slight ammonium feeding during mcl-PHA biosynthesis was preferable for maintaining the anabolic activities to accumulate intracellular PHA under ammonium-limited condition (Kim, 2002; Annuar *et al*., 2007). Hence, time points at 12- and 24-h were selected to supplement the culture with C/N mol solution. Supplementation at 12-h was expected to pre-empt strong initial accumulation of mcl-PHA whereas at 24-h to delay the onset of growth decline phase of the culture. The premise of the selected time points was clearly justified as can be seen later in fed-batch fermentation profiles (section 4.1.4). It has been reported that batch fermentation is associated with low PHA productivity since after utilization of the external carbon source, the cells would degrade the accumulated PHA resulting in its reduced content (Amache *et al*., 2013; Zinn *et al*., 2001). From Figure 4.3, it was observed that the pO_2 in the liquid culture decreased from 47 % to 27 % during cell growth .Nevertheless, the pO_2 remained well above 25 % at the end of the cultivation indicating sufficient aeration of the culture.

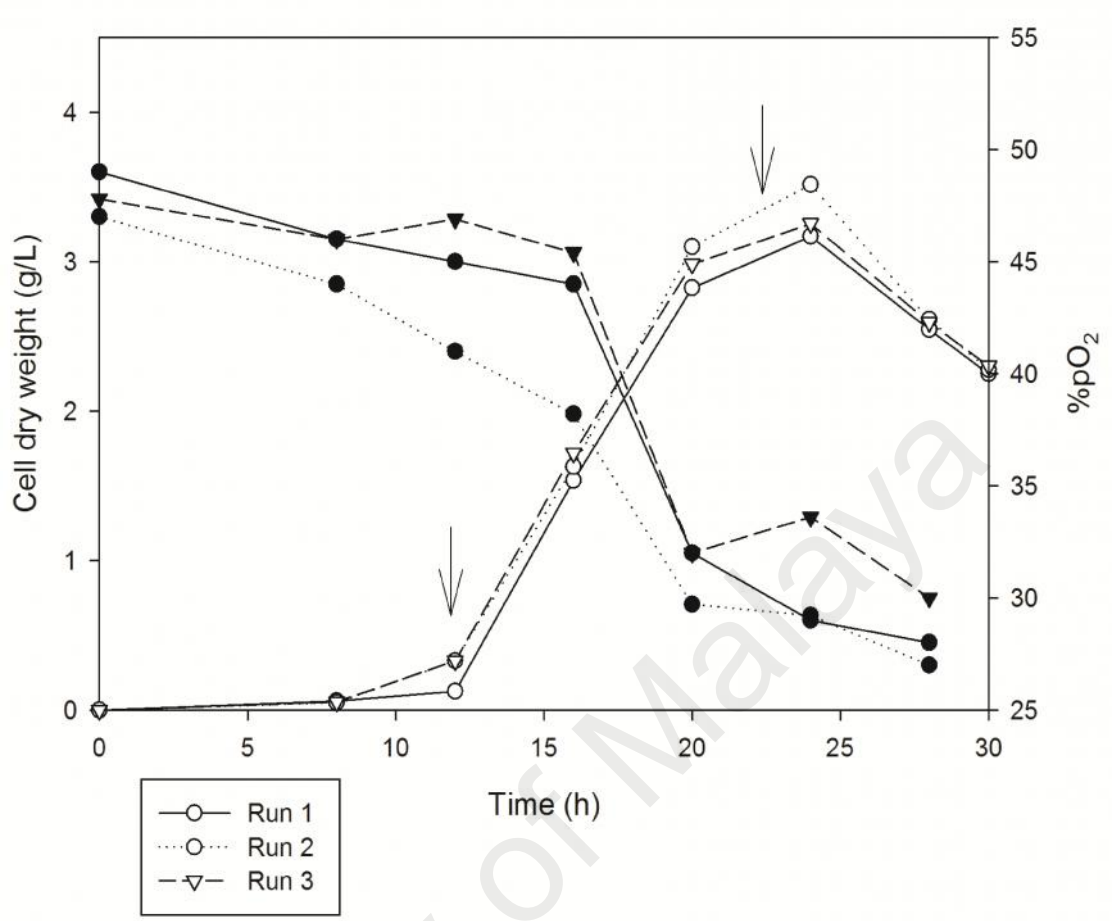

Figure 4.3: Growth profile of *P. putida* BET001 in batch cultivations (Conditions: 600 rpm; aeration 0.5 vvm; pH 7.0; 30 °C; arrows indicate potential feeding points of C/N mol solution; open and closed symbols indicate cell dry weight data and % pO_2 data, respectively)

4.1.4 Fed-batch fermentation of *P. putida* BET001

Culture condition is one of the main factors that affects the production of mcl-PHA. Various types of mcl-PHA monomeric composition can be synthesized by providing different carbon sources in the cultivation medium (Razaif-Mazinah *et al.*, 2015). In this study, mcl-PHA was produced through fed-batch fermentation process by *P. putida* BET001.It has been reported that *P. putida* BET001 is a growth-associated mcl-PHA producer whereby the mcl-PHA fraction from the total biomass increases with its specific growth rate (Gumel *et al.*, 2012). Fed-batch fermentation was employed in the investigation to extend the cell growth phase and concomitant mcl-PHA accumulation, with the octanoic acid and nitrogen source supplementation. From Figure 4.4, a solution at C/N 10 mol ratio was added to supplement the consumption of carbon and nitrogen sources by the cell culture that was growing and accumulationg mcl-PHA at the same time. Combined solution of octanoic acid and $NaNH_4HPO_4.4H_2O$ (10.3 mL) in the indicated mol ratio was added as a whole to the culture at 12- and 24 h. In addition, 3 g L^{-1} of octanoic acid (3.3 mL) was supplied to the culture every 4 hours in order to prevent depletion of the carbon substrate during fermentation. For efficient growth and production of mcl-PHA in the producer organism used in the study, the octanoic acid supplementation was kept below the inhibitory level of 4 g L^{-1} (Chardron *et al*., 2010). Consequently, 8.6 g L^{-1} of cell dry weight with 63 % mcl-PHA content was obtained after 48 hours fermentation. The cell mass and mcl-PHA content increased with the fermentation time (Figure 4.4). The pO_2 values decreased from 47 % to 23% during cell growth (Figure 4.2). It was also concluded that sufficient aeration was provided to the culture as no observable oxygen depletion was recorded throughout the fermentation. Analyses showed that the mcl-PHA produced was composed of three different monomers *viz.* 3-hydroxyoctanoate, 3-hydroxyhexanoate and 3-

hydroxydecanote at 90 mol %, 8 mol % and 2 mol % respectively with weight average molecular weight of ~130 kDa.

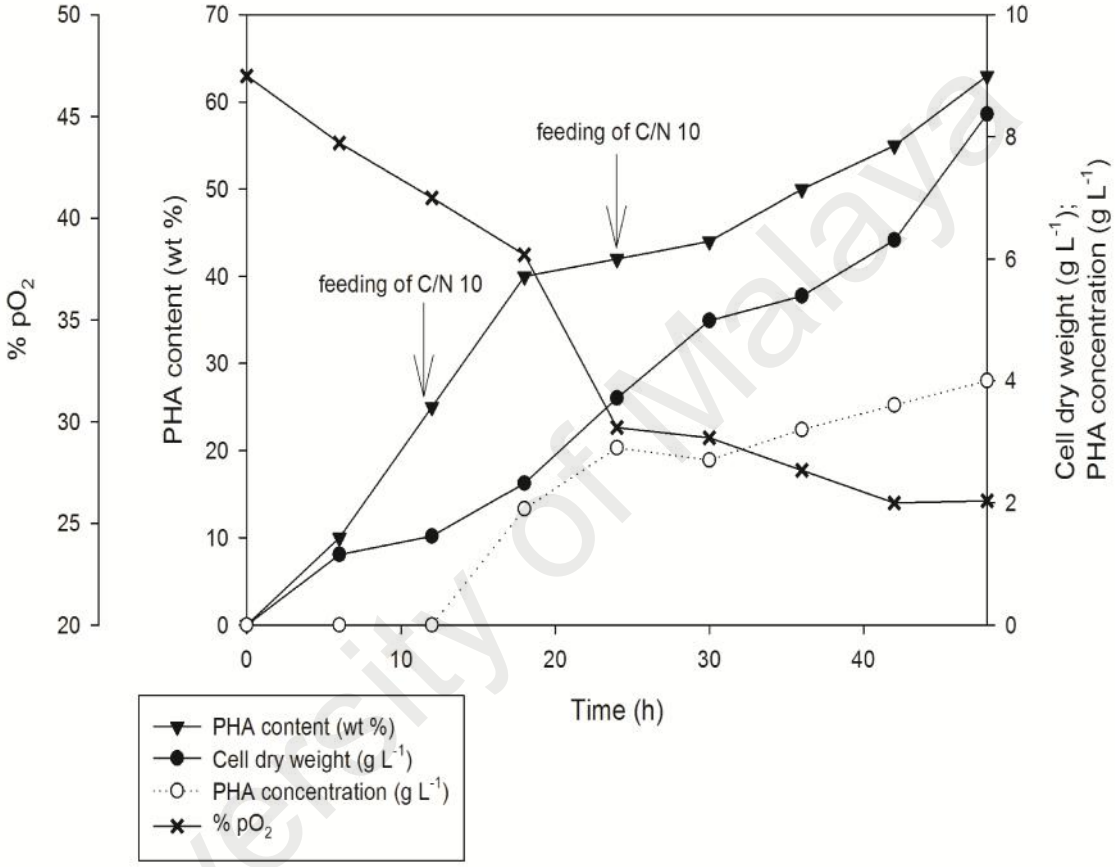

Figure 4.4: Growth and biosynthesis of mcl-PHA by *P. putida* BET001 in fed-batch fermentation

4.2 Blending of P(3HO-*co*-3HHX) with hydroxyapatite (HA)

4.2.1 Characterization of polymer composite

4.2.1.1 Fourier transform infrared spectroscopy (FTIR)

The chemical functional groups of P(3HO-*co*-3HHX), P(3HO-*co*-3HHX)/10 % HA and P(3HO-*co*-3HHX)/30 % HA and HA were examined by FTIR spectroscopy, as shown in Figure 4.5. Absorptions at 2926 and 2861 cm^{-1} were attributed to both asymmetric CH_3- and symmetric CH_2- vibrations in the samples, respectively. The presence of carbonyl ester bond in pure mcl-PHA sample was assigned to the absorption at 1725 cm^{-1} (Figure 4.5(A)). In the composite of P(3HO-*co*-3HHX)/10 % HA and P(3HO-*co*-3HHX)/30 % HA, carbonyl band absorptions were shifted to 1726 cm^{-1} and 1727 cm^{-1}, respectively. It was reported that spectral changes (intensities and position) of carbonyl band at 1740–1720 cm^{-1} was observed during PHA crystallization (Kansiz *et al.*, 2007; Xu *et al.*, 2002). The bands at 563, 601, 604, 1030, 1032 and 1092 cm^{-1} corresponded to the phosphate group of HA (Moradi *et al.*, 2013; Pramanik *et al.*, 2009; Wang *et al.*, 2005). The spectra of P(3HO-*co*-3HHX)/HA composite (Figure 4.5 (B and C)) showed the vibrational bands at 1727 cm^{-1} based on C=O of P(3HO-*co*-3HHX) and 1043 cm^{-1} based on PO_4^{3-} of the hydroxyapatite, indicating the presence of P(3HO-*co*-3HHX) and HA. Figure 4.5(D) showed the bands at 563, 600 and 1032 cm^{-1} corresponding to the phosphate group of HA. At 1042 cm^{-1}, different intensities of phosphate group for HA of P(3HO-*co*-3HHX)/10 % HA and P(3HO-*co*-3HHX)/30 % HA were observed. Peak shifts from 1043 cm^{-1} (C–O) to 1021cm^{-1} (P–O) were observed for both P(3HO-*co*-3HHX)/10 % HA and P(3HO-*co*-3HHX)/30 % HA samples after blending, which indicated that HA had been well blended into P(3HO-*co*-3HHX).

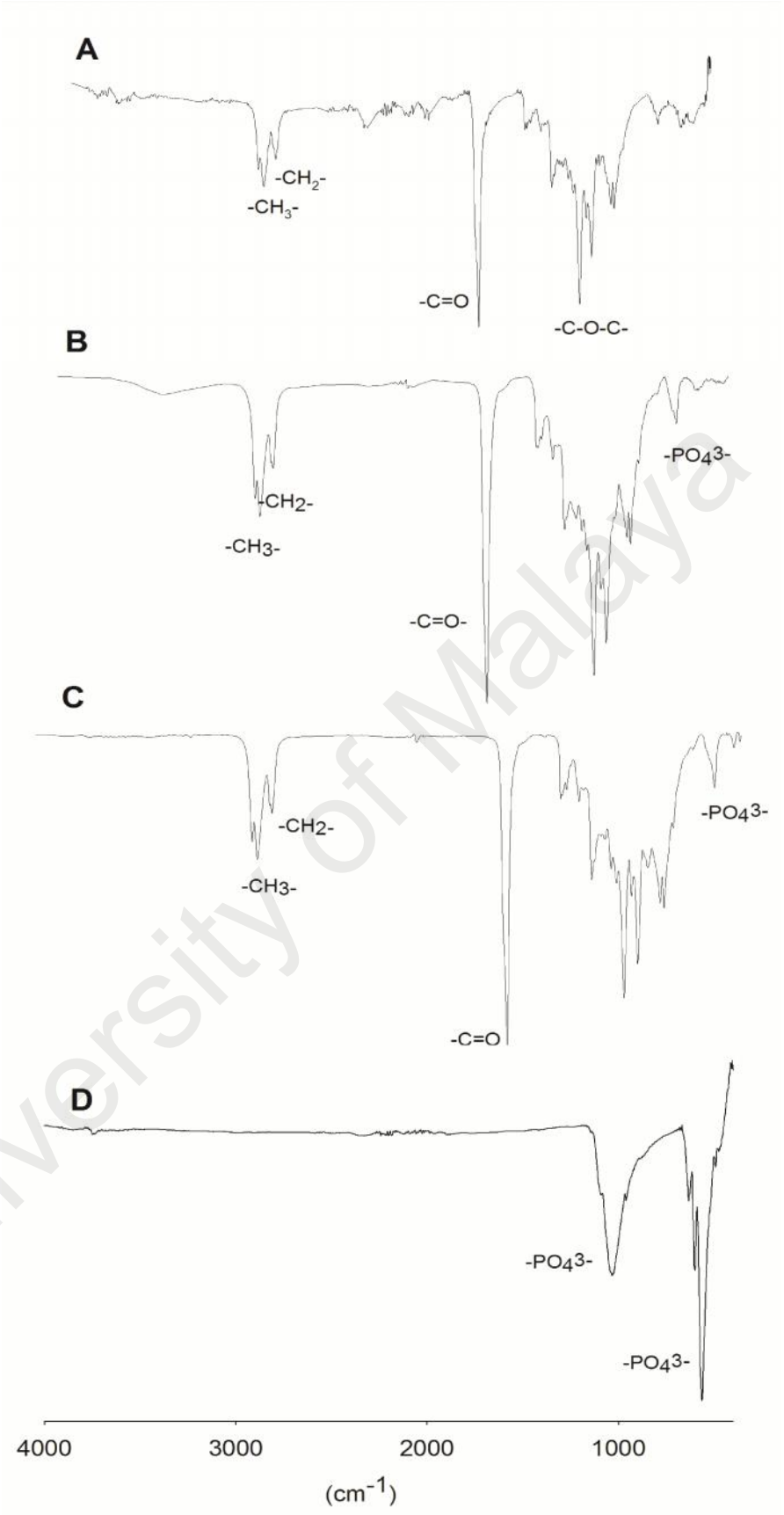

Figure 4.5: FTIR spectra of (A) P(3HO-*co*-3HHX); (B) P(3HO-*co*-3HHX)/10 % HA; (C) P(3HO-*co*-3HHX)/30 % HA; and (D) HA powder

4.2.1.2 X-ray diffraction (XRD)

The X-ray diffraction patterns of the P(3HO-*co*-3HHX), P(3HO-*co*-3HHX)/10 % HA and P(3HO-*co*-3HHX)/30 % HA composites are shown in Figure 4.6 A-C. The crystalline nature of P(3HO-*co*-3HHX)/HA composite scaffold was further confirmed following XRD analysis. Taking into account the broadening of each peak in XRD, mean crystallite size was calculated using Scherrer's equation, that is, $D = 0.9 \lambda/\beta \cos \theta$, where D is the average crystallite size in ° A, β is the peak broadening of the diffraction line measured at half of its maximum intensity in "radian," λ is the wavelength of X-rays, and θ is the Bragg's diffraction angle (Pramanik *et al.*, 2009). The major HA reflection peaks, such as (002), (211), (300), (004) at 25.8°, 31.7°, 32.1°, 32.9° 2θ, are shown in Figure 4.6 D. The standard P(3HO-*co*-3HHX) was observed to display the typical polymeric crystallite reflection at (020), (110), (111) and (040) planes at 17.9°, 19.5°, 21.9°, 26.5° 2θ. It has been reported that the 040 reflection peak in the neat PHA was observed to be broader due to the presence of less perfect crystal structure in the mcl-PHA (Gumel *et al.*, 2014).

In composite scaffold (P(3HO-*co*-3HHX)/HA) samples, the peaks HA (211) and (300) were observed. This suggested the presence of interfacial binding between HA particles and polymer matrix. In addition, P(3HO-*co*-3HHX)/30 % HA samples showed higher intensity peak of HA compared to the P(3HO-*co*-3HHX)/10 % HA samples, which indicated that the HA was well blended into the polymer matrix. It was found that the crystallite size of the pure P(3HO-*co*-3HHX) decreased from 17.9 to 14.9 nm and 10.1 nm after incorporation of 10 % and 30 % of HA particles into the polymer matrix (Table 4.1). The crystallinity of the P(3HO-*co*-3HHX) scaffold was decreased after composite formation indicating that crystal structures of both P(3HO-*co*-3HHX)

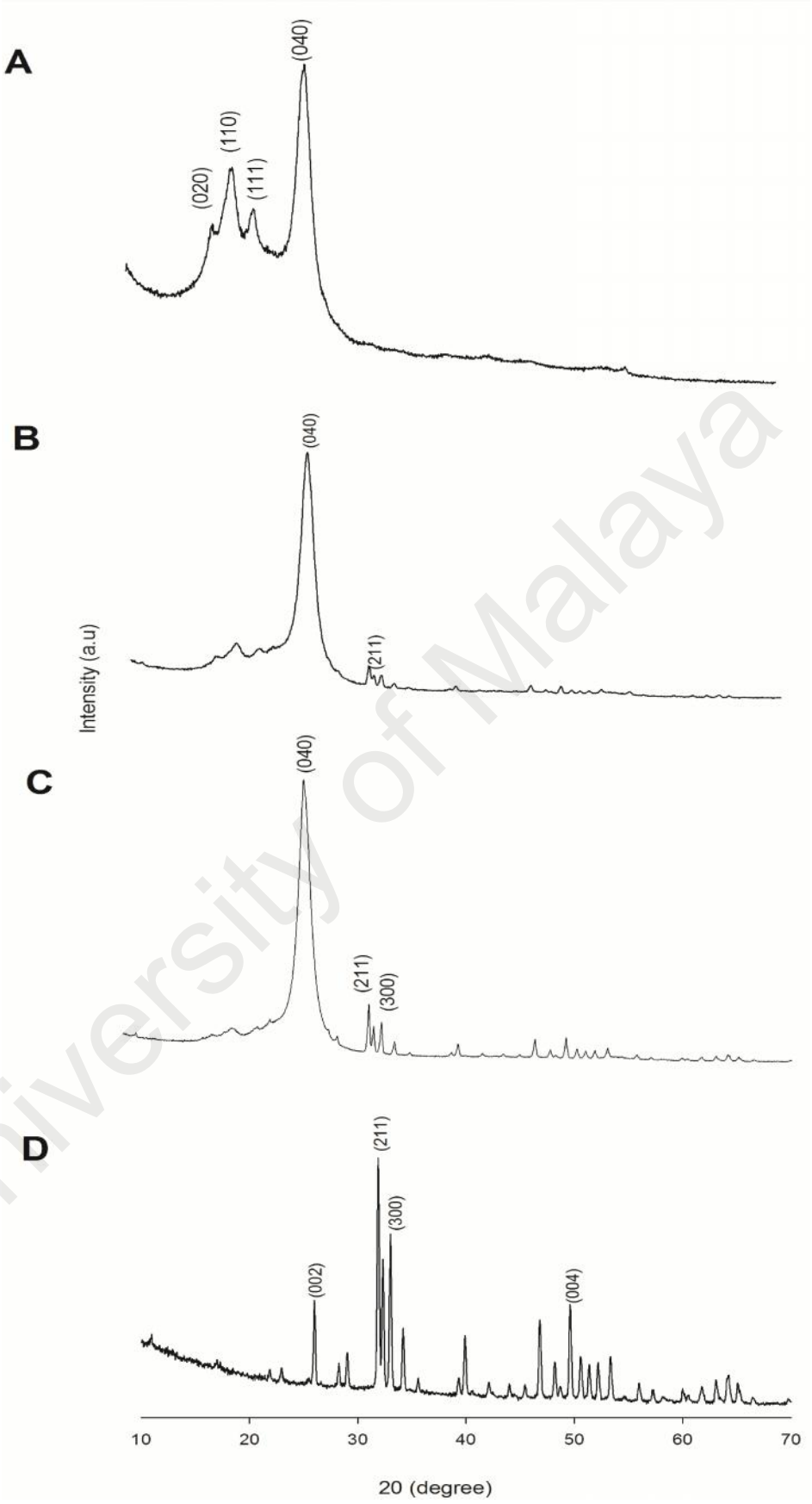

Figure 4.6: XRD spectra of (A) P(3HO-*co*-3HHX); (B) P(3HO-*co*-3HHX)/10 % HA; (C) P(3HO-*co*-3HHX)/30 % HA and (D) HA

and HA have been altered after the composite formation. Similarly, it was reported that the addition of HA particles has led to lower degree of crystallinity of the PHBV matrix in a composite scaffold (Sultana & Khan, 2012). The XRD peaks, (211) and (300) were shifted to higher 2θ values in the case of P(3HO-*co*-3HHX)/HA composite as compared to pure HA (i.e. from 2θ = 31.9 to 32.1 and 32.9 to 33.3, respectively). This was possibly due to compression from the contracting polymeric matrix through interfacial bonding (Pramanik *et al.*, 2009). In addition, the crystalline peak of neat mcl-PHA at 2θ = 26.7 has shifted to 25.8. The shift and decrease in crystallinity of each peak of the polymer as well as HA after composite formation clearly indicated the presence of interfacial binding between HA particles and porous polymer matrix.

4.2.1.3 Differential scanning calorimetry (DSC)

The thermal properties, crystallinity and porosity data of the scaffolds are shown in Table 4.1. The T_m values of the polymers were increased from 54.9 °C to 55.2 °C and 55.7 °C after blending of P(3HO-*co*-3HHX) with 10 % HA and 30 % HA, respectively. The crystallinities of the polymers was decreased from 7.9 % to 6.9 % after blending with HA. The observed decrease in polymer crystallinity as a result of HA composition was corroborated by the data obtained from XRD analysis. It has been reported that polymer with lower degree of crystallinity is degraded faster (El-Hadi *et al.*, 2002). Thus, it can be expected that P(3HO-*co*-3HHX)/HA composite scaffold would exhibit higher rate of degradation *in vitro* and *in vivo* than neat P(3HO-*co*-3HHX) scaffolds. In contrast, the porosity of the polymer did not show significant difference before and after incorporation of HA particles.

Table 4.1: Physical and mechanical properties of P(3HO-*co*-3HHX) and P(3HO-*co*-3HHX)/HA composites

Scaffolds	[a]T_g (°C)	[a]T_m (°C)	[a]ΔH_m (J g^{-1})	[a]X_c (%)	[b]D_{040} (nm)	Porosity %
P(3HO-*co*-3HHX)	-33.7	54.9	11.2	7.9	17.9	80.2 ± 1.2
P(3HO-*co*-3HHX)/10 % HA	-32.9	55.2	10.4	7.4	14.9	75.4 ± 0.8
P(3HO-*co*-3HHX)/30 % HA	-33.1	55.7	9.7	6.9	10.1	78.1 ± 1.6

[a]Calculated from DSC analysis. T_g: Glass transition temperature; T_m: Melting temperature; ΔH_m: Enthalpy of melting; X_c: polymer crystallinity

[b]Calculated from XRD analysis. D_{040}: Crystallite size at 040 plane

4.2.1.4 Energy Dispersive X-ray Analysis (EDX)

Energy Dispersive X-ray Analysis (EDX, map of Ca) was performed in order to investigate the distribution of hydroxyapatite particles in the P(3HO-*co*-3HHX)/HA composite scaffold. Figure 4.7A showed the EDX spectra of neat P(3HO-*co*-3HHX) with the presence of carbon and oxygen elements. In contrast, P(3HO-*co*-3HHX) composite with HA showed the presence of carbon, oxygen, calcium and phosphorus elements (Figure 4.7B and 4.7C), which clearly showed the presence of HA in the composite matrix. EDX analysis showed a relatively higher level of calcium and phosphorus on the surfaces of P(3HO-*co*-3HHX)/30 % HA composite scaffolds compared to P(3HO-*co*-3HHX)/10 % HA samples. Ca/P molar ratios on the surfaces of P(3HO-*co*-3HHX)/10 % HA and P(3HO-*co*-3HHX)/30 % HA were determined at 2.48 and 1.85, respectively. In the EDX spectra, the carbon and oxygen peaks were derived from the polymer (Table 4.2). The presence of HA was revealed by the Ca and P peaks (Rizzi *et al.*, 2001).

In addition, EDX was applied to the composites to monitor HA exposure at the composite surface of porous PHO/HA scaffolds. The weight and atomic percentage of Ca and P element in P(3HO-*co*-3HHX)/30 % HA samples were higher (2.9, 7.0, 1.3, 2.4) than the P(3HO-*co*-3HHX)/10 % HA samples (0.4, 1.5, 0.2, 0.5), respectively. These results showed that the HA particles were successfully incorporated into the P(3HO-*co*-3HHX) matrix. Moreover, it is suggested that high energy ultrasound irradiation (25 kHz) helped to enhance the dispersion of HA particle in the polymer matrix. According to a previous study, ultrasonication has been shown to be an effective means to overcome the agglomeration of particles in the biopolymer (Baei & Rezvani, 2011). Furthermore, good dispersion of inorganic filler in the composite assists to improve the mechanical properties of the composite material (Chen *et al.*, 2005).

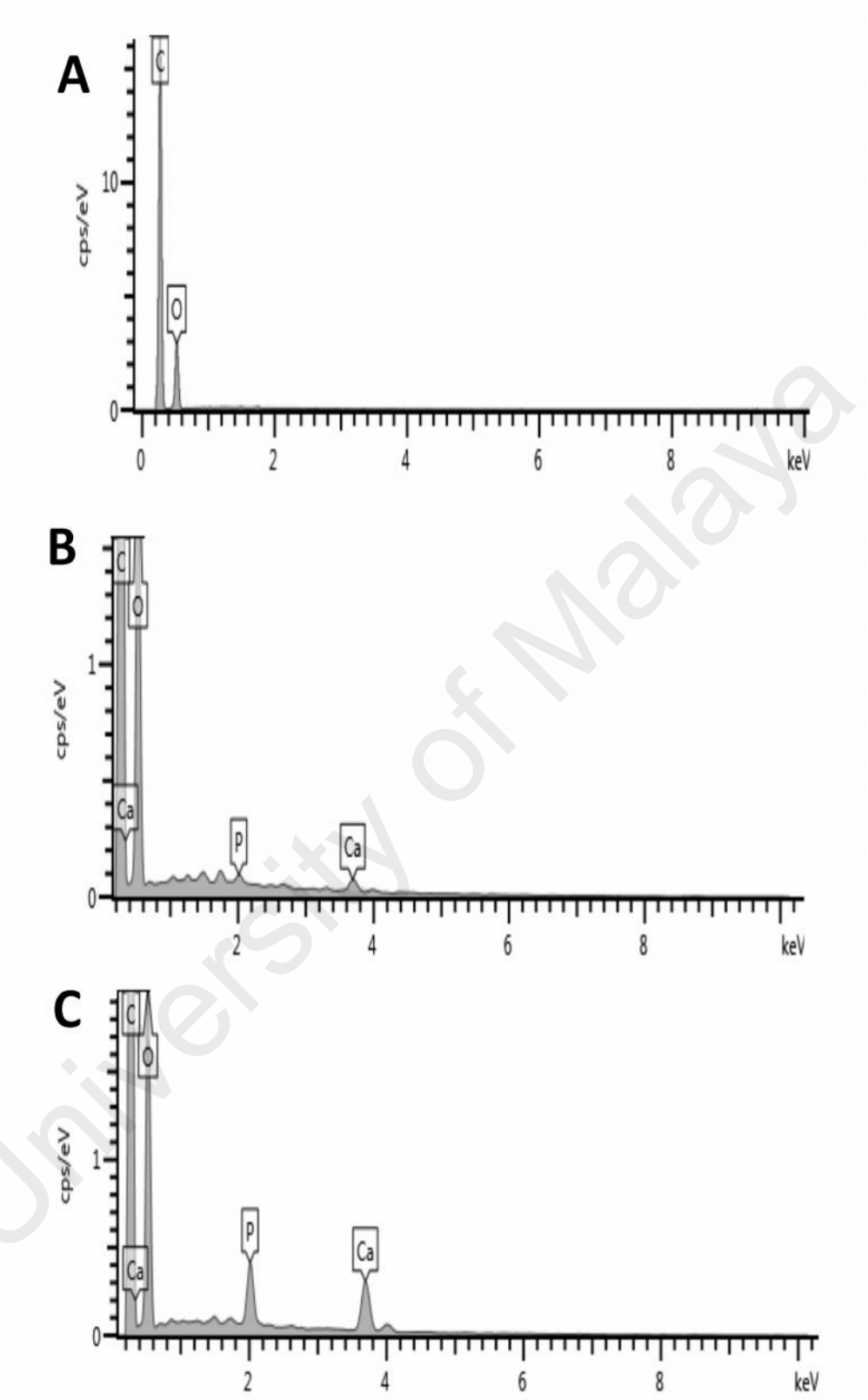

Figure 4.7: EDX spectrum obtained at 10 keV on the (A) P(3HO-*co*-3HHX); (B) P(3HO-*co*-3HHX)/10 % HA and (C) P(3HO-*co*-3HHX)/30 % HA

Table 4.2: Elemental analysis of HA using EDX analysis of P(3HO-*co*-3HHX), P(3HO-*co*-3HHX)/10 % HA and P(3HO-*co*-3HHX)/30 % HA scaffolds.

Element	**Percentage of elements**	
	Weight %	**Atomic %**
P(3HO-*co*-3HHX)		
C	74.4 ± 0.5	79.4 ± 0.4
O	25.6 ± 0.5	20.5 ± 0.4
P(3HO-*co*-3HHX)/10 % HA		
C	71.9 ± 0.8	78.0 ± 0.7
O	26.2 ± 0.7	21.3 ± 0.6
P	0.4 ± 0.0	0.2 ± 0.0
Ca	1.5 ± 0.1	0.5 ± 0.0
P(3HO-*co*-3HHX)/30 % HA		
C	64.4 ± 1.7	74.1 ± 1.1
O	25.7 ± 0.3	22.2 ± 0.5
P	2.9 ± 0.5	1.3 ± 0.3
Ca	7.0 ± 0.9	2.4 ± 0.3

4.2.1.5 Field Emission Scanning Electron Microscope (FESEM)

The morphologies of the scaffolds are shown in Figure 4.8. Both the neat P(3HO-*co*-3HHX) and composite scaffolds showed spongy appearance, high porosity and extensive inter-pores connectivities (Figures 4.8 A, C and E). The porosity of the scaffolds was observed to be in the range of 75 % to 80 % (Table 4.1). The P(3HO-*co*-3HHX)/HA scaffolds (Figures 4.8 C and E) retained porous morphology as that of neat P(3HO-*co*-3HHX) scaffolds (Figure 4.8 A). Pores are necessary for bone tissue formation because they allow migration and proliferation of osteoblasts and mesenchymal cells as well as vascularization. In addition, a porous surface improves mechanical interlocking between the implant biomaterial and the surrounding natural bone, thus providing greater mechanical stability at this critical interface (Karageorgiou & Kaplan, 2005; Pramanik *et al.*, 2009). From SEM images, the mean pore diameter was determined approximately around 100-180 µm. Previous researches suggested that human osteoblasts cells penetrate faster within the scaffolds containing large pores (> 100 µm), meanwhile the extent of mineralization was not affected by the pore size (Akay *et al.*, 2004; Nguyen *et al.*, 2012).

It was found the osteoblast cells were favourably attached to the P(3HO-*co*-3HHX)/30 % HA scaffolds (Figure 4.8 F) as compared to P(3HO-*co*-3HHX)/10 % HA scaffolds (Figure 4.8 D), and significantly less osteoblast cells were found to be able to attach themselves to neat P(3HO-*co*-3HHX) scaffolds (Figure 4.8 B). This was attributed to the increased concentration of dispersed HA that helped to promote the proliferation of osteoblast cells throughout the polymer matrixes. As far as the composite scaffolds prepared in this study were concerned, their porosities were sufficient for good interconnection and transportation of nutrition as evidenced by good cell growth. Hence, the pore size of the scaffolds were favorable for good cell growth.

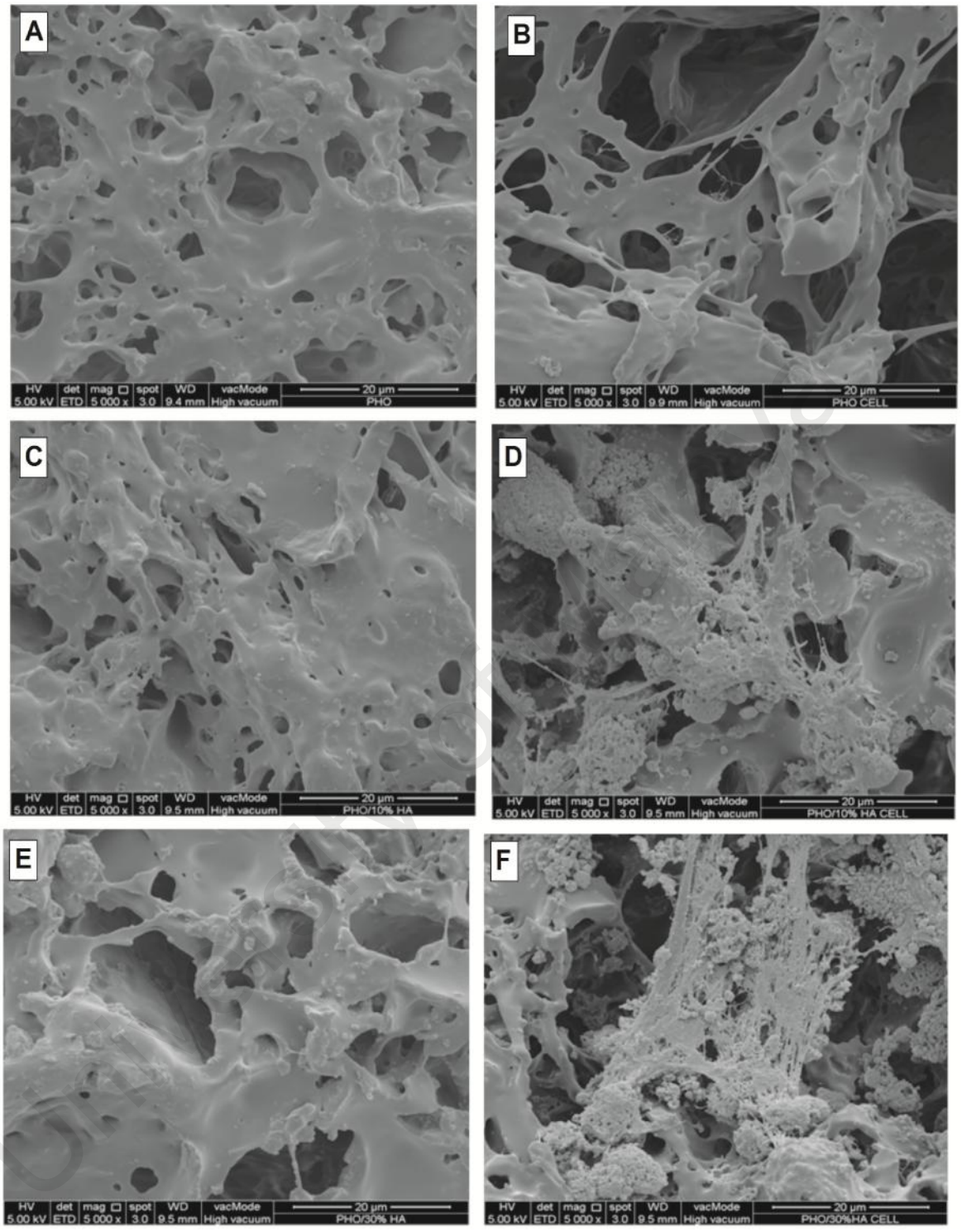

Figure 4.8: FESEM image of the scaffolds (A) P(3HO-*co*-3HHX) (B) cells on scaffold surface P(3HO-*co*-3HHX) (C) composite P(3HO-*co*-3HHX)/10 % HA (D) cells on scaffold surface P(3HO-*co*-3HHX)/10 % HA (E) composite P(3HO-*co*-3HHX)/30 % HA (F) cells on scaffold surface P(3HO-*co*-3HHX)/30 % HA (magnification 5000 ×).

Jack *et al.* (2009) fabricated the PHBV/HA composite scaffolds with high porosity and controlled pore architecture. Their results showed that the incorporation of HA microparticles increased the stiffness and strength and improved the *in vitro* bioactivities of the scaffolds. For bone tissue engineering, biodegradable composite scaffolds containing HA hold great promises. The current investigation demonstrated that HA particles could be homogeneously incorporated into the mcl-PHA to make osteo-conductive porous composite scaffolds.

4.2.2 Biological response of osteoblast cells to P(3HO-*co*-3HHX)/HA composite scaffolds

Further investigation was carried out with osteoblasts cells seeded on pure P(3HO-*co*-3HHX) and P(3HO-*co*-3HHX) matrices containing 10 % and 30 % HA. The attachment and growth of osteoblast cells were assessed using the Alamar Blue Assay (Figure 4.9A). The metabolic activities of the osteoblast cells were analyzed at day 1, 7 and 14. It was found that the percentage of resazurin reduction increased with culture time. From calibration data, it was found that the percentage of resazurin reduction was positively correlated with the cell density. All matrices were able to support the growth of osteoblast cells during 14 days of culture. The percentage of resazurin reduction in neat scaffolds was lower compared to P(3HO-*co*-3HHX)/10 % HA and P(3HO-*co*-3HHX)/30 % HA scaffolds, which indicated that the HA composite scaffolds provided a more favourable physical environment for cell attachment and growth. It has been reported that when the HA content were increased, more particles will be exposed on the surface of the porous scaffold, hence favored the increase in the proliferation of the cells (Huang *et al.*, 2007; Wang *et al.*, 2005). No significant differences were found between P(3HO-*co*-3HHX)/10 % HA and P(3HO-*co*-3HHX)/30 % HA scaffold after 7 and 14 days of culture.

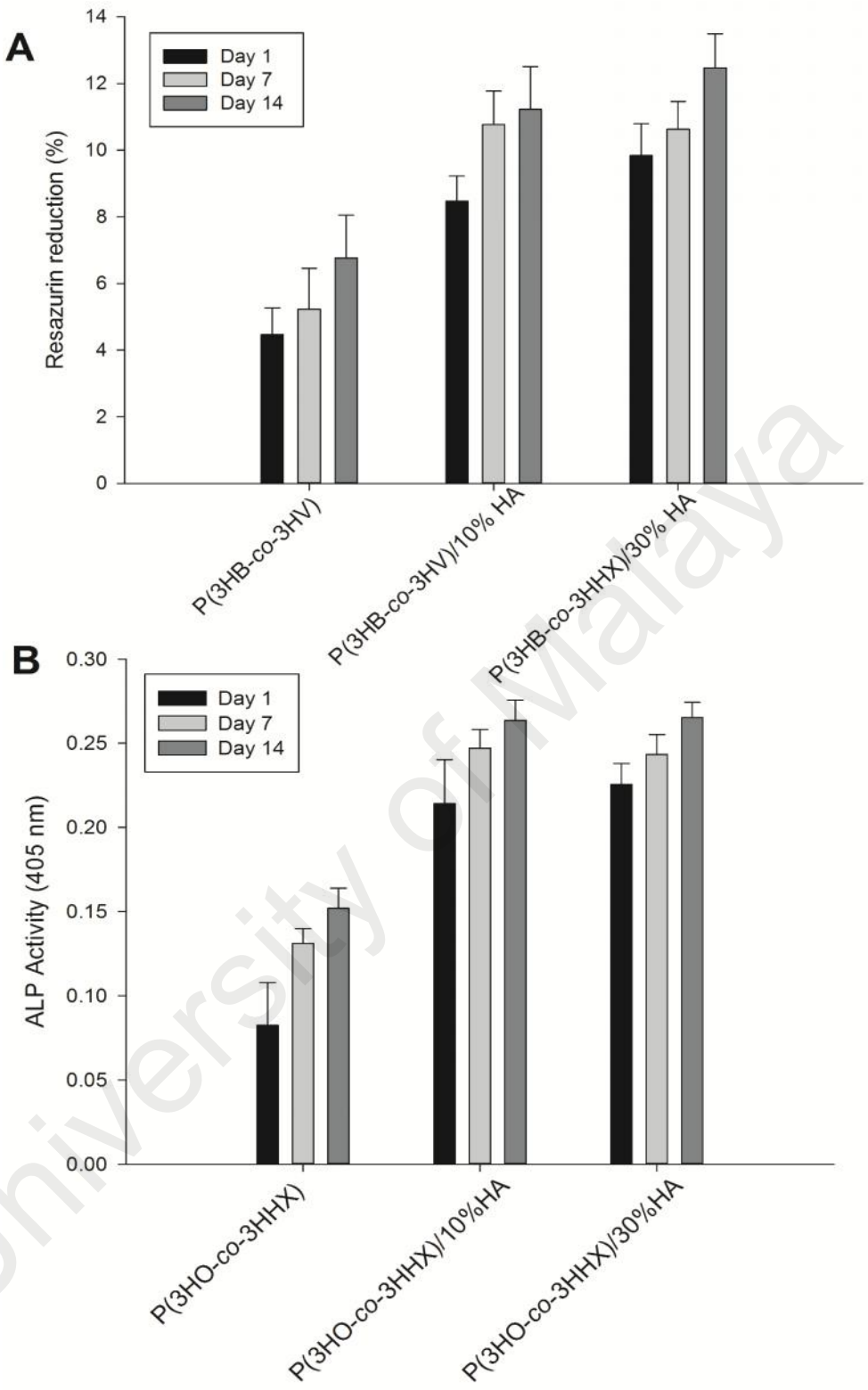

Figure 4.9: (A) Growth of human osteoblast cells (Alamar Blue Assay) (B) ALP activities of human osteoblast cells on P(3HO-*co*-3HHX) PHO, P(3HO-*co*-3HHX)/10 % HA and P(3HO-*co*-3HHX)/30 % HA scaffolds (n = 6)

Both P(3HO-*co*-3HHX)/10 % HA and P(3HO-*co*-3HHX)/30 % HA scaffolds showed highest percentage of resazurin reduction on day 14 relative to neat P(3HO-*co*-3HHX) scaffolds indicating that the recorded cells activities was primarily attributed to their response from HA exposure. In addition, incorporation of hydroxyapatite particles into the composite scaffold has been reported to significantly increase protein adsorption (Wei & Ma, 2004). The microporous structure of composite scaffold provided for greater surface-to-volume ratio, which could have contributed to further increase the proliferation of the osteoblast cells.

The differentiation process of osteoblast cells on neat P(3HO-*co*-3HHX) and P(3HO-*co*-3HHX)/HA composites have been studied from the alkaline phosphatase (ALP) assay (Figure 4.9B). Generally, the ALP activities of cells grown on all scaffolds increased continuously until day 14. In contrast, there was no significant difference on osteoblast cells proliferation between P(3HO-*co*-3HHX)/10 % HA and P(3HO-*co*-3HHX)/30 % HA scaffold after 7 and 14 days of culture. Both P(3HO-*co*-3HHX)/30 % HA and P(3HO-*co*-3HHX)/10 % HA scaffolds showed the highest ALP activities on day 14. The ALP activities of osteoblast cells grown on the neat P(3HO-*co*-3HHX) scaffolds for various culture times were significantly lower than that of the composite HA scaffolds. The results suggested that the presence of dispersed HA within the polymer matrix helped to improve the differentiation of osteoblast cells. The observation was consistent with the previous reports that the polymer–HA scaffolds were superior to the pure polymer scaffolds for tissue engineering because the presence of HA hydroxyl groups promote calcium and phosphate precipitations hence improved interactions with osteoblast cells (Xi *et al.*, 2008).

4.3 Functionalization of mcl-PHA by graft copolymerization P(3HO-*co*-3HHX) with glycerol 1,3-diglycerolate acetate (GDD)

4.3.1 Authentication of P(3HO-*co*-3HHX)-*g*-GDD graft copolymer

4.3.1.1 Fourier transform infrared spectroscopy (FTIR)

Graft copolymerization of glycerol 1,3-diglycerolate (GDD) onto the poly(3-hydroxyoctanoate-*co*-3-hydroxyhexanoate) P(3HO-*co*-3HHX) was carried out with benzoyl peroxide (BPO) as initiator. Figure 4.10 showed the FTIR spectra of neat P(3HO-*co*-3HHX), monomer GDD and grafted copolymer P(3HO-*co*-3HHX)-*g*-GDD with 0.3 and 0.6 mM of initial GDD concentrations. Absorptions at 2930 and 2860 cm^{-1} were attributed to both asymmetric CH_3- and symmetric CH_2- vibrations in the samples, respectively. The presence of carbonyl ester bond in pure mcl-PHA sample was assigned to the absorption at 1727 cm^{-1} (Figure 4.10(a)), and the carbonyl stretching region of GDD monomer at 1718 cm^{-1}. In the grafted copolymer (Figure 4.10 (b) and (c)), carbonyl band absorption was shifted to 1728 cm^{-1}. The broad adsorption at 3431 cm^{-1} was assigned to the stretching vibration of –O-H in hydroxyl group of GDD monomer (Figure 4.10(d)). P(3HO-*co*-3HHX)-*g*-GDD copolymer (Figure 4.10 (b) and (c)) showed a new absorption band at 3415-3450 cm^{-1}, which was attributed to the stretching of the -OH groups in GDD. IR spectra authenticated the grafting of GDD monomer onto the P(3HO-*co*-3HHX) backbone.

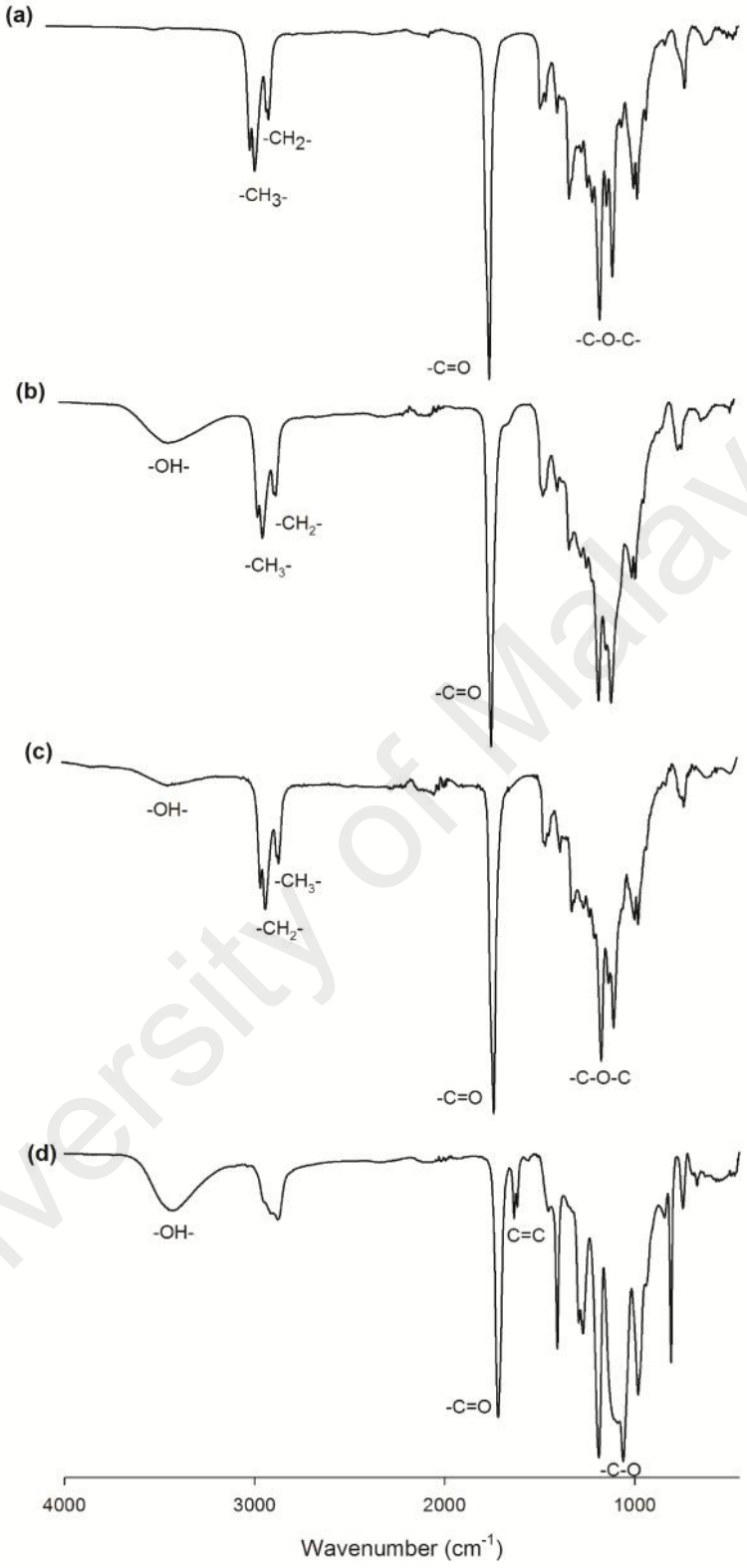

Figure 4.10: FTIR spectra of (a) P(3HO-*co*-3HHX); (b) P(3HO-*co*-3HHX)-*g*-GDD (0.6 mM); (c) P(3HO-*co*-3HHX)-*g*-GDD (0.3 mM); and (d) GDD monomer

4.3.1.2 Proton (^{1}H) nuclear magnetic resonance (NMR)

The chemical structure of the grafted polymer was further authenticated by NMR spectroscopy. Figure 4.11 showed the ^{1}H-NMR spectrum of the grafted copolymer P(3HO-*co*-3HHX)-*g*-GDD. The grafted copolymer was dissolved in deuterated chloroform ($CDCl_3$). In the NMR spectrum of P(3HO-*co*-3HHX)-*g*-GDD, typical signals of mcl-PHA and those of GDD segments were observed. Using internal standard tetramethylsilane (TMS) as the reference, the observed multiplet peaks at 2.6 ppm (1) and at triplets peaks at 5.2 ppm (2) were assigned to methylene ($-CH_2$) and methine (-CH) protons of α- and β- carbon of mcl-PHA backbone, respectively. The signals 1.3 ppm (4) and 0.9 ppm (5) were assigned to methylene ($-CH_2$) proton and terminal methyl ($-CH_3$) proton of the P(3HO-*co*-3HHX) side chain, respectively. The appearance of a new signal for (CH_2-C) at 1.8 ppm (a) constituted evidence that GDD was successfully grafted into the backbone of P(3HO-*co*-3HHX). Chemical shifts *c*, *d*, and *e* were assigned to α, β-protons of methylene group of GDD monomer -COO-CH_2, CH_2-CH(OH) and CH_2-COO-, respectively. Hence, based on the signal analysis, we proposed that the GDD monomers were grafted onto the C-3 carbon of mcl-PHA backbone. The assignment was found to be in accordance with previously reported literatures (Ilter *et al.*, 2001; Lao *et al.*, 2007; Nakas *et al.*, 2015; Renard *et al.*, 2003).

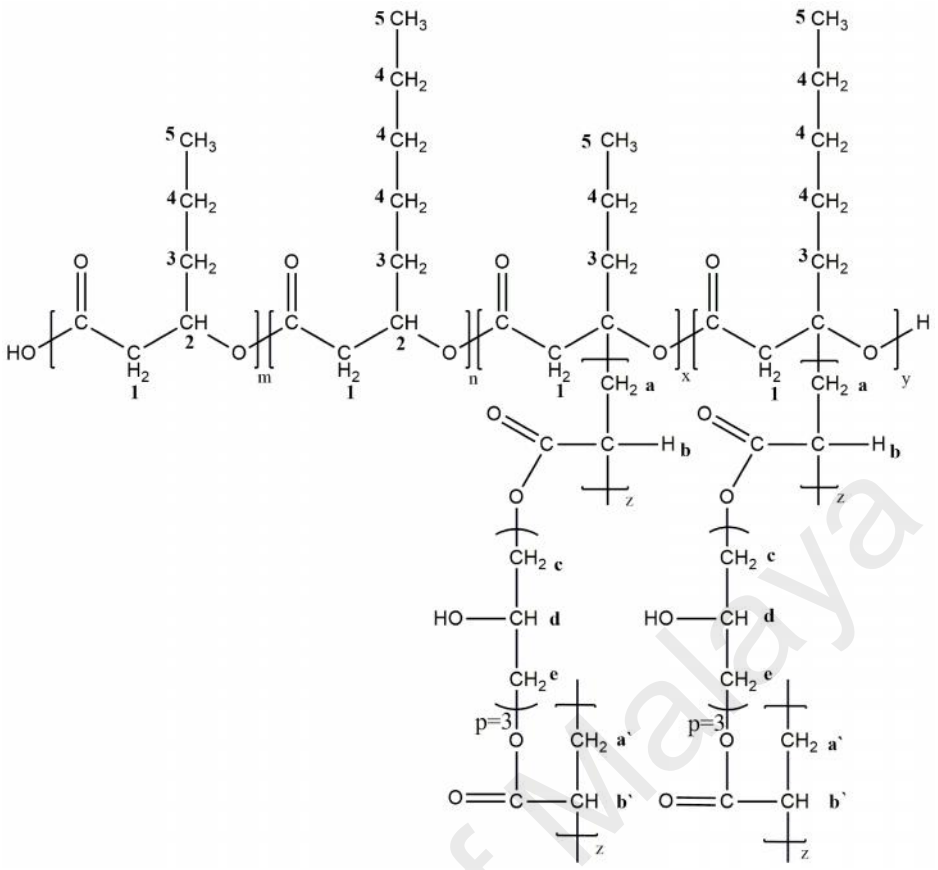

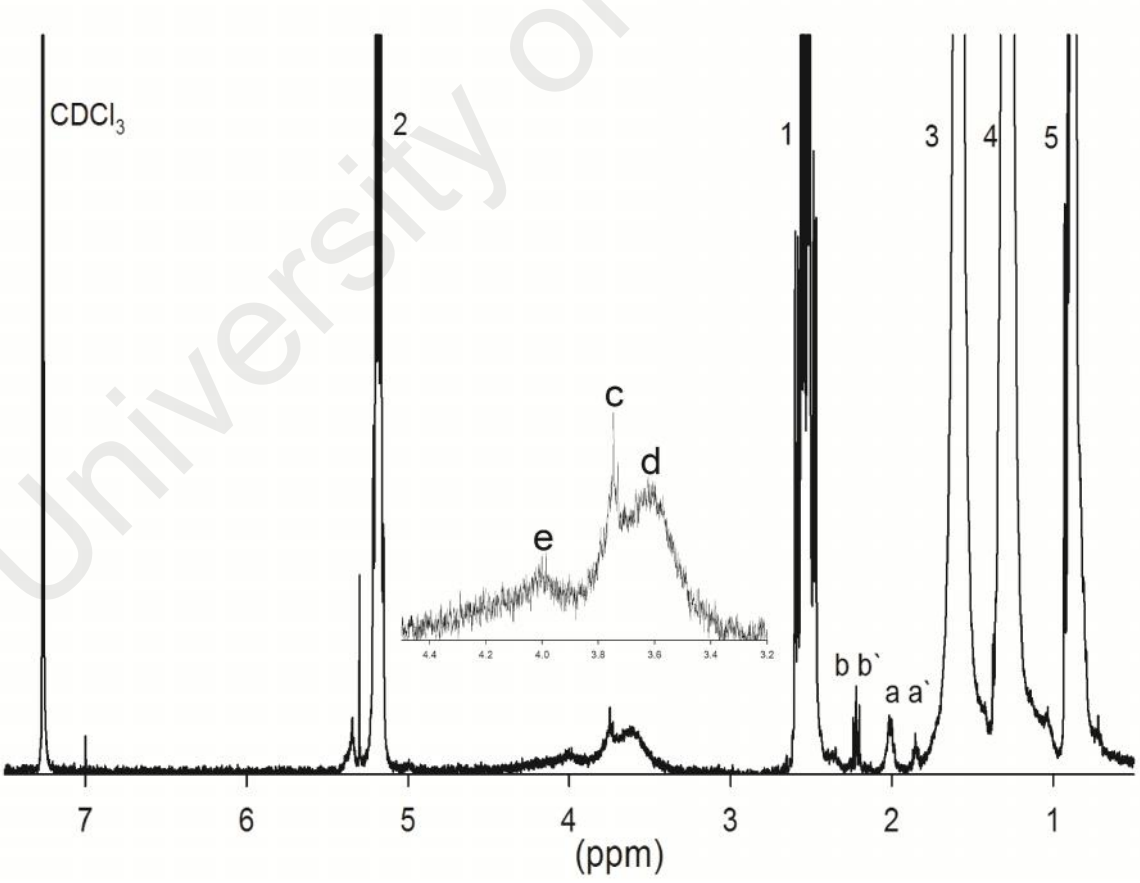

Figure 4.11: ^{1}H NMR of the P(3HO-*co*-3HHX)-*g*-GDD in $CDCL_3$-d_6i (Graft yield = 30 %)

4.3.2 Mechanism of P(3HO-*co*-3HHX) grafting with GDD

Based on the experimental results and previous researches on graft copolymerization, the mechanism for graft copolymerization of P(3HO-*co*-3HHX) by GDD is proposed (Figure 4.12). It is hypothesized that the grafting of GDD monomer onto P(3HO-*co*-3HHX) proceeds *via* three steps which include initiation, propagation and termination reactions. Grafting of GDD onto P(3HO-*co*-3HHX) backbone is proposed to occur *via* three ways: (1) random hydrogen abstraction from P(3HO-*co*-3HHX) backbone by direct attack of initiator radicals (i.e. benzoyl peroxide); (2) chain transfer of GDD growing radicals into P(3HO-*co*-3HHX) backbone; (3) the recombination of GDD and P(3HO-*co*-3HHX) growing radicals. However, during free radical polymerization reaction, both homopolymerization and graft copolymerization could also take place. Chain transfer reaction of GDD proceeds *via* the creation of secondary macroradical of GDD. Consequently, macroradicals could perform reaction with each other, thus generating inter-grafted species of homopolymeric composition (Figure 4.12).

During grafting reactions, polymer radicals produced from active polymers can cause cleavage as well as proton abstraction from the polyester chain (Hazer, 1996; Lao *et al.*, 2007). In free radical polymerization reaction, initiation is the first reaction of a chain carrier with a polymer or monomer molecule to generate a new covalent bond and regenerate reactive centre at a new location. The thermodynamic driving force of these reactions is the replacement of high energy π bond by σ bond (addition) or the replacement of weaker R−H bond by a stronger R′−H (abstraction) (Bhattacharya *et al.*, 2009). The initiation could occur *via* addition, where the radical adds across a double bond of GDD monomer, or by abstraction, where the radical removes a labile H- atom from C-3 carbon of mcl-PHA macromolecule. Grafting is achieved when active

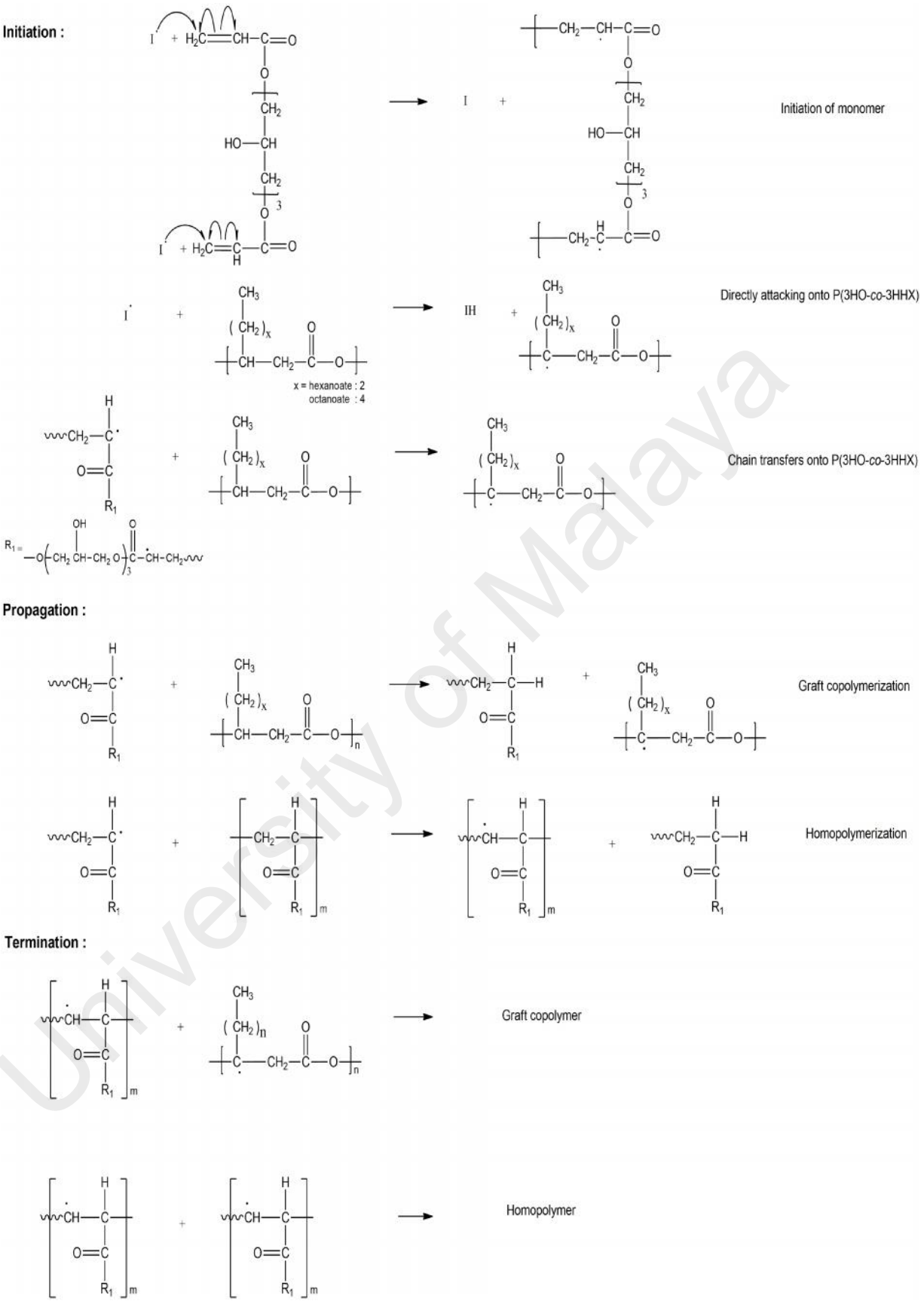

Figure 4.12: Proposed mechanism for the reaction of GDD monomer grafting onto P(3HO-*co*-3HHX) (*I*: initiator benzoyl peroxide; *m* = 1, 2, 3, 4,…..)

polymer decomposes into macroradical, which involves abstracting the proton at the C-3 carbon, and in turn creating radical(s) along the P(3HO-*co*-3HHX) main chain. Coupling of the GDD macroradicals onto the free-radical sites of P(3HO-*co*-3HHX) produced graft copolymer. The presence of diacrylate (-C=C-) in the structure of GDD monomers promotes the formation of radical at both ends. Thus, rapid growth of active chain is enhanced by the formation of graft copolymer. BPO is usually employed as a source of radicals for the initiation of vinyl polymerization and cross-linking of both saturated and unsaturated polymers (Lao *et al.*, 20007). Therefore, the presence of diacrylate in the structure of GDD monomers could promote crosslinking between the chains of PHA.

Ilter *et al.* (2001) reported the presence of double bond opens up possibilities of functionalization in biopolyesters to improve their mechanical and viscoelastic properties. Lao *et al.* (2007) reported the methine protons of PHBHV, which are the most acidic protons, may be abstracted from the backbone to generate macroradicals on the chains of PHBV, thus initiating graft polymerization. Several studies of graft polymerization of PHA also reported that free radical grafting can be initiated at C-3 carbon (-CH(R)-) of the PHA, where the protons are abstracted by free radicals such benzoyl peroxide to form PHA macroradicals. These protons are the most acidic ones along the PHA chains. Alternatively, free radical grafting could proceed *via* polymer chain radical transfer to the PHA backbone (Lao *et al.*, 2007; Lee & Lee, 1997; Nguyen, 2008; Wang *et al.*, 2007). Active radical sites along the PHA backbone chain generated from abstracting the protons at the C-3 carbon positions have been exploited to graft vinyl chains *via* monomer polymerization (Li *et al.*, 2016).

4.3.3 Thermal properties of P(3HO-*co*-3HHX)-*g*-GDD graft copolymer

Thermal analysis of graft copolymer was performed using TGA and DSC. The thermal properties of neat P(3HO-*co*-3HHX) and P(3HO-*co*-3HHX)-*g*-GDD copolymers are listed in Table 4.3. P(3HO-*co*-3HHX)-*g*-GDD copolymers showed higher glass transition temperature (T_g) and lower melting temperature (T_m) compared to neat P(3HO-*co*-3HHX). The T_g and T_m of graft copolymers increased slightly from -33.7 °C to -32.9 °C and decreased signficantly from 54.9 °C to 51.1 °C, respectively, as the concentration of GDD in the copolymers increased. The observation is equally applicable with increasing graft yield from 23 to 127 % (Table 4.3). The presence of GDD groups in the copolymer caused significant structural changes in the P(3HO-*co*-3HHX) chains. It was reported that grafted GDD groups on the poly-3-hydroxyoctanoate (PHO) backbone result in the formation of inter-molecular and intra-molecular hydrogen bonding between GDD grafted chains (Kim *et al.*, 2008). The results suggested that GDD grafting led to the decrease of crystallization ability of P(3HO-*co*-3HHX). Hence, introduction of GDD monomer hindered the crystallization of P(3HO-*co*-3HHX) by introducing chain structural irregularities.

Figure 4.13 showed the TGA curves of neat P(3HO-*co*-3HHX), GDD monomer and P(3HO-*co*-3HHX)-*g*-GDD copolymer samples with different initial concentrations of GDD for grafting reaction. TGA analyses of P(3HO-*co*-3HHX) and graft copolymers were performed to investigate the effects of different initial concentrations of GDD on the thermal degradability of the composites (Figure 4.13(A) and 4.13(B)). Initial degradation temperatures from TGA and maximum degradation temperatures from derivative TGA were reported in Table 4.3. It can be observed that T_d and T_{max} values of neat mcl-PHA were decreased from 277 to 269 °C and 295 to 287 °C, respectively, after being grafted with different concentrations of GDD monomer (Table 4.3).

Table 4.3: Molecular weight, thermal, water uptake and graft yield data of neat P(3HO-*co*-3HHX) and copolymer P(3HO-*co*-3HHX)-*g*-GDD with different concentrations of GDD monomer

Samples	Molecular weights		Thermal analysis				Water uptake (%)	Graft yield (%)
	[a]M_n (x10^3) Da	[a]M_w/M_n	[b]T_d (°C)	[b]T_{max} (°C)	[c]T_m (°C)	[c]T_g (°C)		
P(3HO-*co*-3HHX)	43 ± 0.8	1.89	277	295	54.9	-33.7	2.3 ± 0.3	-
P(3HO-*co*-3HHX)-*g*-GDD								
0.1 mM	47 ± 1.3	1.78	270	285	54.4	-32.6	12.1 ± 0.7	23
0.3 mM	49 ± 2.5	1.67	271	286	50.4	-33.0	22.8 ± 1.9	39
0.4 mM	53 ± 1.9	1.64	273	287	51.4	-33.2	28.2 ± 0.8	59
0.6 mM	61 ± 2.1	1.47	269	287	51.1	-32.9	32.9 ± 1.8	127

[a]Calculated from GPC analysis; [b]Calculated from STA analysis; [c]Calculated from DSC analysis.

M_n number average molecular weight, M_w/M_n polydispersity index, T_d: degradation temperature; T_m: Melting temperature, T_g: glass transition temperature. Reaction condition: P(3HO-*co*-3HHX) 0.2 g; BPO 0.04 mM; 80 °C; 2 h

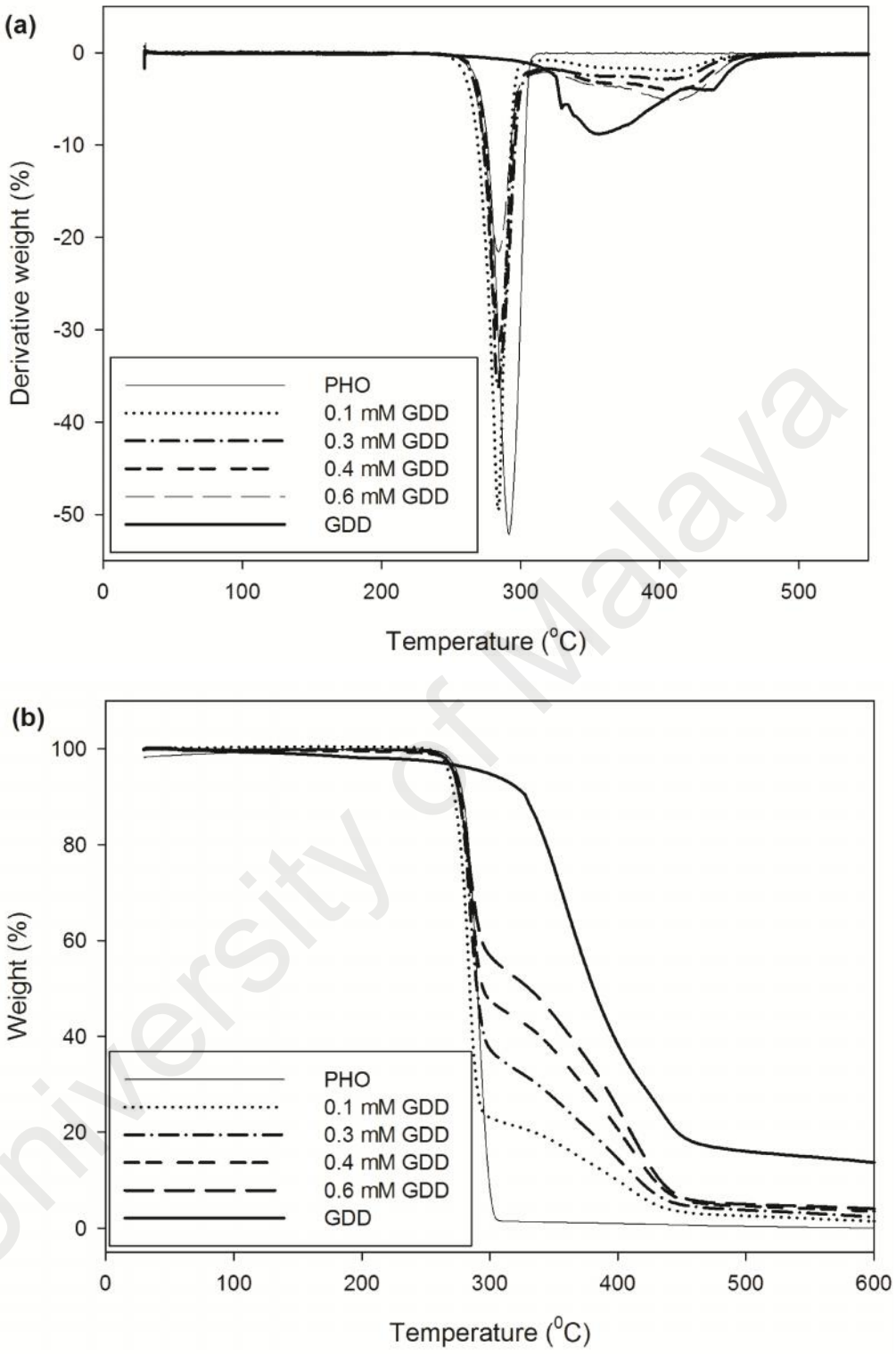

Figure 4.13: (A) Derivative weight percentages of neat P(3HO-*co*-3HHX), GDD monomer and P(3HO-*co*-3HHX)-*g*-GDD with various GDD monomer concentrations. (B) TGA curves of neat P(3HO-*co*-3HHX) and P(3HO-*co*-3HHX)-*g*-GDD with various GDD monomer concentrations

Degradation of GDD monomer and P(3HO-*co*-3HHX)-*g*-GDD began around 100 °C, which was attributed to loss of water (Lao *et al.*, 2007). Although GDD was the first to decompose (T_d 316 °C), it showed the highest thermal stability (T_{max} 327 °C). The shape of all TGA curves was generally similar indicating the thermal degradation of copolymer P(3HO-*co*-3HHX)-*g*-GDD with different graft yields followed similar mechanism. Wang *et al.* (2007) reported that the pattern of TGA curves for PHBV-*g*-PVP was also similar at different graft yields owing to similar mechanism of their thermal degradation.

4.3.4 Molecular weight analysis of P(3HO-*co*-3HHX)-*g*-GDD graft copolymer

GPC was used to obtain the molecular weight and polydispersity data of the graft copolymers (Table 4.3). The measurements showed a single peak corresponding to the molecular weight of the polymer for each sample tested. The number average molecular weights (M_n) of the P(3HO-*co*-3HHX)-*g*-GDD copolymers increased from 4.3 x 10^4 to 6.1 x 10^4 Da with increased initial concentration of GDD. In addition, the polydispersity (M_w/M_n) of the grafted copolymer decreased from 1.89 to 1.47, as the graft yield increased from 23 to 127 % (Table 4.3). It was reported that the radicals produced by hydrogen abstraction following the initiation reaction were involved in secondary reactions which could lead to a degradation of the polymer backbone or crosslinking (Fei *et al.*, 2004; Lao *et al.*, 2007). Thus, the observed results could be ascribed to the hydrogen bonding and possible crosslinking that took place during modification. In other study, grafting of GDD monomer onto the PHO backbone also resulted in a similar increase in molecular weight, hence increased degree of polymer grafting (Kim *et al.*, 2008). Moreover, the increase in molecular weights of P(3HO-*co*-3HHX)-*g*-GDD copolymers and graft yield showed that GDD had been successfully grafted onto P(3HO-*co*-3HHX) chains. Grafting of GDD onto P(3HO-*co*-3HHX)

increased the water uptake ability of the ensuing material (12 – 33 %) relative to neat P(3HO-*co*-3HHX) (2.3 %) (Table 4.3). The observed increase in water uptake ability is primarily due to the hydrophilic properties of GDD monomers. The results also attested to the amphiphilic nature of the graft copolymer.

4.3.5 Reaction parameters of graft copolymerization

4.3.5.1 Effects of the initial monomer concentration

Figure 4.14 showed the graft yield of P(3HO-*co*-3HHX) as a function of GDD monomer concentration in the presence of 0.04 mM BPO as radical initiator for 2 h reaction time at 80 °C. When the initial concentration of GDD monomer was increased from 0.1 to 0.9 mM, the graft yield was also improved from 20 to 170 %, respectively. Increasing the initial monomer concentration helped to increase the probability of the growing chain radical to react with a radical monomer (Lao *et al.*, 2007).

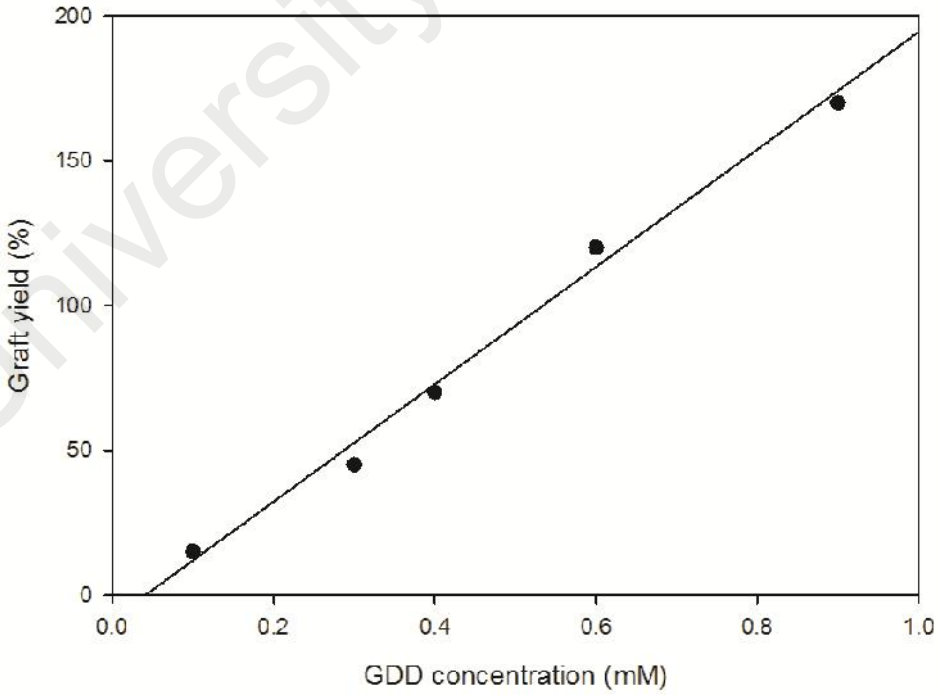

Figure 4.14: Graft yield as a function of the GDD monomer concentration. Reaction conditions: P(3HO-*co*-3HHX) 0.2 g; 80 °C; BPO 0.04 mM; 2 h

4.3.5.2 Effects of reaction time

Free radical reaction is known to be a fast reaction. Figure 4.15 (A) and (B) showed the effects of reaction time and GDD monomer concentration on graft yield in the presence of 0.04 mM BPO at 80 °C and 95 °C, respectively. The graft yield increased as a function of monomer concentration and reaction time. The increase in monomer concentration between 0.1 to 0.9 mM resulted in higher percentage of graft yield. The yield increased rapidly during early phase of reaction period and levelled off after 2 h reaction time. It was attributed to the termination of the polymerization reaction thus formation of dead polymer. Wang *et al.* (2007) reported that after 60 min of reaction time, the yield of PHBV grafted with vinyl group levelled off due to the termination of polymerization reaction. The kinetic chain of radical polymerization could also be ended by the pairing of two radicals to form non radical species (Bhattacharya *et al.*, 2009). The initial rate of grafting (Figure 4.16) was calculated from the initial slope of the curves for each concentration of GDD shown in Figure 4.15 (A) and (B). Higher initial rates of grafting were observed at all initial concentrations of GDD as the reaction temperature was increased from 80 C° to 95 °C. The activation energy (E_a) was calculated based on the Arrhenius equation and the apparent E_a calculated for the graft copolymerization was ~ 51 kJ mol^{-1}.

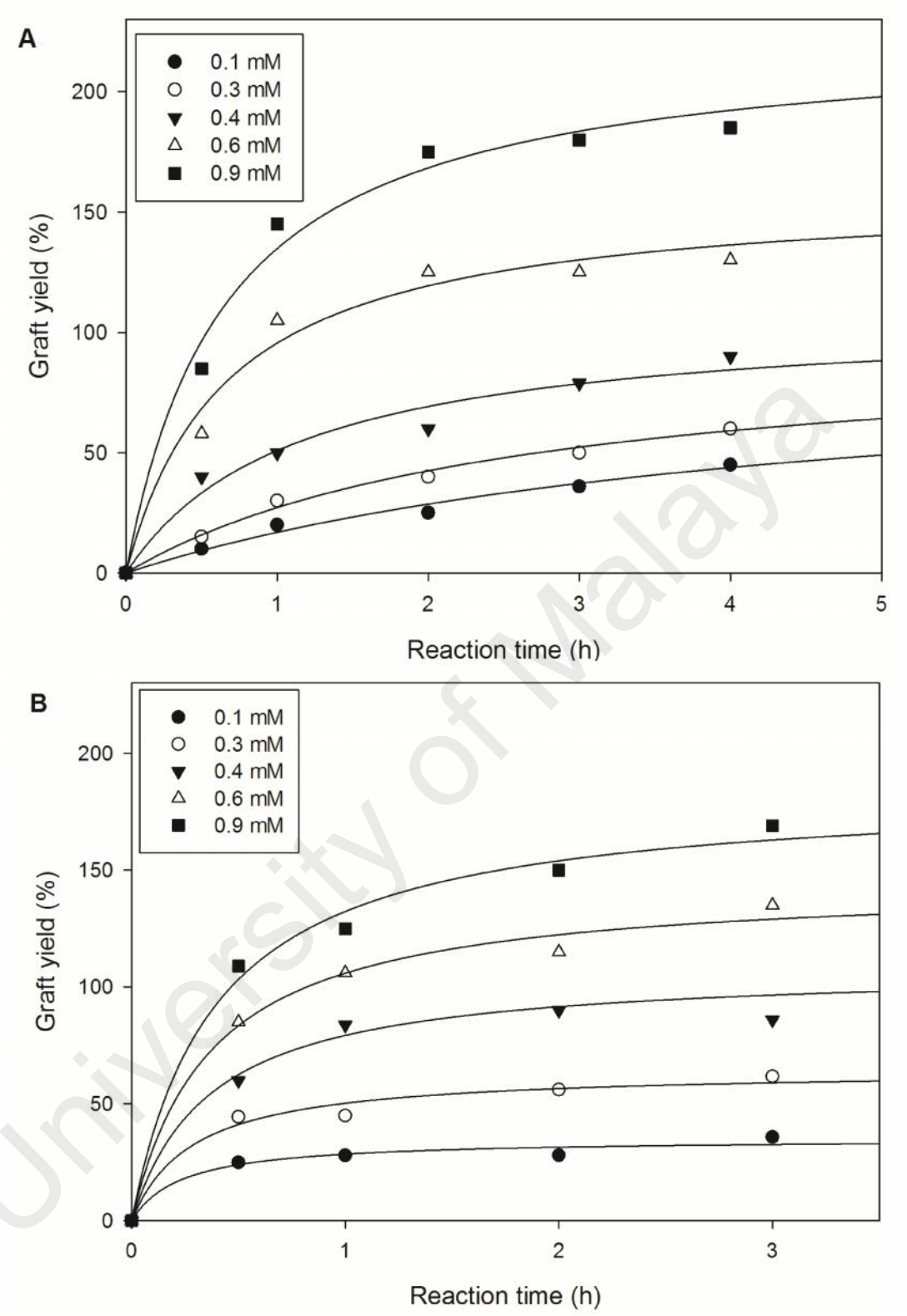

Figure 4.15: Plots of percentage of graft yield as a function of reaction time (h) at different GDD concentrations (mM) and different temperatures (A) 80 °C (B) 95 °C. Reaction conditions: P(3HO-*co*-3HHX) 0.2 g; BPO 0.04 mM; 4 mL acetone (standard deviation of the triplicate measurement was < ± 8 %)

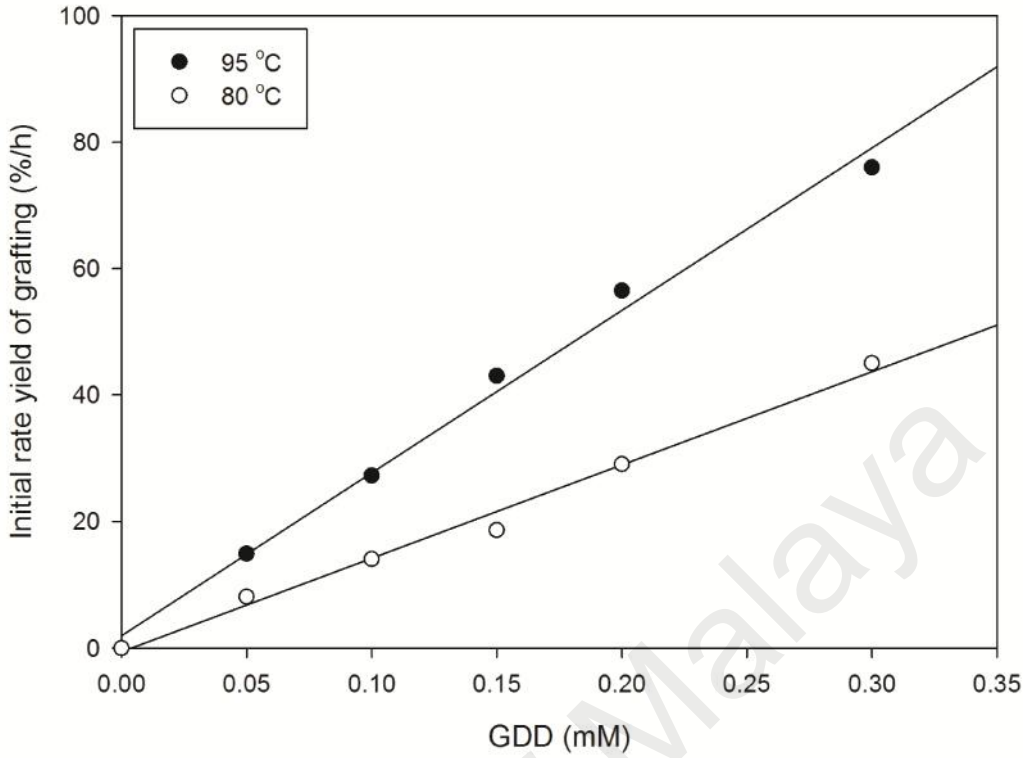

Figure 4.16: Initial rate of grafting as a function of GDD monomer concentration and temperature. Reaction conditions: P(3HO-*co*-3HHX) 0.2 g; 95 °C; BPO 0.04 mM; 4 mL acetone (standard deviation of the triplicate measurement was < ± 5 %)

.3.5.3 Effects of reaction temperature

The effects of reaction temperature on the graft copolymerization are shown in Figure 4.17. The concentration of GDD monomer and BPO were fixed at 0.4 mM and 0.04 mM, respectively, alongside with reaction time of 3 h. The percentage of graft yield was increased as the reaction temperature increased from 70 to 90 °C. The observed effect was associated with the increased in dissociation rate of initiator benzoyl peroxide with temperature (Celik, 2004).

Furthermore, diffusion of GDD monomer into the reaction mixture was likely to be enhanced by the thermal effects. In addition, swellability and mobility of P(3HO-*co*-3HHX) and GDD monomer were also expected to increase as the temperature became higher, and it improved the chances of successful collisions between GDD monomer molecules and P(3HO-*co*-3HHX) macroradicals. Langer and Wilkie (1998) reported that with higher temperature, the swelling of the polymer increased and more radical initiators migrated into the polymer matrix. However, no grafting was observed at temperatures below 65 °C, even after 3 h of reaction. It was attributed to the low rate of initiator benzoyl peroxide dissociation and curtailment of GDD monomer diffusion to penetrate the P(3HO-*co*-3HHX) polymer coil in solution.

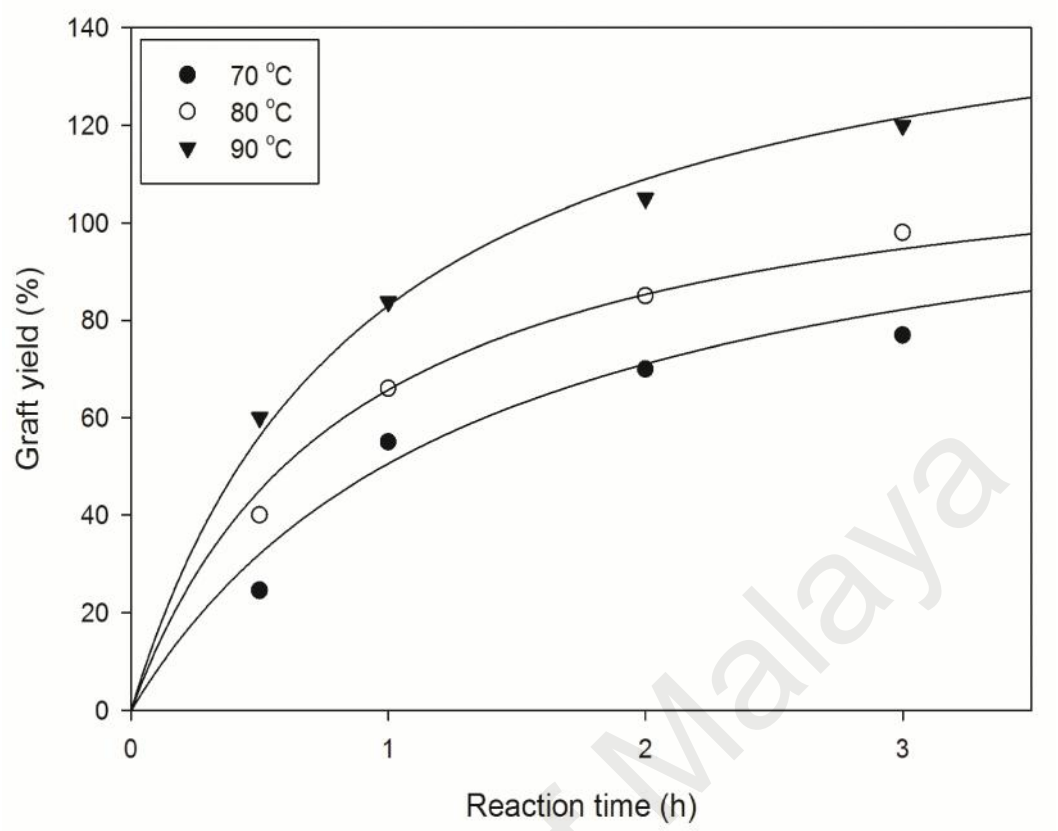

Figure 4.17: Effects of reaction temperature on the graft yield copolymerization of P(3HO-*co*-3HHX)-*g*-GDD. Reaction condition: 0.2 g P(3HO-*co*-3HHX), 0.4 mM GDD, 0.04 mM BPO, 2 h (standard deviation of the triplicate measurement was < ± 5 %)

4.3.5.4 Effects of benzoyl peroxide

The effects of benzoyl peroxide (BPO) concentration on the graft yield is shown in Figure 4.18. The radical initiator concentration was varied from 0.01 to 0.2 mM at 0.4 mM GDD monomer concentration and 80 °C reaction temperature for 3 h reaction time. The graft yield increased with BPO concentration at the beginning, reaching maximum graft yield value of 91 % at 0.04 mM BPO. Subsequently, the graft yield was decreased at higher BPO concentration range i.e. 0.1 to 0.2 mM. Excessive radical concentration in the reaction medium caused the rate of termination reaction to increase, and concomitantly a decrease in graft yield (Celik, 2004).

Similar observation was reported previously and it was attributed to the increased probability of the termination reaction through combination of the growing active chains (Lee & Lee, 1997). The threshold level can be defined as the concentration of radical initiator where the grafting rate and yield started to decline. The initial increase in percentage of graft yield was ascribed to efficient hydrogen abstraction from the backbone at lower concentrations of BPO, which subsequently facilitate the transfer of GDD growing chain to the P(3HO-*co*-3HHX) backbone.

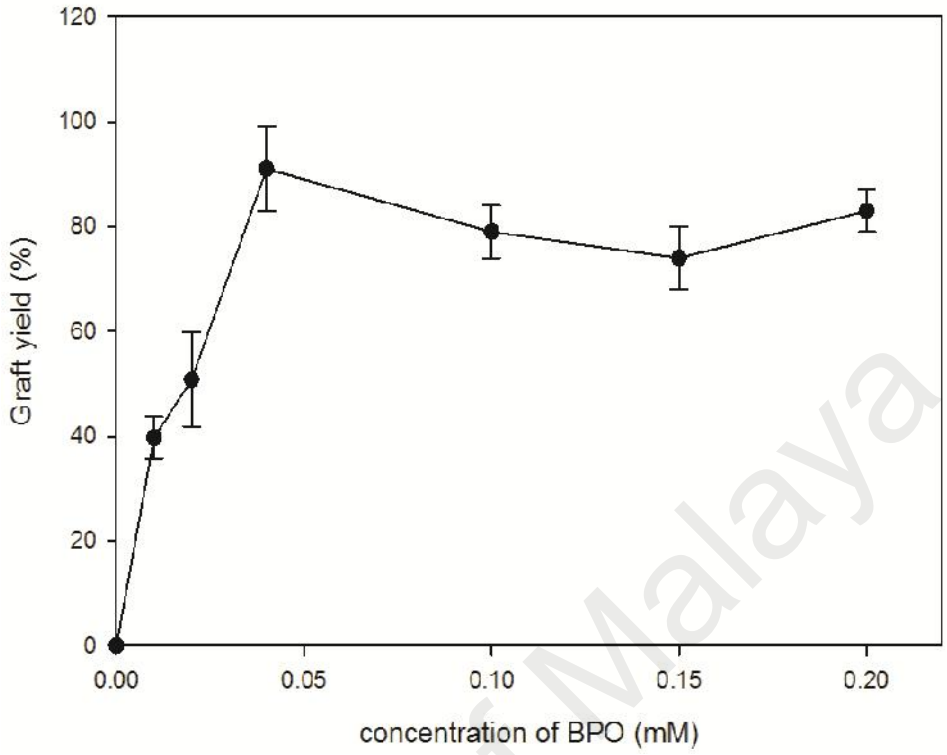

Figure 4.18: Effects of radical initiator (BPO) concentration on the graft yield

4.4 Authentication of P(3HO-*co*-3HHX)-*g*-GDD/HA

Modification of P(3HO-*co*-3HHX) *via* graft copolymerization with GDD (0.1 mM) and blending with 10 weight % of HA led to a novel composite P(3HO-*co*-3HHX)-*g*-GDD/HA. The chemical functional groups of P(3HO-*co*-3HHX)-*g*-GDD/HA were examined by FTIR spectroscopy, as shown in Figure 4.19. The spectra exhibited vibrational bands at 1722 cm^{-1} based on C=O bond of P(3HO-*co*-3HHX) and 732 cm^{-1} based on PO_4^{3-} of the hydroxyapatite, indicating the presence of HA in the polymer matrix. Absorption at 3402 cm^{-1} corresponds to the presence of -OH group of GDD. The results suggested that GDD and HA was successfully grafted and blend into the P(3HO-*co*-3HHX) matrix, respectively.

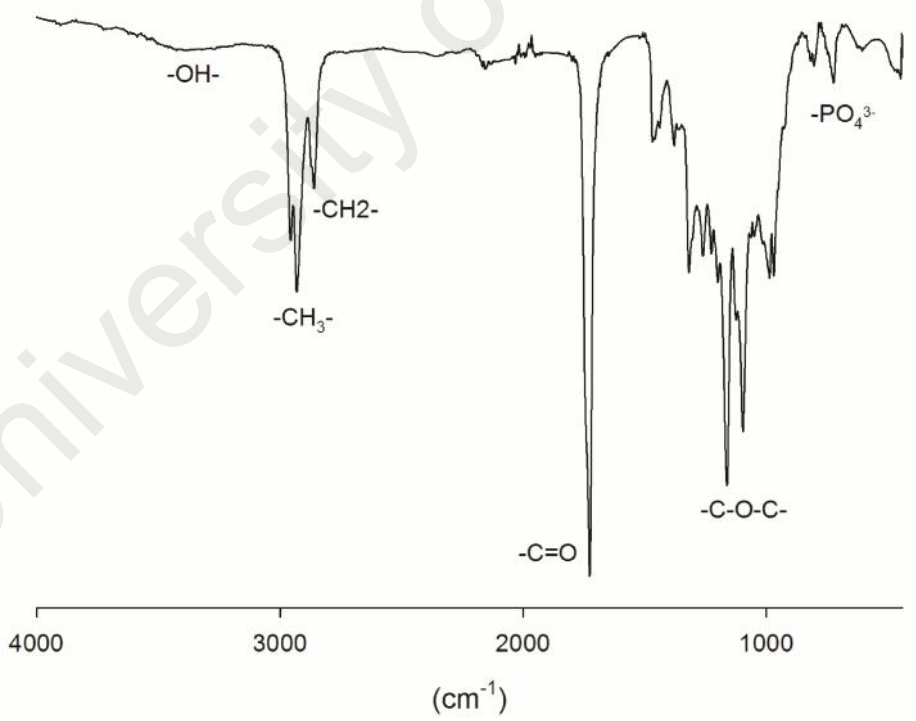

Figure 4.19: FTIR spectra of P(3HO-*co*-3HHX)-*g*-GDD/HA

EDX analysis was applied to establish the distribution of HA particles within the P(3HO-*co*-3HHX)-*g*-GDD/HA composite matrix. Figure 4.20 showed the EDX spectra of P(3HO-*co*-3HHX)-*g*-GDD/HA with the presence of carbon, oxygen, calcium and phosphorus elements, which clearly supported the presence of HA in the composite. The presence of HA was revealed by the Ca and P peaks (Rizzi *et al.*, 2001). The value of Ca/P molar ratio on the surface of P(3HO-*co*-3HHX)-*g*-GDD/HA was determined at 1.25. The weight and atomic percentage of Ca and P element were 1.6, 0.5 and 1.0, 0.4, respectively (Table 4.4). The results showed that the HA particles were successfully incorporated into the P(3HO-*co*-3HHX)-*g*-GDD matrix.

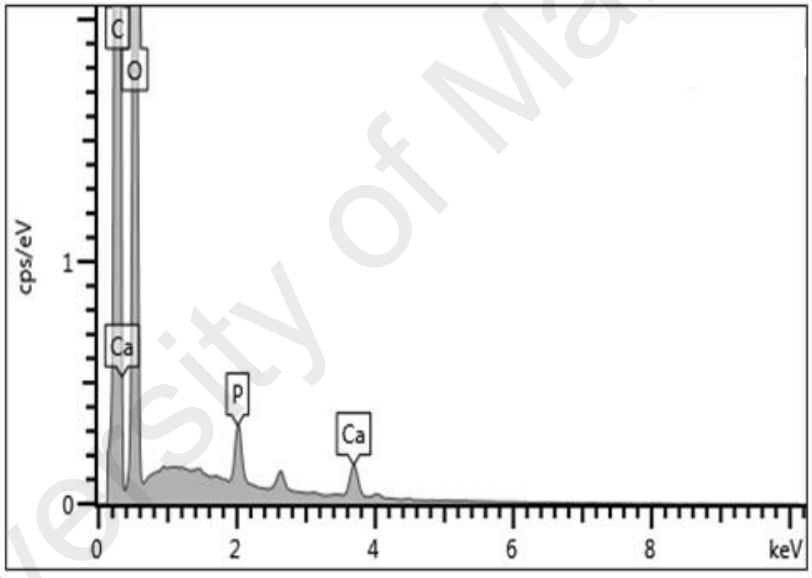

Figure 4.20: EDX spectrum of P(3HO-*co*-3HHX)-*g*-GDD/HA obtained at 10 keV

Table 4.4: Percentage of elements from EDX analysis of P(3HO-*co*-3HHX)-*g*-GDD/HA composite

Element	**Percentage of elements**	
	Weight %	**Atomic %**
P(3HO-*co*-3HHX)-*g*-GDD/HA		
C	72.0 ± 0.6	78.3 ± 0.7
O	25.4 ± 1.2	20.8 ± 0.9
P	1.0 ± 0.2	0.4 ± 0.0
Ca	1.6 ± 0.5	0.5 ± 0.0

4.4.1 Toxicity test of P(3HO-*co*-3HHX)-*g*-GDD/HA using brine shrimp lethality assay (BSLA)

Brine shrimp lethality assay (BSLA) was used to determine the toxicity of polymeric composite of P(3HO-*co*-3HHX)-*g*-GDD/HA. The bioassay is a practical implement for preliminary estimation of biological activities of a wide variety of synthetic and natural products. BSLA is known as the most practical test for toxicology and cytotoxicity of compounds due to its rapidity, convenience and cost-effectiveness (Pelka *et al.*, 2000; Rajabi *et al.*, 2015).

Table 4.5 showed the mean percentage of mortality of *A. franciscana* nauplii after 24 h exposure to aqueous solutions with different concentrations of P(3HO-*co*-3HHX)-*g*-GDD/HA composite. The mean percentage of mortality in negative control was 1.7 %. Meanwhile, the mean percentage of mortality at composite concentrations of 6.25, 12.5, 25, 50 and 100 % was 2.5, 3.3, 2.1, 2.5 and 1.2 %, respectively. No significant difference was found between negative control and aqueous solutions of test material at different concentrations after 24 hours exposure. Thus, it was concluded that toxicity effect of P(3HO-*co*-3HHX)-*g*-GDD/HA composite towards *A. franciscana* nauplii was not observed at all concentrations tested.

Table 4.5: Mean percentage of mortality of *A. franciscana* nauplii after 24 h exposure to aqueous solutions with different concentrations of P(3HO-*co*-3HHX)-*g*-GDD/HA composite

Concentration of sample (%)	Mean mortality of *A. franciscana* (%)
Negative control	1.7 ± 0.2
6.25	2.5 ± 0.1
12.5	3.3 ± 0.2
25	2.1 ± 0.4
50	2.5 ± 0.1
100	1.2 ± 0.1

*Values are mean of three independent experiments with three replicates per sample concentration

CHAPTER 5

CONCLUSIONS

5.1 Conclusions

Medium-chain-length poly(3-hydroxyalkanoates) (mcl-PHA) have been produced by fed-batch fermentation of *P. putida* BET001. 8.6 g L^{-1} of cell dry weight with 63 % mcl-PHA content was obtained after 48 hours fermentation. The mcl-PHA was composed of three different monomers *viz.* 3-hydroxyoctanoate, 3-hydroxyhexanoate and 3-hydroxydecanote at 90 mol %, 8 mol % and 2 mol % respectively.

Modification of P(3HO-*co*-3HHX) *via* physical blending with hydroxyapatite (HA) and chemical grafting with glycerol 1,3-diglecerol diacrylate (GDD) was carried out. A porous composite scaffold made of mcl-PHA and hydroxyapatite (HA) was successfully fabricated using facile particulate leaching technique. Based on FESEM and EDX analyses, the scaffolds were found to be highly porous with interconnecting pore structures and the HA particles were homogeneously dispersed in the polymer matrix. The scaffolds showed excellent biocompatibility and osteoconductivity characteristics based on strong proliferation and differentiation of osteoblast cells on them. Thus, scaffolds made from P(3HO-*co*-3HHX)/HA composites are viable candidate materials for bone tissue engineering application.

Moreover, GDD monomer was successfully grafted onto P(3HO-*co*-3HHX) using benzoyl peroxide as radical initiator. P(3HO-*co*-3HHX)-*g*-GDD graft copolymer were formed following chain transfer and chain termination by recombinant reactions. Introduction of hydroxyl group onto P(3HO-*co*-3HHX) backbone improved the wettability and impart amphilicity to the grafted polymer, thus potentially improving their abilities for cellular interaction. The graft yield could be modulated by varying the

monomer concentration, initiator concentration, temperature and reaction time. The optimum concentration of radical initiator was determined at 0.04 mM and graft yield was observed to increase with initial monomer concentration. Amphiphilic copolymer such as P(3HO-*co*-3HHX)-*g*-GDD obtained from the grafting of natural biopolyester adds to the available repertoire of functional materials.

P(3HO-*co*-3HHX)-*g*-GDD/HA composite was also successfully fabricated *via* graft copolymerization reaction and physical blending of HA to further improve the properties of the neat mcl-PHA. Toxicity of the composite was studied against *Artemia franciscana* in brine shrimp lethality assay. No significant mortality of the test organism was recorded, thus implied that the novel scaffold posed negligible toxicity risk to the cell. It is concluded that P(3HO-*co*-3HHX)-*g*-GDD/HA composite is potentially useful for biomedical applications. It is also envisaged that future exploration with regards to other composite materials and compositing methods for fabrication of biologically active materials using medium-chain-length PHA as base component would undoubtedly discover more potentialities, hence future applications.

5.2 Future research plan

The findings of this study have generated interesting directions for pursuing future works. There are still much to be investigated regarding the modification of mcl-PHA. Suggestions for future research following the current study are as follows:

1. The composite copolymer P(3HO-*co*-3HHX)/ HA can be further tailor-designed using different techniques such as elctrospinning, freeze-drying method, melt-compressed etc. in order to meet specific requirements of intended applications;

2. *In vivo* study of P(3HO-*co*-3HHX)/HA scaffold to be carried out by material implantation in laboratory animals with femoral defect to determine associated biological responses ;

3. The grafted copolymer P(3HO-*co*-3HHX)-*g*-GDD showed a good potential as scaffold material, hence it is necessary to determine its biocompatibility using *in vitro* and *in vivo* studies;

4. Further studies on the biodegradability behavior of the modified copolymer are suggested in view of potential theranostic applications.

REFERENCES

Akay, G., Birch, M. & Bokhari, M. (2004). Microcellular polyhipe polymer supports osteoblast growth and bone formation *in vitro*. *Biomaterials, 25*(18), 3991-4000.

Aldor, I. S. & Keasling, J. D. (2003). Process design for microbial plastic factories: metabolic engineering of polyhydroxyalkanoates. *Current Opinion in Biotechnology, 14*(5), 475-483.

Ali, I. & Jamil, N. (2016). Polyhydroxyalkanoates: current applications in the medical field. *Frontiers in Biology, 11*(1), 19-27.

Amache, R., Sukan, A., Safari, M., Roy, I. & Keshavarz, T. (2013). Advances in PHAs production. *Chemical Engineering, 32*, 931-936.

Annuar, M., Tan, I. K. & Ramachandran, K. (2008). Evaluation of nitrogen sources for growth and production of medium-chain-length poly-(3-hydroxyalkanoates) from palm kernel oil by *Pseudomonas Putida* PGA1. *Asia Pacific Journal of Molecular Biology and Biotechnology, 16(1)*, 11-15.

Annuar, M. S. M., Tan, I., Ibrahim, S. & Ramachandran, K. (2006). Production of medium-chain-length poly (3-hydroxyalkanoates) from saponified palm kernel oil by *Pseudomonas Putida*: kinetics of batch and fed-batch fermentations. *Malaysian Journal of Microbiology, 2*(2), 1-9.

Annuar, M. S. M. (2004). *Production of medium-chain-length poly (3-hydroxyalkanoates) from saponified palm kernel oil by Pseudomonas putida*. (Doctoral dissertation) University of Malaya.

Arslan, H., Hazer, B. & Yoon, S. C. (2007a). Grafting of poly (3-hydroxyalkanoate) and linoleic acid onto chitosan. *Journal of Applied Polymer Science, 103*(1), 81-89.

Arslan, H., Yeşilyurt, N. & Hazer, B. (2007b). The synthesis of poly (3-hydroxybutyrate)-g-poly(methylmethacrylate) brush type graft copolymers by atom transfer radical polymerization Method. *Journal of Applied Polymer Science, 106*(3), 1742-1750.

Avci, D. & Mathias, L. J. (2004). Synthesis and photopolymerizations of new hydroxyl-containing dimethacrylate crosslinkers. *Polymer, 45*(6), 1763-1769.

Baei, M. S. & Rezvani, A. (2011). Nanocomposite (PHBHV/HA) fabrication from biodegradable polymer. *Middle-East Journal of Scientific Research, 7*(1), 46-50.

Baek, J.-Y., Xing, Z.-C., Kwak, G., Yoon, K.-B., Park, S.-Y., Park, L. S. & Kang, I.-K. (2012). Fabrication and characterization of collagen-immobilized porous PHBV/HA nanocomposite scaffolds for bone tissue engineering. *Journal of Nanomaterials, 2012*, 1-11.

Bassas-Galià, M., Gonzalez, A., Micaux, F., Gaillard, V., Piantini, U., Schintke, S., Zinn, M., & Mathieu, M. (2015). Chemical modification of polyhydroxyalkanoates (PHAs) for the preparation of hybrid biomaterials. *CHIMIA International Journal for Chemistry, 69*(10), 627-630.

Bayram, C., Denkbaş, E. B., Kiliçay, E., Hazer, B., Çakmak, H. B. & Noda, I. (2008). Preparation and characterization of triamcinolone acetonide-loaded poly (3-hydroxybutyrate-co-3-hydroxyhexanoate)(PHBHX) microspheres. *Journal of Bioactive and Compatible Polymers, 23*(4), 334-347.

Bhatt, R., Shah, D., Patel, K. & Trivedi, U. (2008). Pha–rubber blends: synthesis, characterization and biodegradation. *Bioresource Technology, 99*(11), 4615-4620.

Bhattacharya, A. & Misra, B. (2004). Grafting: a versatile means to modify polymers: techniques, factors and applications. *Progress in Polymer Science, 29*(8), 767-814.

Bhattacharya, A., Rawlins, J. W. & Ray, P. (2009). *Polymer grafting and crosslinking*: Wiley Online Library.

Bian, Y.Z., Wang, Y., Aibaidoula, G., Chen, G.-Q. & Wu, Q. (2009). Evaluation of poly (3-hydroxybutyrate-co-3-hydroxyhexanoate) conduits for peripheral nerve regeneration. *Biomaterials, 30*(2), 217-225

Boeree, N., Dove, J., Cooper, J., Knowles, J. & Hastings, G. (1993). Development of a degradable composite for orthopaedic use: mechanical evaluation of an hydroxyapatite-polyhydroxybutyrate composite material. *Biomaterials, 14*(10), 793-796

Boccaccini, A. R. & Blaker, J. J. (2005). Bioactive composite materials for tissue engineering scaffolds. *Expert Review of Medical Devices, 2*(3), 303-317.

Brigham, C. J. & Sinskey, A. J. (2012). Applications of polyhydroxyalkanoates in the medical industry. *International Journal of Biotechnology for Wellness Industries, 1*(1), 52.

Cakmakli, B., Hazer, B. & Borcakli, M. (2001). Poly(styrene peroxide) and poly(methyl methacrylate peroxide) for grafting on unsaturated bacterial polyesters. *Macromolecular Bioscience, 1*(8), 348-354.

Celik, M. (2004). Graft copolymerization of methacrylamide onto acrylic fibers initiated by benzoyl peroxide. *Journal of Applied Polymer Science, 94*(4), 1519-1525.

Chan, S. M. (2012). *Thermodegradation of medium-chain-length poly(3-hydroxyalkanoates), and assessment of the biopolyesters and oligoesters as plasticizer for poly(vinyl chloride).* (Doctoral dissertation) University of Malaya.

Chanprateep, S., Katakura, Y., Visetkoop, S., Shimizu, H., Kulpreecha, S. & Shioya, S. (2008). characterization of new isolated *Ralstonia Eutropha* strain A-04 and kinetic study of biodegradable copolyester poly(3-hydroxybutyrate-*co*-4-hydroxybutyrate) production. *Journal of Industrial Microbiology & Biotechnology, 35*(11), 1205-1215.

Chardron, S., Bruzaud, S., Lignot, B., Elain, A. & Sire, O. (2010). Characterization of bionanocomposites based on medium chain length polyhydroxyalkanoates synthesized by *Pseudomonas Oleovorans*. *Polymer Testing, 29*(8), 966-971.

Chen, G. Q. & Wu, Q. (2005). The application of polyhydroxyalkanoates as tissue engineering materials. *Biomaterials, 26*(33), 6565-6578.

Chen, G., Ushida, T. & Tateishi, T. (2002). Scaffold design for tissue engineering. *Macromolecular Bioscience, 2*(2), 67-77.

Chen, Q., Liang, S. & Thouas, G. A. (2013). Elastomeric biomaterials for tissue engineering. *Progress in Polymer Science, 38*(3), 584-671.

Chen, W., Tao, X., Xue, P. & Cheng, X. (2005). Enhanced mechanical properties and morphological characterizations of poly(vinyl alcohol)–carbon nanotube composite films. *Applied Surface Science, 252*(5), 1404-1409

Chen, X., Yang, X., Pan, J., Wang, L. & Xu, K. (2010). Degradation behaviors of bioabsorbable P3/4HB monofilament suture in vitro and in vivo. *Journal of Biomedical Materials Research Part B: Applied Biomaterials*, 92(2), 447-455

Chung, C. W., Kim, H. W., Kim, Y. B. & Rhee, Y. H. (2003). Poly(ethylene glycol)-grafted poly(3-hydroxyundecenoate) networks for enhanced blood compatibility. *International Journal of Biological Macromolecules, 32*(1), 17-22.

Chung, M. G., Kim, H. W., Kim, B. R., Kim, Y. B. & Rhee, Y. H. (2012). Biocompatibility and antimicrobial activity of poly(3-hydroxyoctanoate) grafted with vinylimidazole. *International Journal of Biological Macromolecules, 50*(2), 310-316.

Du, G. & Yu, J. (2002). Metabolic analysis on fatty acid utilization by Pseudomonas oleovorans: mcl-poly (3-hydroxyalkanoates) synthesis versus *β*-oxidation. *Process Biochemistry*, 38(3), 325-332.

Doi, Y. (1990). *Microbial polyesters.* New York: VCH Publishers, Inc., Yokohama, Japan.

Doyle, C., Tanner, E. & Bonfield, W. (1991). In vitro and in vivo evaluation of polyhydroxybutyrate and of polyhydroxybutyrate reinforced with hydroxyapatite. *Biomaterials, 12*(9), 841-847

El-Hadi, A., Schnabel, R., Straube, E., Müller, G. & Henning, S. (2002). Correlation between degree of crystallinity, morphology, glass temperature, mechanical properties and biodegradation of poly(3-hydroxyalkanoate) PHAs and their blends. *Polymer Testing, 21*(6), 665-674.

Fei, B., Chen, C., Chen, S., Peng, S., Zhuang, Y., An, Y. & Dong, L. (2004). Crosslinking of poly[(3-hydroxybutyrate)-*co*-(3-hydroxyvalerate)] using dicumyl peroxide as initiator. *Polymer International, 53*(7), 937-943.

Freier, T., Kunze, C., Nischan, C., Kramer, S., Sternberg, K., Saß, M., . . . Schmitz, K.-P. (2002). *In vitro* and *in vivo* degradation studies for development of a biodegradable patch based on poly (3-hydroxybutyrate). *Biomaterials, 23*(13), 2649-2657.

Furrer, P., Panke, S. & Zinn, M. (2007). Efficient recovery of low endotoxin medium-chain-length poly([R]-3-hydroxyalkanoate) from bacterial biomass. *Journal of Microbiological Methods, 69*(1), 206-213.

Gumel, A. M., Annuar, M. S. & Heidelberg, T. (2012). Biosynthesis and characterization of polyhydroxyalkanoates copolymers produced by *Pseudomonas Putida* Bet001 isolated from palm oil mill effluent. *PLOS ONE, 7*(9), e45214.

Gumel, A., Annuar, M., Ishak, K. & Ahmad, N. (2014). Carbon nanofibers-poly-3-hydroxyalkanoates nanocomposite: ultrasound-assisted dispersion and thermostructural properties. *Journal of Nanomaterials, 2014*,123.

Gumel, A., Aris, M. & Annuar, M. (2014). Modification of polyhydroxyalkanoates (PHAs). In I. Roy & P. M. Visakh (Eds.), *Polyhydroxyalkanoate (PHA) based blends, composites and nanocomposites* (pp. 141-182). UK: The Royal Society of Chemistry.

Gursel, I., Yagmurlu, F., Korkusuz, F. & Hasirci, V. (2002). *In vitro* antibiotic release from poly (3-hydroxybutyrate-*co*-3-hydroxyvalerate) rods. *Journal of Microencapsulation, 19*(2), 153-164

Guzmán, D., Kirsebom, H., Solano, C., Quillaguamán, J. & Hatti-Kaul, R. (2011). Preparation of hydrophilic poly(3-hydroxybutyrate) macroporous scaffolds through enzyme-mediated modifications. *Journal of Bioactive and Compatible Polymers, 26*(5), 452-463.

Hazer, B. (1996). Poly (β-hydroxynonanoate) and polystyrene or poly(methyl methacrylate) graft copolymers: microstructure characteristics and mechanical and thermal behavior. *Macromolecular Chemistry and Physics, 197*(2), 431-441.

Hazer, B. (2010). Amphiphilic poly (3-hydroxyalkanoate)s: potential candidates for medical applications. *International Journal of Polymer Science, 2010*, 1-8.

Hazer, B. & Steinbüchel, A. (2007). Increased diversification of polyhydroxyalkanoates by modification reactions for industrial and medical applications. *Applied Microbiology and Biotechnology, 74*(1), 1-12.

Hazer, D. B., Kılıçay, E. & Hazer, B. (2012). Poly(3-hydroxyalkanoate)s: Diversification and biomedical applications: A state of the art review. *Materials Science and Engineering: C, 32*(4), 637-647.

Hu, S. G., Jou, C. H. & Yang, M. C. (2003). Antibacterial and biodegradable properties of polyhydroxyalkanoates grafted with chitosan and chitooligosaccharides *via* ozone treatment. *Journal of Applied Polymer Science, 88*(12), 2797-2803.

Huang, J., Lin, Y. W., Fu, X. W., Best, S. M., Brooks, R. A., Rushton, N. & Bonfield, W. (2007). Development of nano-sized hydroxyapatite reinforced composites for tissue engineering scaffolds. *Journal of Materials Science: Materials in Medicine, 18*(11), 2151-2157.

Ilter, S., Hazer, B., Borcakli, M. & Atici, O. (2001). Graft copolymerisation of methyl methacrylate onto a bacterial polyester containing unsaturated side chains. *Macromolecular Chemistry and Physics, 202*(11), 2281-2286.

Jack, K. S., Velayudhan, S., Luckman, P., Trau, M., Grøndahl, L. & Cooper-White, J. (2009). The fabrication and characterization of biodegradable ha/phbv nanoparticle–polymer composite scaffolds. *Acta Biomaterialia, 5*(7), 2657-2667.

Jenkins, D. W. & Hudson, S. M. (2001). Review of vinyl graft copolymerization featuring recent advances toward controlled radical-based reactions and illustrated with chitin/chitosan trunk polymers. *Chemical Reviews, 101*(11), 3245-3274.

Jiang, X. J., Sun, Z., Ramsay, J. A. & Ramsay, B. A. (2013). Fed-batch production of mcl-pha with elevated 3-hydroxynonanoate content. *AMB Express, 3*(1), 1-8.

Jung, K., Hazenberg, W., Prieto, M. & Witholt, B. (2001). Two-stage continuous process development for the production of medium-chain-length poly(3-hydroxyalkanoates). *Biotechnology and Bioengineering, 72*(1), 19-24.

Kabilan, S., Ayyasamy, M., Jayavel, S. & Paramasamy, G. (2012). *Pseudomonas* sp. as a source of medium chain length polyhydroxyalkanoates for controlled drug delivery: perspective. *International Journal of Microbiology, 2012*, 1-10.

Kai, D. & Loh, X. J. (2013). Polyhydroxyalkanoates: Chemical modifications toward biomedical applications. *ACS Sustainable Chemistry & Engineering, 2*(2), 106-119.

Kai, Z., Ying, D. & Guo-Qiang, C. (2003). Effects of surface morphology on the biocompatibility of polyhydroxyalkanoates. *Biochemical Engineering Journal, 16*(2), 115-123

Kansiz, M., Domínguez-Vidal, A., Mcnaughton, D. & Lendl, B. (2007). Fourier-transform infrared (FTIR) spectroscopy for monitoring and determining the degree of crystallisation of polyhydroxyalkanoates (PHAs). *Analytical and Bioanalytical Chemistry, 388*(5-6), 1207-1213.

Karageorgiou, V. & Kaplan, D. (2005). Porosity of 3D biomaterial scaffolds and osteogenesis. *Biomaterials, 26*(27), 5474-5491.

Katti, D. S., Vasita, R. & Shanmugam, K. (2008). Improved biomaterials for tissue engineering applications: surface modification of polymers. *Current Topics in Medicinal Chemistry, 8*(4), 341-353.

Kim, D. Y., Kim, H. W., Chung, M. G. & Rhee, Y. H. (2007). Biosynthesis, modification, and biodegradation of bacterial medium-chain-length polyhydroxyalkanoates. *The Journal of Microbiology*, 87-97.

Kim, H. W., Chung, C. W. & Rhee, Y. H. (2005a). UV-induced graft copolymerization of monoacrylate-poly(ethylene glycol) onto poly(3-hydroxyoctanoate) to reduce protein adsorption and platelet adhesion. *International Journal of Biological Macromolecules, 35*(1), 47-53.

Kim, H. W., Chung, C. W., Hwang, S. J. & Rhee, Y. H. (2005b). Drug release from and hydrolytic degradation of a poly (ethylene glycol) grafted poly (3-hydroxyoctanoate). *International Journal of Biological Macromolecules, 36*(1), 84-89.

Kim, H. W., Chung, M. G., Kim, Y. B. & Rhee, Y. H. (2008). Graft copolymerization of glycerol 1, 3-diglycerolate diacrylate onto poly(3-hydroxyoctanoate) to improve physical properties and biocompatibility. *International Journal of Biological Macromolecules, 43*(3), 307-313.

Knowles, J., Hastings, G., Ohta, H., Niwa, S. & Boeree, N. (1992). Development of a degradable composite for orthopaedic use: *in vivo* biomechanical and histological evaluation of two bioactive degradable composites based on the polyhydroxybutyrate polymer. *Biomaterials, 13*(8), 491-496

Köse, G. T., Korkusuz, F., Korkusuz, P., Purali, N., Özkul, A. & Hasırcı, V. (2003). Bone generation on PHBV matrices: an *in vitro* study. *Biomaterials, 24*(27), 4999-5007

Kokubo, T., Kim, H.-M. & Kawashita, M. (2003). Novel bioactive materials with different mechanical properties. *Biomaterials, 24*(13), 2161-2175.

Kunasundari, B. & Sudesh, K. (2011). Isolation and recovery of microbial polyhydroxyalkanoates. *Express Polymer Letters, 5*(7), 620-634.

Langer, N. M. & Wilkie, C. A. (1998). Surface modification of polyamide-6: graft copolymerization of vinyl monomers onto polyamide-6 and thermal analysis of the graft copolymers. *Polymers for Advanced Technologies, 9*(5), 290-296.

Lao, H. K., Renard, E., Langlois, V., Vallée-Rehel, K. & Linossier, I. (2010). Surface functionalization of PHBV by HEMA grafting via UV treatment: Comparison with thermal free radical polymerization. *Journal of Applied Polymer Science, 116*(1), 288-297.

Lao, H.-K., Renard, E., Linossier, I., Langlois, V. & Vallée-Rehel, K. (2007). Modification of poly(3-hydroxybutyrate-*co*-3-hydroxyvalerate) film by chemical graft copolymerization. *Biomacromolecules, 8*(2), 416-423.

Le Meur, S., Zinn, M., Egli, T., Thöny-Meyer, L. & Ren, Q. (2012). Production of medium-chain-length polyhydroxyalkanoates by sequential feeding of xylose and octanoic acid in engineered *Pseudomonas Putida* KT2440. *BMC Biotechnology, 12*(1), 53.

Lee, H. S. & Lee, T. Y. (1997). Graft polymerization of acrylamide onto poly(hydroxybutyrate-*co*-hydroxyvalerate) films. *Polymer, 38*(17), 4505-4511.

Leenstra, T., Kuijpers-Jagtman, A. & Maltha, J. (1998). The healing process of palatal tissues after palatal surgery with and without implantation of membranes: an experimental study in dogs. *Journal of Materials Science: Materials in Medicine, 9*(5), 249-255

Li, H. & Chang, J. (2005). Preparation, characterization and *in vitro* release of gentamicin from PHBV/wollastonite composite microspheres. *Journal of Controlled Release, 107*(3), 463-473

Li, Z. & Loh, X. J. (2015). Water soluble polyhydroxyalkanoates: Future materials for therapeutic applications. *Chemical Society Reviews, 44*(10), 2865-2879.

Li, Z., Yang, J. & Loh, X. J. (2016). Polyhydroxyalkanoates: Opening doors for a sustainable future. *NPG Asia Materials, 8*, e265.

Löbler, M., Sternberg, K., Stachs, O., Allemann, R., Grabow, N., Roock, A., . . . Hanh, B. D. (2011). Polymers and drugs suitable for the development of a drug delivery drainage system in glaucoma surgery. *Journal of Biomedical Materials Research Part B: Applied Biomaterials, 97*(2), 388-395

Madison, L. L. & Huisman, G. W. (1999). Metabolic engineering of poly(3hydroxyalkanoates): From DNA to plastic. *Microbiology and Molecular Biology Reviews, 63*(1), 21-53.

Malm, T., Bowald, S., Bylock, A., Busch, C. & Saldeen, T. (1994). Enlargement of the right ventricular outflow tract and the pulmonary artery with a new biodegradable patch in transannular position. *European Surgical Research, 26*(5), 298-308

Martin, D. P. & Williams, S. F. (2003). Medical applications of poly-4-hydroxybutyrate: a strong flexible absorbable biomaterial. *Biochemical Engineering Journal, 16*(2), 97-105

Meng, D.-C., Shen, R., Yao, H., Chen, J.-C., Wu, Q. & Chen, G.-Q. (2014). Engineering the diversity of polyesters. *Current Opinion in Biotechnology, 29*, 24-33.

Misra, S. K., Valappil, S. P., Roy, I. & Boccaccini, A. R. (2006). Polyhydroxyalkanoate (PHA)/inorganic phase composites for tissue engineering applications. *Biomacromolecules, 7*(8), 2249-2258.

Misra, S. K., Nazhat, S. N., Valappil, S. P., Moshrefi-Torbati, M., Wood, R. J., Roy, I. & Boccaccini, A. R. (2007). Fabrication and characterization of biodegradable poly (3-hydroxybutyrate) composite containing bioglass. *Biomacromolecules, 8*(7), 2112-2119

Mosahebi, A., Fuller, P., Wiberg, M. & Terenghi, G. (2002). Effect of allogeneic schwann cell transplantation on peripheral nerve regeneration. *Experimental neurology, 173*(2), 213-223

Moradi, A., Dalilottojari, A., Pingguan-Murphy, B. & Djordjevic, I. (2013). Fabrication and characterization of elastomeric scaffolds comprised of a citric acid-based polyester/hydroxyapatite microcomposite. *Materials & Design, 50*, 446-450.

Muhr, A., Rechberger, E. M., Salerno, A., Reiterer, A., Schiller, M., Kwiecień, ... Koller, M. (2013). Biodegradable latexes from animal-derived waste: biosynthesis and characterization of mcl-pha accumulated by *Ps. Citronellolis*. *Reactive and Functional Polymers, 73*(10), 1391-1398.

Nair, L. S. & Laurencin, C. T. (2006). Polymers as biomaterials for tissue engineering and controlled drug delivery. In K. Lee & D. Kaplan (Eds.), *Tissue engineering I* (pp. 47-90). Berlin, Heidelberg: Springer Berlin Heidelberg.

Nakas, J. P., Zhu, C., Perrotta, J. A. & Nomura, C. T. (2015). Methods for producing polyhydroxyalkanoates from biodiesel-glycerol: U.S Patents 8,956,835,B2.

Nguyen, L. H., Annabi, N., Nikkhah, M., Bae, H., Binan, L., Park, S *et al*. (2012). Vascularized bone tissue engineering: Approaches for potential improvement. *Tissue Engineering Part B: Reviews, 18*(5), 363-382.

Nguyen, S. (2008). Graft copolymers containing poly(3-hydroxyalkanoates)- A review on their synthesis, properties, and applications. *Canadian Journal of Chemistry, 86*(6), 570-578.

Nguyen, S. & Marchessault, R. H. (2004). Synthesis and properties of graft copolymers based on poly(3-hydroxybutyrate) macromonomers. *Macromolecular Bioscience, 4*(3), 262-268.

Ni, J. & Wang, M. (2002). *In vitro* evaluation of hydroxyapatite reinforced polyhydroxybutyrate composite. *Materials Science and Engineering: C, 20*(1), 101-109.

Novikov, L. N., Novikova, L. N., Mosahebi, A., Wiberg, M., Terenghi, G. & Kellerth, J.-O. (2002). A novel biodegradable implant for neuronal rescue and regeneration after spinal cord injury. *Biomaterials, 23*(16), 3369-3376

Panith, N., Assavanig, A., Lertsiri, S., Bergkvist, M., Surarit, R. & Niamsiri, N. (2016). Development of tunable biodegradable polyhydroxyalkanoates microspheres for controlled delivery of tetracycline for treating periodontal disease. *Journal of Applied Polymer Science, 133*(42)

Peschel, G., Dahse, H. M., Konrad, A., Wieland, G. D., Mueller, P. J., Martin, D. P. & Roth, M. (2008). Growth of keratinocytes on porous films of poly (3-hydroxybutyrate) and poly (4-hydroxybutyrate) blended with hyaluronic acid and chitosan. *Journal of Biomedical Materials Research Part A, 85*(4), 1072-1081

Pelka, M., Danzl, C., Distler, W. & Petschelt, A. (2000). A new screening test for toxicity testing of dental materials. *Journal of Dentistry, 28*(5), 341-345.

Pham, B. T., Tonge, M. P., Monteiro, M. J. & Gilbert, R. G. (2000). Grafting kinetics of vinyl neodecanoate onto polybutadiene. *Macromolecules, 33*(7), 2383-2390.

Philip, S., Keshavarz, T. & Roy, I. (2007). Polyhydroxyalkanoates: Biodegradable polymers with a range of applications. *Journal of Chemical Technology & Biotechnology, 82*(3), 233-247.

Poblete-Castro, I., Rodriguez, A. L., Lam, C. M. & Kessler, W. (2014). Improved production of medium-chain-length polyhydroxyalkanoates in glucose-based fed-batch cultivations of metabolically engineered *Pseudomonas putida* strains. *Journal of Microbiology and Biotechnology, 24*(1), 59-69.

Porter, J. R., Ruckh, T. T. & Popat, K. C. (2009). Bone tissue engineering: A review in bone biomimetics and drug delivery strategies. *Biotechnology Progress, 25*(6), 1539-1560.

Pouton, C. W. & Akhtar, S. (1996). Biosynthetic polyhydroxyalkanoates and their potential in drug delivery. *Advanced Drug Delivery Reviews, 18*(2), 133-162.

Pramanik, N., Mishra, D., Banerjee, I., Maiti, T. K., Bhargava, P. & Pramanik, P. (2009). Chemical synthesis, characterization, and biocompatibility study of hydroxyapatite/chitosan phosphate nanocomposite for bone tissue engineering applications. *International Journal of Biomaterials, 2009*, 512417.

Qu, X.-H., Wu, Q. & Chen, G.-Q. (2006). *In vitro* study on hemocompatibility and cytocompatibility of poly(3-hydroxybutyrate-*co*-3-hydroxyhexanoate). *Journal of Biomaterials Science, Polymer Edition, 17*(10), 1107-1121.

Rai, R., Keshavarz, T., Roether, J., Boccaccini, A. R. & Roy, I. (2011). Medium chain length polyhydroxyalkanoates, promising new biomedical materials for the future. *Materials Science and Engineering: R: Reports, 72*(3), 29-47.

Rajabi, S., Ramazani, A., Hamidi, M. & Naji, T. (2015). *Artemia Salina* as a model organism in toxicity assessment of nanoparticles. *DARU Journal of Pharmaceutical Sciences, 23*(1), 1.

Razaif-Mazinah, M., Rafais, M., Annuar, M., Suffian, M. & Sharifuddin, Y. (2015). Effects of even and odd number fatty acids cofeeding on pha production and composition in *Pseudomonas Putida* Bet001 isolated from palm oil mill effluent. *Biotechnology and Applied Biochemistry*, *63*, 92-100.

Reddy, C., Ghai, R. & Kalia, V. C. (2003). Polyhydroxyalkanoates: An overview. *Bioresource Technology*, *87*(2), 137-146.

Renard, E., Tanguy, P. Y., Samain, E. & Guerin, P. (2003). *Synthesis of novel graft polyhydroxyalkanoates.* Paper presented at the Macromolecular Symposia.

Rezwan, K., Chen, Q. Z., Blaker, J. J. & Boccaccini, A. R. (2006). Biodegradable and bioactive porous polymer/inorganic composite scaffolds for bone tissue engineering. *Biomaterials, 27*(18), 3413-3431.

Rizzi, S. C., Heath, D., Coombes, A., Bock, N., Textor, M. & Downes, S. (2001). biodegradable polymer/hydroxyapatite composites: Surface analysis and initial attachment of human osteoblasts. *Journal of Biomedical Materials Research, 55*(4), 475-486.

Saadat, A., Behnamghader, A., Karbasi, S., Abedi, D., Soleimani, M. & Shafiee, A. (2013). Comparison of acellular and cellular bioactivity of poly(3-hydroxybutyrate/hydroxyapatite nanocomposite and poly(3-hydroxybutyrate) scaffolds. *Biotechnology and Bioprocess Engineering, 18*(3), 587-593.

Sabir, M. I., Xu, X. & Li, L. (2009). A review on biodegradable polymeric materials for bone tissue engineering applications. *Journal of Materials Science, 44*(21), 5713-5724.

Shabna, A., Saranya, V., Malathi, J., Shenbagarathai, R. & Madhavan, H. (2013). Indigenously produced polyhydroxyalkanoate based co-polymer as cellular supportive biomaterial. *Journal of Biomedical Materials Research Part A 102(10),* 3470-3476.

Shishatskaya, E., Khlusov, I. & Volova, T. (2006). A hybrid PHB–hydroxyapatite composite for biomedical application: production, *in vitro* and *in vivo* investigation. *Journal of Biomaterials Science, Polymer Edition, 17*(5), 481-498

Shishatskaya, E., Volova, T., Puzyr, A., Mogilnaya, O. & Efremov, S. (2004). Tissue response to the implantation of biodegradable polyhydroxyalkanoate sutures. *Journal of Materials Science: Materials in Medicine, 15*(6), 719-728

Shrivastav, A., Kim, H.-Y. & Kim, Y.-R. (2013). Advances in the applications of polyhydroxyalkanoate nanoparticles for novel drug delivery system. *BioMed Research International, 2013,*1-12.

Sodian, R., Sperling, J. S., Martin, D. P., Egozy, A., Stock, U., Mayer Jr, J. E. & Vacanti, J. P. (2000). Technical report: Fabrication of a trileaflet heart valve scaffold from a polyhydroxyalkanoate biopolyester for use in tissue engineering. *Tissue Engineering, 6*(2), 183-188.

Steinbüchel, A. & Lütke-Eversloh, T. (2003). Metabolic engineering and pathway construction for biotechnological production of relevant polyhydroxyalkanoates in microorganisms. *Biochemical Engineering Journal, 16*(2), 81-96.

Sudesh, K. & Iwata, T. (2008). Sustainability of biobased and biodegradable plastics. *CLEAN–Soil, Air, Water, 36*(5-6), 433-442.

Sudesh, K., Abe, H. & Doi, Y. (2000). Synthesis, structure and properties of polyhydroxyalkanoates: biological polyesters. *Progress in Polymer Science, 25*(10), 1503-1555.

Sultana, N. & Khan, T. H. (2012). *In vitro* degradation of PHBV scaffolds and nHA/PHBV composite scaffolds containing hydroxyapatite nanoparticles for bone tissue engineering. *Journal of Nanomaterials, 2012*, 1-12.

Sultana, N. & Wang, M. (2008). PHBV/PLLA-based composite scaffolds containing nano-sized hydroxyapatite particles for bone tissue engineering. *Journal of Experimental Nanoscience, 3*(2), 121-132.

Tan, Q., Li, S., Ren, J. & Chen, C. (2011). Fabrication of porous scaffolds with a controllable microstructure and mechanical properties by porogen fusion technique. *International Journal of Molecular Sciences, 12*(2), 890-904.

Tesema, Y., Raghavan, D. & Stubbs, J. (2004). Bone cell viability on collagen immobilized poly (3-hydroxybutrate-*co*-3-hydroxyvalerate) membrane: Effect of surface chemistry. *Journal of Applied Polymer Science, 93*(5), 2445-2453

Tsuge, T. (2002). Metabolic improvements and use of inexpensive carbon sources in microbial production of polyhydroxyalkanoates. *Journal of Bioscience and Bioengineering, 94*(6), 579-584

Verlinden, R. A., Hill, D. J., Kenward, M., Williams, C. D. & Radecka, I. (2007). Bacterial synthesis of biodegradable polyhydroxyalkanoates. *Journal of Applied Microbiology, 102*(6), 1437-1449.

Wang, W., Zhang, Y. & Chen, Y. (2007). Graft copolymerization of N-vinylpyrrolidone onto poly(3-hydroxybutyrate-*co*-3-hydroxyvalerate) in homogeneous solution. *Iranian Polymer Journal, 16*(3), 195.

Wang, Y. W., Wu, Q., Chen, J. & Chen, G. Q. (2005). Evaluation of three-dimensional scaffolds made of blends of hydroxyapatite and poly(3-hydroxybutyrate-*co*-3-hydroxyhexanoate) for bone reconstruction. *Biomaterials, 26*(8), 899-904.

Wang, Y.-W., Wu, Q. & Chen, G.-Q. (2004). Attachment, proliferation and differentiation of osteoblasts on random biopolyester poly(3-hydroxybutyrate-*co*-3-hydroxyhexanoate) scaffolds. *Biomaterials, 25*(4), 669-675.

Wei, G. & Ma, P. X. (2004). Structure and properties of nano-hydroxyapatite/polymer composite scaffolds for bone tissue engineering. *Biomaterials, 25*(19), 4749-4757.

Williams, S. F. & Martin, D. P. (2005). Applications of polyhydroxyalkanoates (PHA) in medicine and pharmacy. *Biopolymers 3*,91-128.

Xi, J., Zhang, L., Zheng, Z. A., Chen, G., Gong, Y., Zhao, N. & Zhang, X. (2008). Preparation and evaluation of porous poly(3-hydroxybutyrate-*co*-3-hydroxyhexanoate)—hydroxyapatite composite scaffolds. *Journal of Biomaterials Applications, 22*(4), 293-307.

Xu, J., Guo, B.-H., Yang, R., Wu, Q., Chen, G.-Q. & Zhang, Z.-M. (2002). In situ FTIR study on melting and crystallization of polyhydroxyalkanoates. *Polymer, 43*(25), 6893-6899.

Yu, L., Dean, K. & Li, L. (2006). Polymer blends and composites from renewable resources. *Progress in Polymer Science, 31*(6), 576-602.

Zhao, K., Deng, Y., Chen, J. C. & Chen, G.-Q. (2003). Polyhydroxyalkanoate (PHA) scaffolds with good mechanical properties and biocompatibility. *Biomaterials, 24*(6), 1041-1045

Zinn, M., Witholt, B. & Egli, T. (2001). Occurrence, synthesis and medical application of bacterial polyhydroxyalkanoate. *Advanced Drug Delivery Reviews, 53*(1), 5-21.

PUBLICATIONS AND PAPERS PRESENTED

Publications:

1. Ansari, N. F., Annuar, M. S. M., & Murphy, B. P. (2016). A porous medium-chain-length poly (3-hydroxyalkanoates)/hydroxyapatite composite as scaffold for bone tissue engineering. *Engineering in Life Sciences* 17: 420-429.

2. Ansari, N. F., Annuar, M. S. M. (2017). Functionalization of medium-chain-length poly(3-hydroxyalkanoates) as amphiphilic material by graft copolymerization with glycerol 1,3-diglycerol diacrylate and its mechanism. *Journal of Macromolecular Science, Part A* (accepted – DOI: 10.1080/10601325.2017.1387490)

Conferences:

1. Nor Faezah Ansari, M. Suffian M. Annuar, Belinda Pingguan Murphy. (2015). *A porous composite PHA/hydroxyapatite scaffold for bone tissue engineering and its hydrophilicity enhancement by graft copolymerization with glycerol 1,3-diglycerol diacrylate.* Presented in 20th Biological Science Graduate Congress (BSGC), Chulalongkorn University, Thailand (Oral presentation).

2. Nor Faezah Ansari and M. Suffian M. Annuar. (2016). *Fabrication and characterization of porous P(3HO-co-3HHX)/hydroxyapatite composite scaffold for bone tissue engineering and its hydrophilicity enhancement by graft copolymerization with glycerol 1,3-diglycerol diacrylate.* Presented in 3rd International Conference of Chemical Engineering and Industrial Biotechnology (ICCEIB), Bayou Lagoon Park Resort, Melaka (Oral presentation).